Model Evaluation for Seasonal Forecasting over Southern Africa

Nana Ama Kum Browne

Thesis Presented for the Degree of

DOCTOR OF PHILOSOPHY

In the Department of Environmental and Geographical Science

UNIVERSITY OF CAPE TOWN

December 2011

DEDICATION

To my son Nana Amoono

Model Evaluation for Seasonal Forecasting over Southern Africa

Nana Ama Kum Browne

December 2011

Abstract

This study contributes to a broader effort of institutions toward improving seasonal forecasts over southern Africa. The primary objective is to understand where global models show shortcomings in their simulations, and how this impacts on their seasonal forecast skill. It is proposed that the skill of a model in simulating natural climate variability is an appropriate metric for a model's potential skill in seasonal forecasting. Thus the study investigates the performance of two global models in simulating the regional processes in relation to the processes variability, and how this is related to their forecast skill.

In the study, ensembles of hindcasts from the Community Atmospheric Model version 3 (CAM3) and the Hadley Center Atmospheric Model version 3 (HadAM3) are analyzed. This is to evaluate simulations from both models and the results compared with Climatic Research Unit (CRU) dataset and the National Centers for Environmental Prediction/National Center for Atmospheric Research (NCEP/NCAR) reanalysis dataset. The simulations with the models covered a period of 30 years (1971-2000) and five ensembles from each model used. It was found that both CAM3 and HadAM3 give credible simulations of essential climatic features but with some biases in reproducing other features. For example, CAM3 captured the strength of the wind, direction, and the Inter-Tropical Convergence Zone (ITCZ) but has limitations in simulating the circumpolar waves, while HadAM3 captured the core of the anticyclones and the circumpolar waves but could not adequately capture the wind system over the region. Both models have the ability to simulate the synoptic circulations satisfactorily. However, deficiencies in the simulation of the inter-annual rainfall contribute directly to the models limitation for producing skillful forecasts. Additionally, the models fail to properly project the link between the regional rainfall and Sea Surface Temperature (SST) during El Niño and La Niña years. In cases where the observed rainfall-SST correlation show meaningful results, the limitation of the models to properly

correlate with SST indicate that the models are not setting up teleconnection patterns. This has effect on their forecast skills.

The same global models were evaluated for their seasonal forecast skill in summer rainfall of an El Niño and a La Niña year over southern Africa defined in the study as 40S-0 and 0-70E. Both models demonstrated some skill over southern Africa but showed some bias frequencies. It is noted that the models' skill in predicting seasonal precipitation vary from one sub-region to the other. The sub-regions used are defined as 10S:0 and 7E:30E for North-Western (NW), 20S:5S and 30E:42E for North-east (NE), 34S:28S and 26E:33E for Eastern Cape (EC), and Western Cape (WC).

The study significantly provides more insight into models ability to simulate the general circulation features that modulate rainfall and temperature, and the relationship of rainfall with global SST. This thesis will therefore provide useful information for modellers, forecasters, and climate researchers on the two global models used in the study.

ACKNOWLEDGMENTS

The project is sponsored by the Centre for High Performance Computing, South Africa. I am very grateful to Schlumberger Faculty for the Future, DAAD, AMMSI, and NRF for financial support and Abdus Salam International Centre for Theoretical Physics for granting me various fellowships.

I am heartily thankful to Dr. Babatude Abiodun, whose guidance and support from the initial to the final level enabled me to develop an understanding of the subject. Also Professor Bruce Hewitson and Dr. Mark Tadross, I am grateful for their valuable contributions. CSAGers, I am highly indebted to you for your assistance in diverse ways.

My family has been a constant source of strength in my life. Mum and Dad, thanks for giving me the foundation of my education. Araba Edesima Browne this one is for you little sister; many thanks for your support. Araba Browne Okyireh and Winifred Browne, I appreciate your prayers and encouragement for me. My much loved husband, Kofi Klutse, I am grateful for your endless support.

I offer my regards and blessings to all of those who supported me in various ways for the completion of the project. Bode Gbobaniyi and Tafara Matekaire, for mugs of coffee and walks when the stress level peaked, Bamba Sylla, Kweku Osei for always being supportive and reviewing my drafts. Mavis, Thompson, Kirpal, Eben for asking me “how is the thesis going” every time keeps me awake. Prophet Adjetey, thanks for your prayers. Dr. Kana, that story kept me calm and more focused. Prof Allotey, Prof Fletcher, Prof SY Mensah, and Prof Benyah, your expectation of me challenged me to forge ahead. Thank you.

Table of Contents

Chapter 1

Introduction

This thesis aims to understand where Global Climate Models (GCMs) show shortcomings in their simulations of southern African climate, and how this impacts on their seasonal forecast skill. It is proposed that the skill of a model in simulating climate variability is a useful metric for assessing a model's potential skill in seasonal forecasting. A model's performance in capturing both the climatology and climate variability of a region is very important in seasonal forecasting. Understanding how well GCMs reproduce climate variability may thus inform the generation of better seasonal forecasts.

The following sections represent an overview of seasonal forecasting challenges and needs, methods and practices. These provide a background to the central theme of the thesis on model evaluation for informing seasonal forecasting.

1.1 Seasonal Forecasting: Needs and Challenges

Seasonal forecasting of climate is very important and is linked to a variety of practical applications from socio-economic sectors such as energy management, agricultural management, health planning, and tourism to weather risk and security issues such as disaster forecasts and prevention, food security or water resource management. Information from seasonal forecasts of rainfall and temperature can assist planning, management and mitigation decisions for users from many sectors of the economy.

Seasonal forecasting is useful for southern Africa because the region has a variable climate which affects daily life. The highly complex topography of the region due to the presence of mountain chains and the position of the region between the Atlantic

and Indian Oceans make the region vulnerable to climate variations. The topographic features are variable in spatial extent and contribute to rapid changes in the region's climate. In addition, the geographical location of southern Africa (between the two oceans) exposes it to seasonal changes due to the impacts of the different processes that occur in the oceans. Other factors that cause variable climate for the region are the disturbances of the warming and cooling of the ocean during El Niño Southern Oscillation (ENSO). The effects from the oceans influence different parts of the region differently due to the varying topography. Knowledge of how the climate will change a season in advance will help coping strategies in southern Africa.

Rainfall is considered the most important climatic element that influences agriculture in southern Africa. Because of this, foreknowledge of rainfall conditions is very important in southern Africa since a high percentage of farmers depend on rain-fed agriculture. Practices of farmers are controlled by unreliable rainfall over the region and farmers live with host of uncertainties. In some years there is not enough rain for crops to survive and entire harvests fail. In other years, the total rainfall might be sufficient, but the timing of the rainfall can result in reduced yields. And in other years, heavy rainfall can wash away soil and damage crops. Clearly, ability to predict rainfall variability a season in advance will help these farmers to manage and cope with seasonal changes of the region. The advantages for farmers here will be in improvement of livelihoods and intensifying production through replenishing soil nutrients, adopting improved technology and investing in more profitable enterprises when conditions are favourable or near average; and to more effectively protect their families and farms against the long-term consequences of adverse extremes.

The high variability of the climate of southern Africa makes seasonal forecasting more challenging over the region. Consequently, the outcomes of seasonal forecasting have not achieved the desired precision and accuracy especially for enterprises such as agriculture where slight changes in predicted weather events could cause losses in crop and livestock production. Many efforts to correct this challenge have been successful only to some degree. For example, most of the approaches used in seasonal forecasting first study the potential predictability of internal variability arising from initialisation of slowly-varying components of the climate system (Hurrell *et al*., 2009) so that some level of confidence can be

developed in the forecasts. At this point, an important question to consider will be the level of detail at which regional internal variability needs to be well captured to make forecasts useful to users. Will it be sufficient simply to capture the amplitude of the variability on (say) seasonal time scales, or will it also be necessary to capture higher order aspects such as spells of hot, dry or wet days, or the risk of drought persisting over several seasons or years? These questions limit the ability of forecasters to improve seasonal predictions for societal benefit. Another concern is about what is needed by society. The wide range of needs and expectations from society also limits the application of seasonal predictions for societal benefit. More importantly, can the models deliver these? Models have improved considerably in recent times. There have also been a number of concerted efforts towards improving models to simulate remarkably well current climate and its variability but the accuracy of the models is limited by grid resolution and the ability to describe the complicated atmospheric, oceanic, and chemical processes mathematically. These continue to be overarching concerns for climate researchers and society in southern Africa and other parts of the world. An example of many of the efforts to address the overarching concerns on seasonal forecasting created the EU-funded project entitled "Development of a European Multimodel Ensemble system for seasonal to inTERannual prediction (DEMETER; Palmer *et al*. (2004))". The objective of the project is to develop a well-validated European coupled multi-model ensemble forecast system for reliable seasonal to interannual prediction.

It is well accepted in the forecasting community that a weather system is accurate up to two days ahead (e.g. Shukla, 1998). Conversely, the goal of seasonal forecasting is predicting climate seasonal anomalies a few months in advance (typically 3 or 4 months before the onset of the season). Seasonal forecasting is possible because the ocean circulates on a slower timescale bestowing some memory (due to its larger heat capacity) to the atmosphere thereby enhancing and extending the predictability horizon (Palmer and Anderson, 1994; Anderson, 2008) associated with the atmosphere.

The coupling between the atmosphere and ocean is quite strong in the tropical region giving rise to one of the prime examples of seasonal climate variability El Niño and La Niña phenomena. Although the origins of El Niño and La Niña phenomena lie in

the tropical Pacific, the weather in many places around the world is affected by their events; however the strength of that teleconnection depends strongly on the location and season (Halpert and Ropelewsky, 1992). Southern Africa's rainfall season is influenced by Sea Surface Temperatures (SSTs) in the tropical Pacific associated with ENSO (Ropelewski and Halpert, 1987; Ogallo *et al*., 1988; Indeje *et al*., 2000; Mutai *et al*., 1998), and by SSTs in the Indian Ocean (Goddard and Graham, 1999; Mutai and Ward, 2000). Moreover, while the ENSO has effect on rainfall variability over the southern Africa, Indian Ocean SST anomalies vary independently of ENSO. It is challenging for GCMs to represent such complex variability and that limits our understanding in improving the models for reliable forecasts.

1.2 Seasonal Forecasting Methods and Practices over Southern Africa

For seasonal forecasts to have an impact on society, they have to be reliable, timely, and well presented. Reliability of the forecast helps to build user confidence in the product. There have been many attempts to produce reliable seasonal forecasts through a suite of different approaches. The approaches include a range of indigenous knowledge in which early farmers formulate hypotheses about seasonal rainfall by observing natural phenomena, while the cultural and ritual spiritualists draw predictions from divination, visions and dreams (Roncoli *et al*., 2001). In index-based forecasting, approaches are based on a range of different indices depending on the focus of the research. Climate indices may range from indicators of large-scale see-saw pressure patterns, especially the Southern Oscillation and North Atlantic Oscillation, through regional indices of monsoon strength, down to indices of local station rainfall. The statistical approaches use the past to predict the future by identifying trends and patterns within a data to develop the forecasts. The approach uses statistical methods to correct systematic deficiencies in the response of GCMs to SST forcing. The dynamical approaches have forecasts made from observed SST fields using GCMs. A forecast is made with a regional climate model (RCM) nested within GCM and forced by the GCM's boundary conditions. Recently dynamical and statistical approaches have been combined to compute the climate response to SST forcing (Smith and Livezey 1999; Feddersen *et al*. 1999; Mo and

Straus 2002; Tippett *et al*. 2003; Widmann *et al*. 2003). Each of these approaches have their merits and demerits.

Dynamic seasonal forecasting, however, is based on fundamental physical and dynamical relationships; relationships that are largely invariant to climate and climate change, and are conditioned by assimilating (dynamically) observations of the past and present state. Uncertainty, which grows with the length of a meteorological forecast, is being quantified by generating a series of forecasts under slightly different starting conditions in the model, which reflect the level of uncertainty in not being able to exactly prescribe the current state of weather everywhere, and then analysing the spread in the series of forecasts. This approach, termed ensemble forecasting, allows more appropriate probability statements, i.e. estimates of uncertainty, to be made about a forecast. Ensemble predictions generally provide more robust and reliable assessments of forecast conditions (Palmer *et al*., 2005; Krishnamurti *et al*., 1999).

Understanding of seasonal forecasting and the techniques employed have improved considerably (Hastenrath *et al*., 1995; Barnston *et al*., 1996; Mason *et al*., 1996; Rocha and Simmonds, 1997; Mason, 1998; Landman and Mason, 1999; Landman and Tennant, 2000; Landman and Mason, 2001; Landman and Goddard, 2002) after the occurance of the 1991-92 El Nino-related drought and its associated effects over many parts of the globe including southern Africa. The progress made in exploring prospects for seasonal climate prediction over the region is encouraging. For example, Landman *et al*. (2009) addressed the performance of a number of simulations for various regions of southern Africa. They employed both statistical and dynamical methods in their assessments and found that the statistical method outscored the dynamical method though they showed that increase in ensemble members in the case of dynamical method improves the skill of the GCMs. It is therefore well accepted (Yoo and Kang, 2005 and Kang and Yoo, 2006) that when many ensembles are used in the dynamical method, the probability of producing an accurate forecast is higher.

The dynamical approach is widely used because GCMs remain important tools at hand for modeling, assessing global climate and seasonal forecasting. GCMs show the ability to simulate inter-annual rainfall variability when they are forced with SST

(Palmer and Anderson, 1994; Mason *et al*., 1999; Hunt, 1997). In addition, when many ensembles from GCMs are used, there is high probability of producing accurate forecasts (Palmer *et al*., 2005; Krishnamurti *et al*., 1999). The study uses the Hadley Center Atmospheric Models version 3 (HadAM3) and the NCAR Community Atmospheric Models version 3 (CAM3) to assess the climate variability of southern Africa with a view of improving knowledge of the models' seasonal forecasting skills.

1.3 Research objectives

The main objective of this thesis is to add to our understanding of why global models show marked limitations in their representation of southern African climate and how these affect their seasonal forecast skills. Assessing global models to ascertain how they reproduce known features of climate is key to improving model reliability and predictive accuracy. Knowledge of the performance of global models is relevant in both research and operational seasonal forecasting.

To support the main objective, the thesis addresses the following three specific inquiries:

- How well do global models reproduce the synoptic circulations that control the climate of southern Africa?
- How well do global models reproduce teleconnections between regional rainfall and global SSTs?
- How predictable is the seasonal climate over southern Africa using these global models?

Building on these analyses, the thesis investigates why global models have limitations in reproducing the essential climate features of southern Africa. It could be intuitively assumed that a global model which produces a realistic circulation pattern over a region will give a skillful forecast over that same region. However, this assertion is not always justified. The thesis therefore investigates the two selected global models with respect to the limitations peculiar to each model, and

how this affects their ability to produce reliable seasonal forecasts over southern Africa.

In particular, the study investigates how CAM3 and HadAM3 GCMs reproduce the southern African climate and how their performance affect their seasonal forecast skills over the region. Information from this research will improve our understanding on how models reproduce the climate of southern Africa and why they may exhibit such characteristics. The methods of the investigation will provide useful metrics for concerned climate research groups in their practices and will contribute to the overall robustness of seasonal forecasting methodologies for southern Africa.

1.4 Thesis outline

This thesis is composed of seven chapters. Following the introductory chapter, which gives an overview of seasonal forecasting and a summary of methods employed in the practice, Chapter 2 describes southern African climate and GCMs. Chapter 3 discusses the models, methods and data used in this research and also gives a description of the sub domains used. Chapter 4 explores how well the global models reproduce the specific synoptic circulations that control the climate of southern Africa. By comparing model outputs to the National Centers for Environmental Prediction/National Center for Atmospheric Research (NCEP/NCAR) reanalysis data, the models' skill in replicating the major circulation features, and their variability is examined. This chapter addresses models' performances in reproducing important features pertinent to the southern African climate, and their roles as drivers of rainfall and temperature in the region. Chapter 5 expands on the assessment of the previous chapter by looking at how well the models capture the inter-annual variability of the southern African climate during ENSO years and the relationship between regional rainfall and global SST. The rainfall from four sub-regions - North-Western (NW), North-east (NE), Eastern Cape (EC) and Western Cape (WC) - provided a more robust assessment of the southern African climate for ENSO years. The relationship provides a foundation for the suitability of these models for reliable seasonal forecasting. In Chapter 6, the study investigates how predictable the seasonal climate is, using the global models, and discusses why the models may

exhibit certain forecast skills over particular areas. This chapter considers the question of models skills in predicting summer rainfall of an El Niño and a La Niña year over southern Africa. The same global models are used here. CAM3 has not been previously used for seasonal forecasting over southern Africa but HadAM3 has been in use for about a decade at the Climate Systems Analysis Group (CSAG) and other institutions in southern Africa. These institutions continue to seek for ways of improving their forecasts and this requires in-depth studies of the models. In this chapter, past seasonal forecasts of 2002/2003 El Niño and 2007/2008 La Niña rainfall are evaluated to assess the forecast skills of the models and explain why they exhibit those skills. A suite of statistical verification measures are used to determine the quality of the seasonal forecasts. We can improve our understanding of seasonal forecasting by monitoring the quality of forecasts for specific years. Finally, Chapter 7 presents the synthesis of the study, draws conclusions from the findings and provides recommendations for future studies.

Chapter 2

Southern African Climate and GCMs

The chapter provides an overview of climate variability in general and variability at the seasonal time scale in particular. A background is provided on the climate of southern Africa with focus on the important circulations that affect its climate and discusses how the position of the region and its topography affect it seasonal variability. A review is also provided on the GCMs and dynamical approaches used in seasonal forecasting.

2.1 Mean Climate and Variability

Climate is a statistical description in terms of the mean and variability, of relevant quantities (usually surface variables such as temperature, precipitation, and wind) over a period of time ranging from months to thousands or millions of years. Practically, 30 years is used as a standard normal periods defined by World Meteorological Organisation to describe the climate. The 30 years was chosen as a period long enough to eliminate year-to-year variations in description or application of the climate for one region or the other. The standard normal climate helps in describing the climate and is used as a base to which current conditions can be compared.

The climate is composed of a number of components which include but are not limited to the atmosphere, oceans, cryosphere, and the biosphere. These components are non-linear systems in their own right and their evolution is governed by various physical, chemical, and biological processes (Kiehl and Ramanathan, 2006). Each

component exhibits different response at different timescales and thermodynamic properties (Bard, 2002). The climate is influenced strongly by the interaction and feedbacks of these components. The influence that manifests in the natural changes of climate with reference to time is climate variability. These natural variations are caused by both external and internal factors. Variations that are directly driven by a periodic external force, like the diurnal or the seasonal cycle of insolation, are due to the rotation of Earth on its axis, the seasonal ones to its revolution around the Sun. They bring about the temperature and precipitation variations between day and night and between summer and winter, respectively. Natural climate variations due to the non-linear interplay of feedbacks within the climate system are complicated. For instance, a temperature drop within the system will increase the amount of snow and ice, and thus lead to further cooling; this is the so-called ice-albedo feedback (North, 1975; North, 1984). On the other hand, the increase of trace-gas concentrations in the atmosphere, such as that of carbon dioxide (CO_2), will increase surface temperatures through the greenhouse effect (Collins and Senior, 2002; Collins *et al.*, 2006). Each climate feedback can enhance or counteract the effect of another feedback (Soden and Held, 2005). The distinct feedback mechanisms identified in the climate system are numerous and complex. Variations associated with random fluctuations in physical or chemical factors can be external to the climate system, such as aerosol loading due to volcanic eruptions (Robock, 2002). They can also be internal to the system, such as weather fluctuations.

Human activities also influence the climate. The major human-induced causes include changes in greenhouse gas concentrations, changes in aerosol levels, and changes in land use and land cover. Land-use change, due to urbanisation and human forestry and agricultural practices, affect the physical and biological properties of the Earth's surface (Steinfeld *et al.*, 2006). Such effects change the radiative forcing and have a potential impact on regional and global climate (IPCC, 2007).

2.1.1 Climate variability at the seasonal time scale

A large portion of climate variability occurs on the seasonal time scales, i.e. on time scales ranging between about 20 and 90 days. This variability is important for the atmosphere in the tropical regions, where it represents a high percentage of the total atmospheric variance (Hoerling *et al.*, 2001; Hoerling and Kumar, 2002). The

dominant mode of variability in the tropics is the Tropical Intra-seasonal Oscillation, also known as the Madden-Julian Oscillation (MJO; Madden and Julian, 1972; Madden and Julian, 2005; Wang, 2005; Zhang, 2005). The MJO influences both the tropics and the subtropics between 30°S and 30°N (Tazalika and Jury, 2008; Pohl *et al*., 2007). A good percentage of the seasonal variance in rainfall is explained by MJO signal in parts of southern Africa (south of 15 °S) in summer (Pohl *et al*., 2009). Due to its strong impact on convective activity and circulation anomalies over these regions, the MJO is a crucial component of weather forecast and seasonal predictions. Furthermore, several observational and model studies have shown that the MJO phenomena might interact with phenomena that occur at longer time scales, such as monsoons and inter-annual variability (e.g. Tazalika and Jury, 2008; Pohl *et al*., 2007). These interactions might produce a substantial modulation of the intensity of the seasonal and inter-annual variability. Understanding of the modes that characterize the variability at seasonal time scales is of great importance for a deeper comprehension of the mechanisms that govern climate variability.

2.2 Southern African Climate Variability

Southern Africa experiences a high variable climate. The region is situated at the interface of tropical, subtropical and temperate climate systems, as well as the southern Indian and Atlantic oceans (see figure 2.1). The position of the region, the impact of ocean currents, and the presence of mountain chains, which serve as climatic barriers, makes it susceptible for it varying climate. The sub-continent is influenced by a wide variety of atmospheric and oceanic circulation systems (Chase and Meadows, 2007; Tyson and Preston-Whyte, 2000) and strongly controlled by tropical northerly airflow, which is enhanced by periodic coupling with temperate troughs. In the north and east, climate is primarily dictated by the seasonal interplay between subtropical high-pressure cells and the migrations of easterly flows associated with the Inter-Tropical Convergence Zone (ITCZ; Tyson, 1986; Tyson and Preston-Whyte, 2000; Chase and Meadows, 2007). Summer conditions of the southeastern are often associated with negative sea level pressure (SLP) anomalies over the western Indian Ocean, reducing the northeasterly flux of tropical moisture into the region (Mason and Jury, 1997; Rocha and Simmonds, 1997). Along the

southern and western coasts, winter rainfall results from temperate frontal systems embedded in the westerlies (Tyson and Preston-Whyte, 2000). Between the southern and western coasts is a narrow zone at the central part of the sub-continent, which receives both winter and summer precipitation.

The complex interactions between different synoptic circulation systems determine the southern African climate (Hudson and Jones, 2002; Reason and Jagadheesha, 2005; Anyah *et al*., 2006). In many cases, synoptic features interact with other circulation systems to produce extreme weather conditions. Some circulation systems exist for a long time and are more stable, others are transient and short lived (Tyson and Preston-Whyte, 2000). The transient features enhance, inhibit or have a neutral effect on rainfall over southern Africa. Major rainfall controls in southern Africa includes the subtropical anticyclones (Jones and Simmonds, 1993; Reason, 2002), westerly waves and lows (Taljaard and Bureau, 1985; Garstang *et al*., 1996; d'Abreton and Tyson, 1996), tropical highs, tropical lows (Crimp, 1997; Mason and Jury, 1997), and tropical temperate troughs. The major circulation types over southern Africa are shown in figure 2.1 and the various circulation systems are described in the subsections.

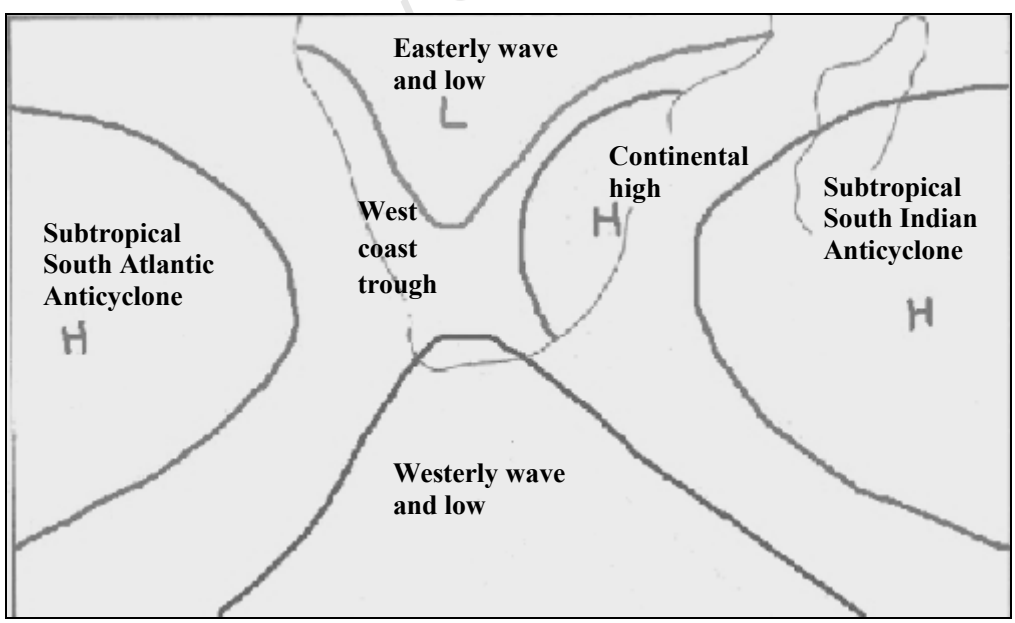

Figure 2.1*: Some important circulation types controlling the climate over southern Africa. (Modified from Tyson and Preston-Whyte, 2000)*

2.2.1 General circulation and synoptic features

Weather and climate of southern Africa is a product of complex interactions between general circulations, synoptic features and mesoscale features, in which topography and Sea Surface Temperature (SST) play significant roles (Tyson, 1981, 1986; Tyson and Preston-Whyte, 2000). The important synoptic features over southern Africa may include the ITCZ, sub-tropical jets, sub-tropical highs and Rossby waves. For instance, the ITCZ controls the location of maximum moisture flux convergences and maximum rainfall over the region (Newell and Kidson, 1984; Kraus, 1977; Klaus, 1978; Nicholson *et al*., 1996; Usman and Reason, 2004; McGregor and Nieuwolt, 1998; Jury and Pathack, 1993; Nicholson, 2000; Cook, 2000; Suzuki, 2010). The subtropical jets organize developing convective storms and induce cyclogenesis, tornadoes, squall lines, mountain waves and turbulence (Thorncroft and Flocas, 1997; Uccellini and Johnson, 1979; Nakamura and Shimpo, 2004; Roca *et al*., 2005). At the same time, the jets can produce divergence and stability. A slow vertical sinking air motion accompanies the subtropical jets and gives rise to predominantly fair weather in its area of influence. The two anticyclones over the Atlantic and Indian oceans produce a strong surface pressure gradient between the continent and oceans. Consequently, moist and unstable air is advected inland to produce strong convection with heavy rainfall and thunderstorms over eastern South Africa. The upper level quasi-stationary circumpolar waves (mainly wave 1 and wave 3) modulate the strength and motion of storms, and other localized features, and thus influence rainfall and temperature over southern Africa. Tyson (1980) links changes in the position of wave 3 with 10-12 year rainfall oscillations over the south coast of South Africa.

Temperate disturbances in the westerlies usually start with a trough (low pressure system) between the Atlantic and Indian Ocean high pressure systems (figure 2.1). The trough produces large scale precipitation over southern Africa, and when influenced by other disturbances like a cold front, it may induce tropical convection leading to thunderstorms (Kumar and Hoerling, 1998; Tyson and Preston-Whyte, 2000). A cold front is a zone of strong discontinuity and temperature gradient between two air-masses of different temperature characteristics which occurs when

cold air replaces warm air over a region. Cold fronts frequently accompany westerly waves passing over southern Africa, and may produce extreme cold weather in winter and extend cold breaks in summer (Hobbs, 1998; Tyson and Preston-Whyte, 2000). Detailed information on cold fronts can be found in Browning and Mason (1980); Fuenzalida *et al*. (2005); Smith and Reeder (1988); and Garreaud (2000). The main temperate disturbance is cut-off lows that develop from the westerlies (Singleton and Reason, 2007). The lows start in the upper troposphere as troughs, and then deepen until they form closed circulations, which extend equatorwards at the surface (Tyson and Preston-Whyte, 2000; Taljaard and Bureau, 1985). The lows induce unstable troposphere at low levels, produce severe convective events that lead to heavy rainfall and floods over large areas, and may trigger severe cyclonegenesis that induces strong wind (Nieto *et al*., 2005; Tyson and Preston-Whyte, 2000). Others like coastal lows (shown in figure 2.1) are very intense synoptic feature, which account for many flood-producing rains over southern Africa.

Tropical disturbances in the tropical easterly flow are usually associated with the ITCZ and the warm, humid easterly winds between the zone and the subtropical high belt. They may take the form of easterly waves, easterly lows or tropical lows. Tropical low pressure systems caused by disturbances in the easterly wave (figure 2.1), and are mostly driven by thermal heating of the tropical interior. They contribute to tropical moisture and energy transfer, a process which significantly facilitates rainfall over the region (Mason and Jury, 1997; Van den Heever *et al*., 1997). When the upper westerly wave coincides with an easterly wave or depression at lower levels, it results in the formation of a Tropical Temperate Trough (TTT). This feature is also associated with tropical moisture and energy transfer and has been known to significantly contribute to summer rainfall over southern Africa (Harangozo and Harrison, 1983; Harrison, 1984a).

2.2.2 Precipitation pattern

A number of processes and systems are associated with precipitation in different parts of southern Africa. The main form of precipitation over southern Africa is rainfall. The rainfall patterns over much of southern Africa are influenced by several circulation features, which include the ITCZ; anticyclones and associated ridging

systems; depressions and associated trough systems; semi-stationary and travelling waves; wave interactions between low- and mid-latitude flow; and jet streams.

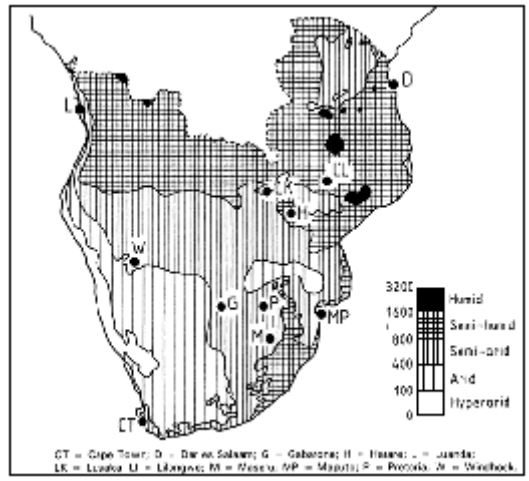

Figure 2.2: *The average rainfall over southern Africa and the major climatic divisions of the region. (Source: FAO Corporate Document Repository; Small water bodies and their fisheries in southern Africa, 1994).*

The distribution of the mean annual precipitation decreases fairly uniformly westwards from the escarpment across the interior plateau of the region. Figure 2.2 shows the various climatic divisions of southern Africa and their average rainfall.

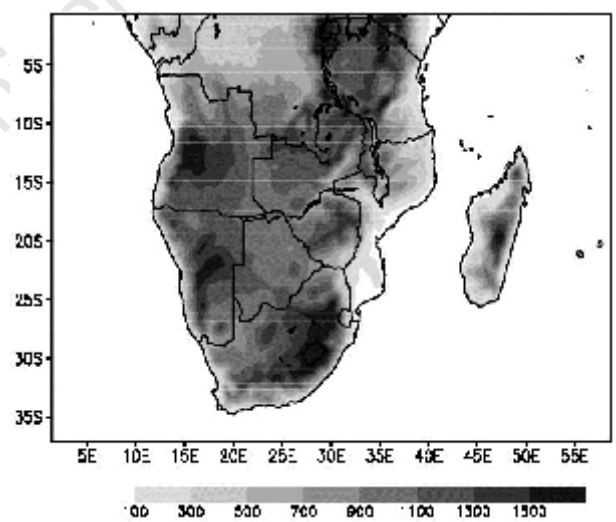

Figure 2.3: *Southern African topography*

The southern and eastern coastal parts have a high complex rainfall pattern due to irregular terrain (Figure 2.3). The Drakensberg Mountains as shown in figure 2.3 run almost parallel to the coast for the entire eastern side of the country, causing the irregular rainfall patterns in that part of the region (Singleton and Reason, 2006). Generally, rainfall increases towards the equator in the humid and semi-humid regions, resulting in more rain in Tanzania, northern Mozambique and Angola, and decreases in the arid and hyperarid regions giving less rainfall in South Africa, Botswana and Namibia. Rainfall over southern Africa is generally seasonal. The peak of the rainy season occurs in summer, between December and March with the exception of the Western Cape which is a winter-rain area. Mean summer rainfall contributes most of the mean annual rainfall over southern Africa. The seasonal rainfall pattern is discussed in several studies including Taljaard (1986) and Harrison (1984b).

2.2.3 Temperature pattern

The spatial and temporal variation of temperature across the sub-continent is not as pronounced as rainfall. However, a distinct variation exists at the seasonal scales. In summer (December, January and February) surface temperatures are higher over the arid regions of Botswana and Namibia to the eastern parts with average temperatures exceeding 26°C. The central portion of the sub-continent experience relatively cooler conditions; and the southeast even more, with average temperatures less than 20°C. This temperature decrease associated with summer rains is as a result of maximum mean cloudiness reducing the shortwave radiation reaching the earth's surface (Hudson and Jones, 2002). Southern Africa experiences decreasing temperatures during March to May, as the colder air masses from the Antarctic push inland (Tomczak and Godfrey, 2003), resulting in average temperatures of 20°C. The northwest experiences warmer temperatures during this period, whilst the east coast experiences average temperatures of 24°C. Only the regions north of 25°S experience temperatures greater than 24°C, during winter (June to August). All other parts have a range of temperatures between 12 and 20°C. From September to November, most parts of southern Africa experience warm temperature due to the absence of clouds. The influences of tropical air cause temperatures greater than 22°C (Tyson and Preston-Whyte, 2000). However, Lesotho, most of South Africa, and the southern part of Namibia experience temperatures of less than 16°C. Most

parts of Tanzania and eastern Congo tend to have temperatures typically around 20°C due to rain bearing clouds.

2.2.4 Wind flow and pressure pattern

The wind circulation is a crucial part of the southern African climate. This circulation oscillates as the seasons of the year change. There is a complexity in the behavior of the air circulation pattern over southern Africa. Rising air at the surface with adequate moisture generally results in convection (Grabowski and Moncrieff, 2004). An ideal situation for intense convection is the existence of an upper level anticyclone and a lower level cyclone. On the other hand, if the situation of the cyclone-anticyclone configuration is reversed such that the anticyclone is near the ground while the cyclone is at the upper level, conditions become unfavorable to convection (Tyson and Preston-Whyte, 2000). There are various configurations of the cyclone-anticyclone centers and moisture fields in the atmosphere in southern Africa at any given time or location (Freiman and Tyson, 2000), which leads to complexities in the distribution of rainfall.

Circulation patterns of importance over southern Africa are adequately described by the lower (850hpa) and upper (500hPa) pressure levels. Wind circulation at the 850hPa level exhibits a more coherent pattern which is coupled with rainfall. For instance, there is cyclonic wind circulation over northern Zambia and southern Angola, which allow intense convective activity over the region (Tyson and Preston-Whyte, 2000; Pohl *et al*., 2008). Another cyclonic centre is dominant over southern Malawi, Central Mozambique, northern Zimbabwe and eastern Zambia. This roughly defines the position of influence of the ITCZ during the southern Hemisphere summer (Pohl *et al*., 2008). The areas north of 10ºS have a predominantly light westerly flow. The anticyclonic activity of the subtropical high pressure exists to the south east of this region, centered over the coastline. The core of the strong easterly winds straddles southwest Zimbabwe, eastern Botswana, and northern South Africa. Another cyclonic centre exists over southern Botswana which causes intense summer heating (Tyson and Preston-Whyte, 2000). A westerly flow exists over the southern oceans (south of 35°S) adjacent to the sub-continent. The rest of the southwestern region has a southerly flow.

The main feature at the upper levels is an anticyclone centered around 17°S. A weak easterly flow exists northward of this anticyclone (Tyson and Preston-Whyte, 2000). This weak easterly regime stretches northward right up to the equator. By contrast, a broad westerly flow lies south of the anticyclone. This westerly regime covers the remainder of neighboring sub-continent, Madagascar, Mauritius, Reunion, and the southern portions of the Indian and Atlantic Oceans adjacent to southern Africa.

In winter, wind circulation pattern at the 850hPa level shows a noticeable difference to the summer pattern. There is a massive anticyclone centered over the Indian Ocean just southwest of Madagascar towards the southeast coast of southern Africa (Tyson and Preston-Whyte, 2000). Consequently, the flow across the bulk of the sub-region is easterly. In contrast, the southwest experiences a strong northwesterly flow but northwest regions experience a southerly flow. The southwest receives more regular precipitation during the period. Strong winds are also experienced over a zone stretching from the Indian Ocean north of 20°S through a large section of Tanzania into Zambia. Elsewhere on the sub-region the winds are relatively light. At the upper levels, the winds are strong over the southwestern fringe of the sub-continent. North of the axis, the wind pattern is mostly easterly with a slight northerly component (Bonnardot *et al*., 2005) and are much weaker in comparison with the stronger westerlies to the south.

2.3 Walker circulation, El Niño-Southern Oscillation and SSTs

The Walker Circulation have a strong influence on rainfall variability over southern Africa (Lindesay *et al.,* 1986). The circulation is caused by the pressure gradient force that results from a high pressure system over the eastern Pacific ocean, and a low pressure system over Indonesia. Walker circulation develops an ascending limb in the Indian Ocean, which is located over tropical Africa with the consequence of enhanced convection over these areas. The meridional cell (Hadley circulation) becomes more dominant and contributes to a pronounced Inter-Tropical Convergence Zone between temperate and tropical synoptic systems (around 20^{o}S) whilst the subtropical anticyclone intensifies near 30^{o}S. Detailed information about the Walker Circulation and its influences on southern African rainfall may be found

in Tyson (1986); Preston-Whyte and Tyson (1988); Tyson and Preston-Whyte (2000); Lindesay, 1986 and in many other articles.

The Walker circulation is directly responsive to sea surface temperatures over the eastern and western Pacific Ocean. As the temperatures change from time to time, a major pressure oscillation develop in the atmosphere. This see-saw pattern of atmospheric pressure between the Indian Ocean and Pacific Oceans (Walker, 1918) has been termed Southern Oscillation (SO). El Niño is closely related to SO. During El Niño episodes lower than normal pressure is observed over the eastern tropical Pacific and higher than normal pressure is found over Indonesia and northern Australia. This pattern of pressure is associated with weaker than normal near-surface equatorial easterly (east-to-west) winds. These features characterize the warm phase of the SO, which is often referred to as an El Niño/Southern Oscillation (ENSO) episode.

Climate variability in southern Africa has also been linked to the Southern Oscillation. The relationship between the Southern Oscillation Index (SOl) and rainfall in southern Africa has been investigated (e.g. Nicholson and Entekhabi, 1986; Lindesay, 1986; Hastenrath, 1995). For example, Lindesay (1986) found a clear pattern of spatial correlation between seasonal rainfall and the SOI for a period of 1935-1983. According to Lindesay (1988) the results of spectral analyses of central South African summer rainfall at periods of the Southern Oscillation confirm the thermodynamics that connect phase changes of the oscillation with changes in circulation over southern Africa. According to Harrison (1984b) the SO modulates the occurrence and preference in location of strong convection which contribute a large part of summer rainfall over South Africa. Preston-Whyte and Tyson (1988) reported that southern Africa rainfall is inversely correlated with rainfall over the equatorial belt of Africa. Detailed discussions on spatial and temporal fluctuations of rainfall over Africa may be found in Nicholson (1986) and Janowiak (1988). Other studies dwell on the relationships between SOl and circulation indices of southern Africa (e.g. Tyson,1984; Lindesay, 1986). Relationships between rainfall across South Africa and atmospheric circulation variables associated with SOl have been investigated by Lindesay (1988). After determining the correlation between SO and rainfall across South Africa, Lindesay (1988) correlated fluctuations in SOl with the

circulation and other meteorological variables over southern Africa for the period 1957 to 1983. Results showed that during the early months of October and November, correlations of both signs were observed over South Africa. Lindesay (1988) found poor correlations and no spatial coherence in the distribution of oppositely correlated areas. Positive correlations, with spatially coherent areas, were found over central parts of South Africa during the months December, January and February while an opposite pattern was found over the southwest Cape province. It was observed that a zone of high positive correlations was 1-15 oriented in the north-west to south-east direction during the months December-March which was probably due to tropical and temperate trough influences. It was found that SOl accounted for 20 percent of rainfall variability over central South Africa.

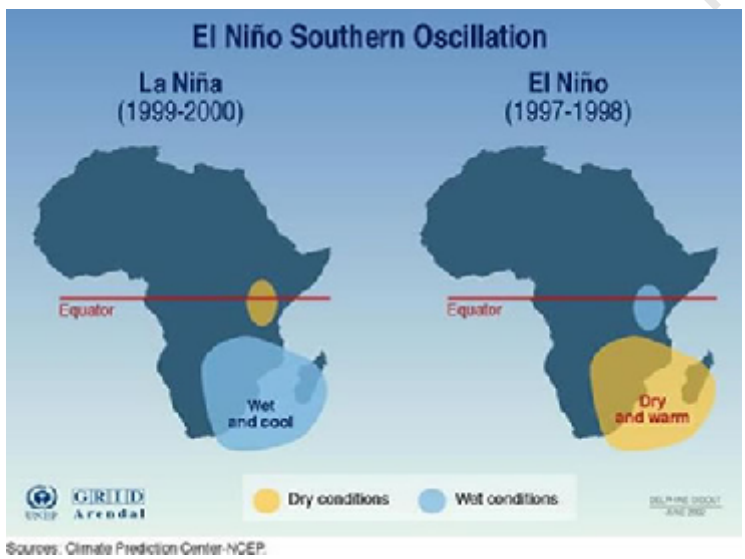

***Figure 2.4**: Impact of El Niño and La Niña events on Southern Africa. (Source: Climate Prediction Center-NCEP)*

The El Niño-Southern Oscillation (ENSO) is the most dominant perturbation responsible for climate variability over southern Africa (Nicholson and Entekhapi, 1986; Nicholson and Selato, 2000). Studies have shown that below normal rainfall is experienced over southern Africa during ENSO years and above normal rainfall during non ENSO years (Nicholson and Entekhabi, 1986; Lindesay, 1988). The

effects of ENSO disturbances over southern Africa vary from region to region and depend on the strength and timing of the phenomenon. ENSO phenomenon causes extreme weather such as floods, droughts and other disturbances in many regions of the world (Rasmusson and Wallace, 1983). For instance, the 1997/1998 El Niño event may have caused extreme wet conditions over eastern Africa, while the 1999-2000 event might have resulted in devastating floods in Mozambique (Nicholson and Entekhapi, 1986). The major impacts of the warm phase of ENSO (El Niño) are temperature anomalies, changes in precipitation variability, floods, and droughts. El Niño is particularly associated with drought over most parts of southern Africa. La Niña events are associated with cooler SSTs and floods over most parts of southern Africa. According to Halpert and Ropelewksi (1992), below normal surface temperatures occur from June through August prior to the onset of summer rainfall for southern Africa (La Niña) while above normal temperatures during the same period precede El Niño years. Consequently observed warmer (cooler) winter temperatures in southern Africa are associated with below (above) normal rainfall the following summer. Figure 2.4 shows a recent impact of the El Niño phenomenon over Africa from the 1999/2000 La Niña and 1997/1998 El Niño events. Some earlier and detailed description of the ENSO phenomenon can be found in the works of Horel and WaIlace (1981); Rasmusson and Carpenter (1982); Cane *et al*., (1986); Ropelewski and Halpert (1987); Philander (1989) and Asnani (1993).

Although changes in SSTs are slow, they affect the circulation over most of the tropical and subtropical regions. In particular, spatial and seasonal changes in global SST modulate the atmospheric circulations (from mesoscale to global scale), which in turn influence the rainfall over southern Africa (e.g. Hirst and Hastenrath, 1983; Reason, 2002). SST are thus an important indicator for monitoring drought and heavy rain conditions over southern Africa. The influence of SST varies from one sub-region to another in the southern Africa and various studies have reported that changes in sub-tropical rainfall are related to changes in the SST. For instance, Hirst and Hastenrath (1983) found a positive correlation between SST over the south east Atlantic and rainfall over Angola from March to April. Reason (2002) showed that the inter-annual variability in rainfall may be related to South Atlantic SST gradients. Therefore, it is essential for GCMs to capture the influence of SST variations on the sub-regional rainfall.

2.4 Atmospheric Global Climate Models

Atmospheric Global Circulation Models (AGCMs) like all other climate models are important tools for evaluating past and current climate to predict future climate and the implications of its changes. AGCMs use extensive mathematical calculations based on the laws of physics, but do not start from perfect representations of the weather system (either in terms of equations or observations) and so do not produce exact forecasts of the future. Indeed, even the smallest of errors in an otherwise perfect model will grow over time (Lorenz, 1982; Toth and Kalnay, 1997), limiting predictability of weather to about 10-14 days.

While GCMs remain important tools at hand for modeling, assessing global climate and seasonal forecasting, they have a limitation in that the current resolution at which they are generally run is too coarse to resolve local scale atmospheric dynamics such as the effects of orography or the interactions of the land surface and boundary layer (McGregor, 1997). This need for local scale information gives rise to downscaling of global climate output. Downscaling can either be statistical or dynamical with each method having unique merits and demerits. Therefore, a successful downscaling from a model would depend on the ability of the model to simulate general circulation features, and any bias in simulating these features would affect the simulated seasonal climate variables at the regional scale (Wang *et al*., 2004; Giorgi and Mearns, 1999).

The seasonal forecasting approach had received less attention as a seasonal forecasting technique for southern Africa until in the last decade. Examples of the studies that considered dynamical approaches include Landman and Goddard (2002); Feddersen *et al*. (1999); Barnston *et al*. (2003); (2005); Landman and Mason (1999); Shongwe *et al*. (2006); Goddard *et al*. (2001); Goddard and Mason (2002). Specifically, Landman and Beraki (2010) used multi-model forecasting approach to assess the skill of mid-summer rainfall over southern Africa. They compared multi-model results with single model results and found that the multi-model combinations outperformed the single model forecasts.

2.4.1 Ensemble Forecasting

Single simulations (usually from Numerical Weather Predictions) give realisations that do not account for the uncertainties of the climate (Talagrand, 1999; Toth *et al*., 1998), since it only considers the mean climate instead of a probability distribution. The uncertainties are due to the chaotic character of the atmospheric flow and small initial differences in the atmosphere grow rapidly and attain large amplitude (Lorenz, 1982; Toth and Kalnay, 1997). Multiple ensembles are normally generated to capture the envelope of possible time-evolutions of the climate. The idea behind ensemble forecasting is to consider and estimate uncertainties in prediction systems. This technique was first introduced by Epstein (1969) and later used by Leith (1974) and confirmed by Toth and Kalnay (1993) to provide information of probabilistic prediction systems.

It has been shown that ensemble forecasting is one of the best methods for reducing errors associated with climate uncertainties over individual model ensemble prediction (Krishnamurti *et al*., 1999). Seasonal forecasts show greater accuracy when the ensemble prediction method is used (Palmer *et al*., 2005; Krishnamurti *et al*., 1999). The ensemble technique is suitable for producing probabilistic forecasts (Anderson and Stern, 1996; Toth *et al*., 2003), because the technique predicts events and gives information on the uncertainty of the prediction, which is only present in probabilistic forecasts. Leith (1974) and Palmer *et al*. (2004; 2005) applied ensemble technique and showed that averaging the ensemble forecasts gives a forecast of greater accuracy. In this technique, forecasts are produced by using different perturbed initial conditions of SST as input to a model. The inter-annual variation due to external forcing (signal) can be estimated by the use of several ensembles in the simulation of the climate system (Krishnamurti *et al*., 1999; Palmer *et al*., 2005). The primary source of the signal at the seasonal time scale arises from anomalous SST patterns (Barnston, 1994) as lower boundary conditions. The source of these variations and seasonal predictability is obtained from the lower boundary conditions (Charney and Shukla, 1981; Shukla, 1998) since the atmosphere cannot produce random variations that persist for months. A two-tiered climate prediction approach is used with AGCMs (e.g. Barnston *et al*., 2003; Hunt, 1997; Bengtsson *et al*., 1993), in which the boundary conditions, being the signal from the SST, are predicted first

and are then used to force the atmosphere. The atmosphere is therefore considered a slave to the prescribed boundary conditions.

Other attempts for reducing model errors are by the use of stochastic perturbations due to model physics ("stochastic physics"; Buizza *et al*., 1999; Tompkins and Berner, 2008). A more comprehensive approach by Houtekamer *et al*. (1996) used a number of different versions of the ECMWF model with different physical parametrization schemes and initial condition perturbations. All these systems find that the spread of the ensemble is still too small, indicating that the simulation of the error sources is incomplete. Some of the new approaches to ensemble forecasting, such as multi-model ensembles, are attempting to address some of this additional uncertainty.

2.4.2 Multi-model Ensemble Forecasting

The use of models ensemble in climate studies has attracted interest across a variety of fields. There have been debates in the climate community on whether model combinations really enhance the prediction skill of their composite. It is assumed that for a perfect model, all of the uncertainties reside in the initial conditions. But there is no such thing as a perfect model since there are inherent uncertainties associated with input data and physical formulation of the atmospheric models. The uncertainty associated with the model formulation is contained in the inter-annual variance from stochastic processes of the model. However, the quantification of all aspects of model uncertainty requires multi-model ensembles, ideally as a complement to the exploration of single-model uncertainties through perturbed physics ensemble and/or stochastic physics experiments. In addition, a variety of applications, not only limited to the weather and climate prediction problems, have demonstrated that combining models generally increases the skill, reliability and consistency of model forecasts. Examples include model forecasts in the sectors of public health (e.g. malaria; Thomson *et al*., 2006) and agriculture (e.g. crop yield; Cantelaube and Terres, 2005), where the combined information of several models is reported to be superior to a single-model forecast. Similarly, for weather- and climate-related applications, predictions for the ENSO and seasonal forecasts from multi-model ensembles are generally found to be better than single-model forecasts (Palmer *et al*. 2005; Barnston *et al*., 2003; Doblas-Reyes *et al*. 2005; Yoo and Kang,

2005 and Kang and Yoo, 2006). Likewise, the multi-model ensemble approach has become a standard technique to improve ensemble forecasts on the seasonal time scale.

Chapter 3

Models, data, and methods

This chapter provides a description of the models, data and methods used in the study. It begins with a concise description of the two models used followed by a brief description of the observation and reanalysis data in the study. A description is given on the main domain and the sub-domains of the study. A summary of the simulations is then provided, followed by a discussion of the format of data from the model simulations. Finally, a description of the techniques used in the core analyses is provided.

3.1 The Global Models

HadAM3 and CAM3 are the two available global climate dataset currently at the Climate Systems Analysis Group. For easy access, the study made use of these two models.

3.1.1 HadAM3

The Hadley Centre Atmospheric Model version 3 (HadAM3) is the atmosphere component of the Hadley Centre Coupled Model version 3 (HadCM3). The model was developed at the Hadley Centre for Climate Prediction and Research, UK (Gordon *et al*., 2000; Pope *et al*., 2000). The model employs spherical polar coordinates on a regular latitude-longitude grid. HadAM3 has a resolution of 3.75^{o}x2.5^{o} in latitude and longitude giving a resolution of approximately 300km (about T42 in a spectral model). The convective scheme is Mass Flux scheme (Gregory and Rowntree, 1990) with convective downdraughts (Gregory and Allen, 1991). The development and description of the HadAM3 model are documented in Gordon *et al*. (2000); Pope *et al*. (2000); Jones *et al*. (2005); Murphy *et al*. (2002). HadAM3 used a horizontal resolution 3.75^{o} x 2.5^{o} and 19 vertical levels.

3.1.2 CAM3

The National Center for Atmospheric Research (NCAR) Community Atmospheric Models version 3 (CAM3) is the fifth generation NCAR atmospheric GCM (Collins *et al*., 2004). It is the atmosphere component of the fully coupled Community Climate System Model (CCSM). There are three hydrostatic, dynamic cores in CAM3: Finite Volume (FV), Eulerian Spectral (ES) and Semi-Lagrangian Spectral (SS). For this study, we used FV dynamic core, which solves the equations for horizontal momentum, potential temperature, pressure thickness and transport of constituents (including water vapour) using a conservative flux-form of the semi-Lagrangian scheme in the horizontal (Lin and Rood, 1996), and a Lagrangian scheme with conservative remapping in the vertical. Detailed formulations of other dynamic cores are given in Collins *et al*. (2004). The physics packages in CAM3 consist of moist (precipitation) processes, cloud and radiation calculations, surface models and turbulent mixing processes. In the moist processes, CAM3 uses a plume ensemble scheme (Zhang and McFarlane, 1995) to parameterize deep-convection, a mass flux scheme (Hack, 1994) to represent shallow convection, the Sundqvist (1988) scheme for evaporation of convective precipitation as it falls toward the surface, and a prognostic condensate scheme (e.g. Rasch and Kristjansson, 1998) combined with a bulk microphysical parameterization scheme (Zhang *et al*., 2003) to represent non-convective clouds. Collins *et al*. (2004) give detailed descriptions of CAM3 physics parameterizations. CAM3 used a horizontal resolution of 2.0^{o} x 2.5^{o} and 26 vertical levels.

3.2 The observation and reanalysis data

The following available observation and reanalysis dataset were used to validate the models.

3.2.1 Climatic Research Unit (CRU)

The Climatic Research Unit (CRU) dataset (Hulme *et al*., 1998; Mitchell *et al*, 2003) at the University of East Anglia (UEA) is available as daily precipitation and temperature gridded datasets over land areas and averages for the Northern and Southern Hemispheres and the Globe. It is for a period of 1901 to 2000 and has a

resolution of 0.5 x 0.5 degree latitude/longitude grid. In this study, the period 1971-2000 was extracted. The CRU dataset is freely and readily available for download. CRU produced the original high-resolution climate grids (CRU TS 1.0; New *et al*., 2000) and an update to 1998 (CRU TS 1.1). Mitchell *et al* (2003) revised these grids and extended them to the year 2000 (CRU TS 2.0). The CRU 2.1 data-set revises and extends previous CRU data-sets. The grids have been recalculated in the version 2.1 for 1901-2002 period, following a complete revision of the underlying station databases and using an improved method.

3.2.2 Climate Prediction Center Merged Analysis of Precipitation Data

Climate Prediction Center (CPC) Merged Analysis of Precipitation (CMAP) dataset (Xie & Arkin, 1996) merges satellite and rain gauge data from a number of satellite sources and rain gauge sources. The CMAP dataset uses precipitation from Numerical Weather Prediction (NWP) models, where the NWP data is used primarily to fill in gaps at high latitudes. Details on the component datasets as well as the method used to merge these data are provided by Xie and Arkin (1996, 1997). The analyses are on a 2.5^{o} x 2.5^{o} latitude/longitude grid and ranges from 1979 to present. CMAP is used in chapter 6 as the primary rainfall dataset for diagnosing the intraseasonal climate variability (Xie and Arkin 1997.

The CMAP dataset consists of several climate rainfall products, which merge rainfall estimates from a variety of satellite and ground-based sources. The combination of data from these multiple sources provides long-term climate rainfall datasets suitable for climate studies and has over the years provided credible results (Xie & Arkin, 1996). However, there are a number of issues that affect their use for some climate applications. These include discontinuities in the component datasets, differences in the calibration methods, and the methodology used to weight the individual rain estimates (Xie & Arkin, 1996).

3.2.3 National Centers for Environmental Prediction reanalysis 1 Data

The National Centers for Environmental Prediction/National Center for Atmospheric Research (NCEP/NCAR) reanalysis dataset (Kalnay *et al*. 1996) of the Climate Diagnostics Center (CDC) of the National Oceanic and Atmospheric Administration (NOAA) uses a state-of-the-art analysis/forecast system to perform data assimilation using past data from 1948 to the present. The dataset is available as 4 times daily

format and as daily averages. The data is available also in monthly means with a resolution of 2.0^{o} x 2.0^{o} latitude-longitude grid and has 17 pressure and 28 sigma levels. The NCEP data was used to validate the model for the circulation systems. These are used in the seasonal and inter-annual analyses in terms of monthly mean from 1971 to 2000. The meteorological fields utilized at seasonal time scale are precipitable water, zonal (U) and meridional (V) components of the wind (ms^{-1}), mean sea level pressure (hPa), geopotential height (m) and air temperature (K).

NCEP reanalysis data have been used by many researchers and their qualities have been documented (WMO/D-NO.876, 1997). For example, Cavalcanti *et al.* (1998) studied years of contrasting characteristics using NCEP reanalysis data. Their analysis was based on anomaly fields of precipitation, zonal and meridional components of the wind at 200 hPa, outgoing longwave radiation and specific humidity. Moisture divergence and transport were calculated in the layer 1000 hPa to 300hPa. They analysed four periods of summer and autumn seasons of the dry years 1983 and 1993 in the Northeast Region of Brazil and wet years 1984 and 1994. They observed that results of circulation patterns during these opposite cases were consistent in terms of precipitation observed over Brazil. The differences in atmospheric variables between dry and wet periods defined clearly the characteristics of the atmosphere. Mo *et al.* (1998) also used NCEP reanalysis data and forecasts to examine the atmospheric circulations associated with California rainfall anomalies. They used global gridded analysis of OLR from NCEP covering the period 1973-1995. Their results showed that the six hour precipitation forecasts are able to capture signals associated with inter-annual variability.

In the report from the first World Climate Research Programme (WCRP) international conference on reanalysis that was held at NOAA, USA, NCEP reanalysis data are of high quality and undertaken with fixed state-of-the-art data assimilation/analysis methods to provide multi-year global datasets for a range of investigations of many aspects of climate, particularly inter-annual variability and for model validation and predictability studies. The large spurious effects present in operational analyses arising from changes in assimilation systems are absent from these datasets which thus provide a more homogeneous time series for precipitation,

diabatic heating, surface fluxes and other components of the hydrological cycle (WWO/TD-NO. 876, 1997).

However, one problem with the NCEP reanalysis is the assimilation of surface data over Africa. Evidently, to reduce artificial boundary layers in the model observed fields, only station pressure data are incorporated. Wind, temperature, rainfall and other valuable inputs are ignored. Upper air radiosonde, aircraft and satellite data are incorporated; but the radiosonde network is very sparse over Africa. Hence further model improvements could bring a greater degree of realism to the reanalysis fields.

3.2.4 Reynold's Sea surface temperatures (SSTs)

Reynold's Sea surface temperature (SST; Reynold, 1988), developed by Richard Reynolds from the National Climate Data Center was used in the study. This SST was used to force the GCMs for the simulations and is available at the monthly time scale on a 1° x 1° regular grid and for 1971–2000. Bias correction of all input data to the analysis procedure is critical to obtaining a valid output (see for example Reynolds *et al*, 2002). This is readily available in Reynold's SST and makes it more suitable to be used for this study. Moreover at the present time, the only SST fields available for investigation of SST perturbations of surface winds at latitudes higher than 38S are the Reynolds SST analyses produced by NOAA (Reynolds and Smith 1994).

3.3 Simulations and Techniques

3.3.1 Simulations and SST perturbation

Both HadAM3 and CAM3 were used to produce 30-year (1971-2000) climate simulations. A five member ensemble was integrated forward with observed daily Reynold's SST. The ensemble members were produced from perturbing the initial conditions of the SSTs as input to the models for each ensemble run. Statistical averages of these ensemble members' estimation of the features were used in the analyses. Ensemble forecasting is one of the best methods for reducing errors associated with climate uncertainties over individual model ensemble prediction. The more the ensemble members used, the better the results. Five members are used

for the study due to our limited computing resources. In the simulations, each model used its default resolution; CAM3 used a horizontal resolution of 2.0^{o} x 2.5^{o} and 26 vertical levels; HadAM3 used a horizontal resolution 3.75^{o} x 2.5^{o} and 19 vertical levels. For better comparison of the models with the NCAR/NCEP reanalysis data reanalysis data, the model results were interpolated to the resolution of the NCEP (i.e. 2.5^{o} x 2.5^{o}).

Dynamical ensemble seasonal forecasting done in the study required a set of consistent, but different initial conditions for the atmosphere and ocean components of the coupled model. Simulations are carried out starting with each of these initial conditions leading to an ensemble of forecasts. The initial conditions are consistent in the sense that they are designed to represent the inherent uncertainties the operational analyses. A set of initial conditions is created by adding small perturbations to an initial best-guess unperturbed state. For the atmosphere, these perturbations are calculated using the singular vector method, which computes the modes of the fastest energy growth during the first two days of the forecasts. The ensemble of initial conditions for ocean model forecasts is created by adding small perturbations to the SST.

CMAP was used in Chapter 6 for the forecast assessment. For the forecasts, each model is integrated forward with observed (Reynolds) SSTs. This ensures that aspects of the model (e.g. soil moisture and temperature) are in equilibrium with the model precipitation as forced by historical SSTs. The 10 model restart dumps at the end of this period are then used to start the 10 member ensemble forecast which is integrated for 3 months into the future using persisted SST anomalies. Persisted SSTs are generated by modifying the long term monthly average SST field by the latest observed month SST. For example, a forecast in December, January and February is made in November. The SST fields are generated for the months of November, December, January and February by modifying each month's long term 40 year average by the latest observed SST field, in this example, October. The model is then given these fields and the forecast is produced. Persisted SSTs prediction are generally considered to constitute a good prediction of SST in the first 3-month season (Latif *et al*. 1994, 1998; Stockdale *et al*. 1998; Goddard *et al*. 2001).

3.3.2 Techniques

For the model validation of rainfall in Chapter 4 and 5 of the study, CRU and NCEP were used for comparisons. The simulated winds are validated with NCEP, while the precipitation field is validated with data from CRU and NCEP. To validate the ability of the models in simulating mid-latitude waves, spectral analysis was used to filter the zonal wave numbers 1 and 3 from 500mb geopotential height in the models and NCEP reanalysis. The fortran algorithm used in filtering the zonal waves calculated the correlation coefficient to determine the similarity between multiple waves and spectral density function. The spectral density function transforms the random transform to the wavelength of vertical wave profiling separation and de-noising filter. In the de-noising filter, a spectral estimate with more than 2 degrees of freedom at each Fourier frequency, results in spectral estimators with reduced variance.

The procedure of Self-Organizing Maps (SOMs) and its application to synoptic climatology have been described in detail by Hewitson and Crane (2002). Other applications include extreme events (Cavazos, 1999; 2000), GCM evaluation (e.g. Tennant, 2003) and season definition and classification (Tennant and Hewitson, 2002). Essentially SOMs seek to place an arbitrary number of nodes within the data space such that the distribution of nodes is a representation of the multi-dimensional distribution function, when the nodes become more closely spaced in regions of high data densities (Hewitson and Crane, 2002). We describe the process as a nonlinear projection of the probability density function of multi-dimensional input data onto a two-dimensional array of nodes (SOM map), effectively as a mapping of high dimensionality onto a low dimensionality. The SOM technique is different from other cluster techniques in that representative points (nodes) are identified effectively and span the data space, as opposed to grouping data points. In addition, the SOM offers a powerful means of visualizing the continuum of data space, whereby the reference vectors of the two-dimensional array of nodes may be used to display a continuum of states spanning the range of data space. In this work, SOMs is used to study the climatology of rainfall and to identify Tropical Temperate Troughs (TTTs) over southern Africa. Daily rainfall distribution over southern Africa is classified into SOMs. Association of data points with a SOM node, is accomplished in a postprocessing phase after archetype points within the data space

have been identified. Once the SOM map has been developed, each input data sample is assigned to a best-matching node in the map. This mapping of data points to the SOM nodes allows the calculation of frequencies of each archetype, and which may in turn be displayed as a two-dimensional histogram across the array of states represented by each node. The frequencies show the percentage of data space contributing to a particular pattern in rainfall. The SOM mapping depicts the pattern of TTTs and shows how the nodes relate to each other in data space. TTTs are indicated with high rainfall pattern from the equator diagonally, along the central to the eastern part of southern Africa. The SOMs array of size 5x3 dimensions with a rectangular lattice were initially trained on NCEP reanalysis daily rainfall from 1971 to 2000. The number of SOM nodes was arbitrary chosen to represent the daily circulation over a year. The frequency of each day in the input data to a particular node is mapped in a two-dimensional plane across the 15 nodes (five rows and three columns) of the SOM. Fifthteen nodes were chosen to reduce the dimensionality of the data to a fair degree while still allowing a reasonable number of TTT features to remain. Using the frequency distribution of NCEP "observed" rainfall, the models simulation at the daily time frame are evaluated by how closely they match the observed frequencies. The frequency of association between the models rainfall and SOM nodes are determined in the same way (as the array trained on NCEP) is assigned to the closest matching node in the SOM and termed the standard frequency, which is expressed in percentages. The size of the data space represented by each node, or the variance of TTT formation related to each node, is evaluated by determining the frequency error with which the sample values map to a given node.

For the inter-annual variability of rainfall, the anomalies were obtained with respect to the long-term mean of models, reanalysis and CRU. The anomalies are calculated from the 30-year mean and are expressed in percentage of the mean. For examining the global teleconnection patterns, correlations between the models rainfall were computed and compared with the CRU and NCEP data for four climatic sub-regions over southern Africa.

R (R Development Core Team (2008)) verification package (Pocernich, 2009) was used for forecast evaluation. In the forecast evaluation of the El Niño and La Niña years, CMAP dataset were used for the comparisons. Various verification measures

including the Relative Operative Characteristics (ROC; Jolliffe and Stephenson, 2003) curve, Brier Score (BS; Brier, 1950; Murphy, 1973, 1993; Ferro, 2007), and Ranked Probability Score (RPS; Wilks, 2006), were used for accessing the models.

Forecast verification compares the forecast against a corresponding observation (Jolliffe and Stephenson, 2003). Forecast skill is evaluated in different verification methodologies and a judgment of skill can be dependent on the particular technique employed. Stanski *et al*. (1989) reviewed six attributes of a forecast that make up the total quality. The attributes are reliability, accuracy, skill, resolution, sharpness, and uncertainty. They also made an important point that no single verification measure provides complete information about the quality of a product. In this study, a number of verification measures have been employed to measure forecast accuracy. The measures employed in the study require the forecasts to be probabilistic. It is given in terms of a probability that a considered event would occur (Mason *et al*., 1999). These probability forecasts provide a set of contingency tables (Jolliffe and Stephenson, 2003), one for each probability interval of rainfall exceeding a given threshold; being lower quartile, upper quartile or the mean (the mean is used in the study). The contingency tables indicate the quality of a forecast system by considering its ability to anticipate correctly the occurrence or non-occurrence of predefined events that are expressed in binary terms. For example, rainfall occurrence can be represented on a binary scale by defining the event if rainfall occurred and a nonevent if rainfall did not occur. The occurance or non occurance of events create a set of possible points for plotting a graph of hit/false alarm rate or true positive/false positive rate called the ROC curve (Figure 3.1).

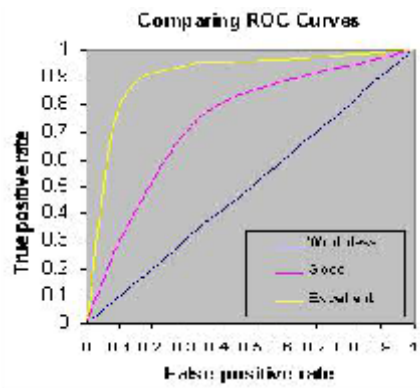

Figure 3.1*: The ROC curve, Perfect: Curve travels from bottom left to top left of diagram, then across to top right of diagram. Diagonal line indicates no skill.*

The area under the ROC curve shown in figure 3.1, describes the accuracy of a forecast (Jolliffe and Stephenson, 2003). When the area equals 1, it signifies a perfect probabilistic forecast system with 100% alarm hit rate and no false alarm rate. ROC scores are used in the study to measure the ability of the forecast to discriminate between two alternative outcomes. The area under the ROC curve is not strictly an estimate of forecast skill but is a useful indicator of forecast quality (Mason *et al*., 1999). One limitation of the ROC area is that it can give a perfect score even when the forecast probability do not agree with the observed probability of an event ROC area is not sensitive to biases. Therefore over- and under-confidence are not penalized. The ROC is a first step towards estimating forecast value (Murphy, 1996; Richardson, 2000) despite these shortcomings.

The BS measures the mean squared probability error of a forecast (Brier, 1950; Murphy, 1973, 1993; Ferro, 2007) and gives its potential predictability. It is the most commonly used measure for forecast verification. The measure is negatively oriented with a lower score representing a higher accuracy; 0 reflects a perfect forecast and 1 reflects a poor forecast. The BS equation is shown in equation 3.1.

$$BS = \frac{1}{N}\sum_{t=1}^{N}(f_t - O_t)^2 \qquad (3.1)$$

where O_t represents the climatological probability of the event, N represents the number of distinct probabilities, f_t is predicted probabilities.

The RPS is expressed as:

$$RPS = \frac{1}{n-1}\sum_{n=1}^{N}[(\sum_{t=1}^{n} f_t) - (\sum_{t=1}^{n} O_t)]^2 \qquad (3.2)$$

where terms are same as defined in equation 3.1.

A RPS is a verification measure that is sensitive to the difference between the probabilities assigned to observed and forecast categories (Wilks, 2006). This measure is negatively oriented, with the best score of zero obtained for a perfect forecast system, and positive scores further away from zero are indicative of a systematically erroneous forecast system. If a high probability was assigned to a certain category and that category occurred, a high score (being 0) will be assigned.

However if the category is not observed, a penalty will be given. RPS can therefore be calculated by the square errors with respect to cumulative probabilities in the forecast and observation distribution of categories (equation 3.2; Wilks, 1995). All the verification measures used in the study are described in details in Jolliffe and Stephenson (2003); Mason *et al*. (1999); Mason and Mimmack (2002); Matheson and Winkler (1976); Mason and Mimmack (2002); Mason (2004).

In effect, a good forecast should have an RPS of 0, a BS of 0, and AUC of 1. A bad forecast is expected to have an RPS of 1, a BS of 1, and AUC of 0. The judgement of a forecast depends on how closer it is to these values.

3.4 Study domain

Previous studies over southern Africa (Engelbrecht *et al*., 2009) have shown that seasonality and interannual variability of rainfall vary greatly from one area of the region to the other, which would explain why the total rainfall over region is difficult to forecast. Based on this difficulty, the region is divided into sub-regions to capture the variations of the rainfall seasonality over different parts of the region. Engelbrecht *et al*. (2009) divided the region into 6 climatic domains; Nicholson divided the region into 10 climatic domains; However, for brevity, the thesis used four domains from Engelbretch *et al*. (2009) division.

The four sub-regions are shown in figure 3.2: 10S:0 and 7E:30E for North-Western (NW), 20S:5S and 30E:42E for North-east (NE), 34S:28S and 26E:33E for Eastern Cape (EC), and Western Cape (WC) sub-regions.

(a)

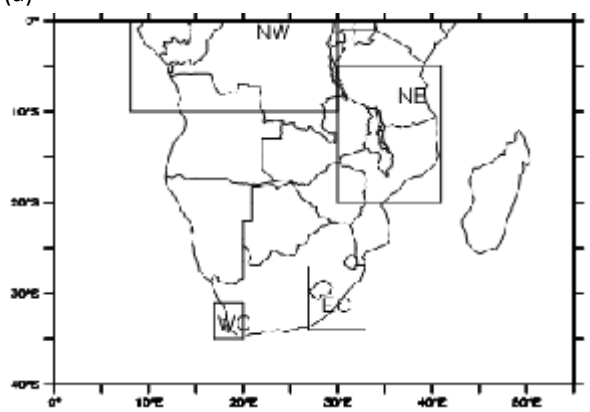

(b)

***Figure 3.2**: The southern African study domain. (a) The boxed areas show the locations of the sub-regions (NW, NE, EC, and WC) used in the study. (b) Political map showing the countries involved.*

Note that while NW and NE are in tropics, EC and WC are in mid-latitude; on the other hand, while the climate of NW and WC have a boundary with the cold Atlantic Ocean, EC and NE have a boundary with warm Indian Ocean. Hence, it is of interest to investigate how the models capture the differences in these climatic domains, in particular, the seasonality, interannual variability of rainfall and the influence of SST on the seasonal rainfall. In obtaining the average data over the domains, the data over the adjacent oceans were masked out as much as possible.

Chapter 4

Simulation of General Circulation

The purpose of this chapter is to demonstrate model representation of the southern Africa climatology. The climate of southern Africa is influenced by the mean circulation of the atmosphere. Thus, when evaluating GCMs, it is important to consider the mean circulation systems prevailing over the region. This chapter evaluates how CAM3 and HadAM3 simulate the important circulation features over southern Africa. The evaluation would help in identifying the strength and weakness of each GCM.

Section 4.1 presents and discusses the models representation of temperature and rainfall climatology in comparison with NCEP reanalysis data, while section 4.2 discusses how the models represent the important controls of rainfall over southern Africa. A model gives a good representation of the climate if it is able to show the essential patterns shown by the observation or reanalysis data. Section 4.3 focuses on why the models show such results after summarising the significant findings of how they represent the climatology of southern Africa.

4.1 African Climate Features

In order to evaluate individual model skill in simulating relevant features of southern African climate, a study of the rainfall and temperature over the continent is conducted prior to assessing the synoptic circulation over southern Africa. The following sections focus on how well the models reproduce the observed climatology of temperature and rainfall.

4.1.1 Temperature climatology

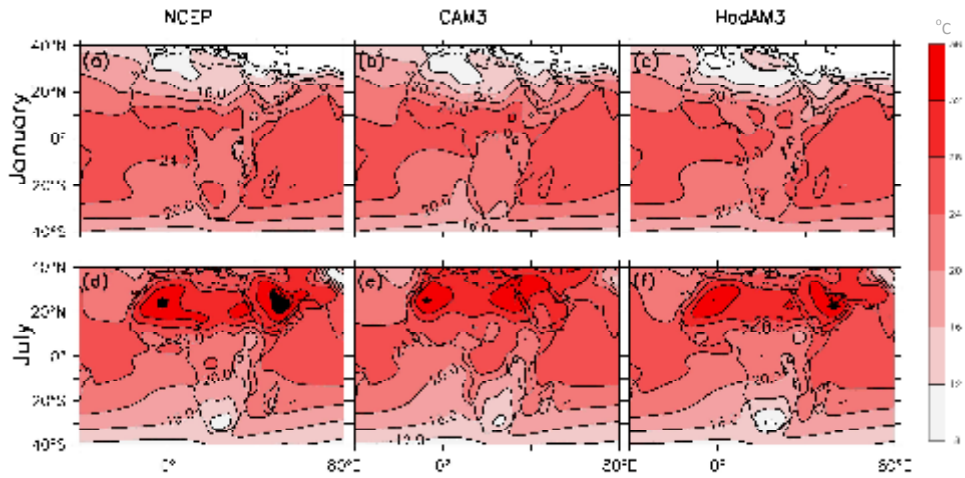

***Figure 4.1**: Comparison of observed and simulated surface temperature (^{O}C) over Africa in January (upper panels) and in July (lower panels) from NCEP reanalysis (left panels), CAM3 (middle panels), and HadAM3 (right panels).*

In figure 4.1, both GCMs capture the essential features in temperature field over Africa in summer (January) and winter (July), but with some biases, presented with the difference between models and NCEP in figure 4.2. In January, three maximum and two minimum centers for temperatures are evident in NCEP (Figure 4.1a). The maxima are located over the West African coast (26^{o}C), Sudan (24^{o}C), and Namibia (26^{o}C), and the minima over Algeria (8^{o}C) and Uganda (22^{o}C).

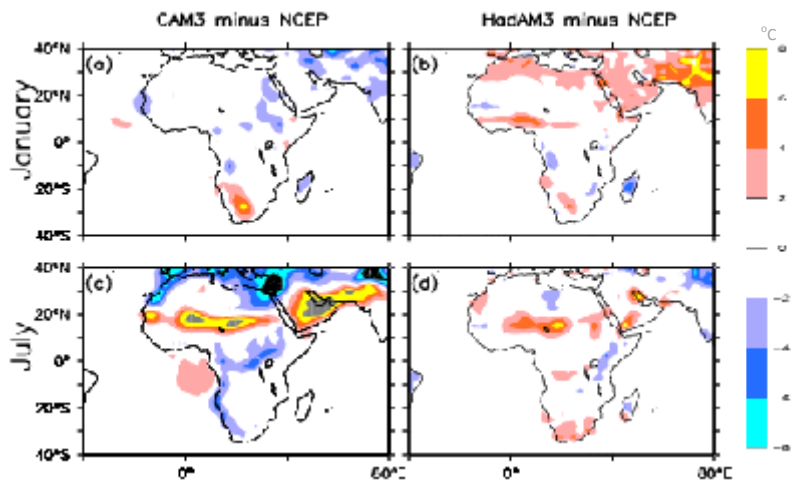

***Figure 4.2**: Differences in temperature (^{O}C) over Africa in January (upper panels) and in July (lower panels) from CAM3 minus NCEP (left panels) and HadAM3 minus NCEP (right panels). Biases above 8 (^{O}C) are shaded in grey and below -8 (^{O}C) are shaded in black.*

The models adequately simulate the locations and magnitudes of these centers, but underestimate the Uganda minimum by 2°C. Additionally, CAM3 (Figure 4.1b) cannot reproduce the Namibian maximum, while HadAM3 (Figure 4.1c) underestimates it by 2°C. However, both models correctly reproduce the Sahelian temperature gradient. In July, the models replicate the location of maximum temperatures (over Sahara, Saudi Arabia, and Congo), the complex terrain-induced minimum temperature (over South Africa), and trough (along the eastern half of southern Africa).

Nevertheless, the simulated maximum temperatures in both models are 2°C lower than that of the NCEP reanalysis. The values of minimum temperature, temperature trough, and Sahel temperature gradient in CAM3 are also too high, when compared with the reanalysis, while the values of minimum temperature and temperature trough in HadAM3 are too low.

4.1.2 Rainfall climatology

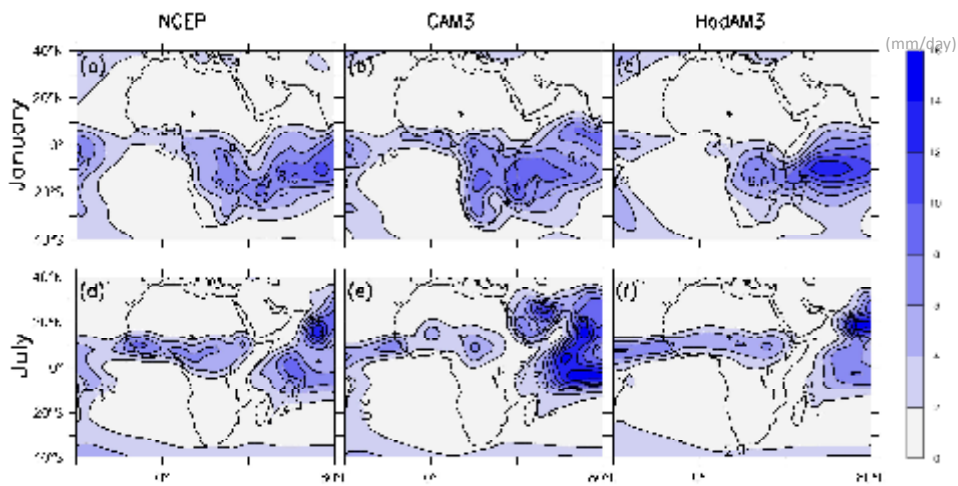

Figure 4.3*: Comparison of observed and simulated mean rainfall (mm/day) over Africa in January (upper panels) and in July (lower panels) from NCEP reanalysis (left panels), CAM3 (middle panels), and HadAM3 (right panels).*

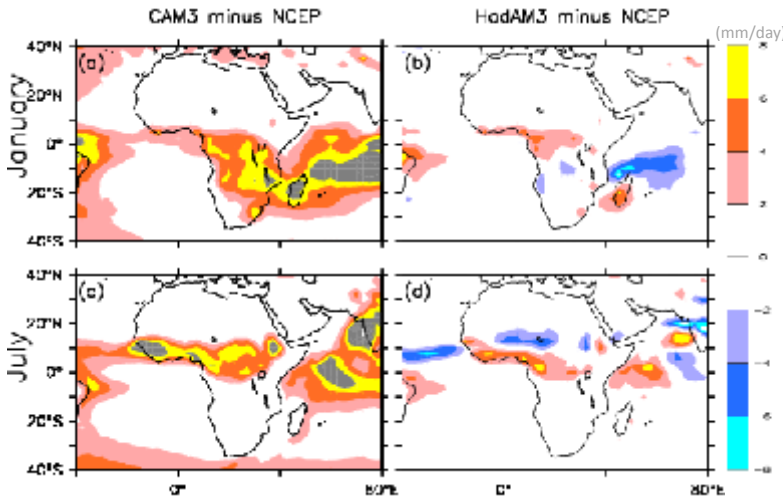

***Figure 4.4**: Differences in rainfall (mm/day) over Africa in January (upper panels) and in July (lower panels) from CAM3 minus NCEP (left panels) and HadAM3 minus NCEP (right panels). Biases above 8 mm/day are shaded in grey.*

Figure 4.3 shows rainfall distribution over Africa for both austral summer and winter seasons. At the peak of the summer season, rainfall is concentrated over the southern part of the continent. Observed rainfall maxima are located along the ITCZ, the Zaire air boundary. In July, rainfall band migrates towards the northern hemisphere in accordance to the displacement of the ITCZ leaving the south sub-continent dry. In this season, maxima are located over the complex terrian of west and east Africa (e.g. Guinea highlands, Cameroon mountains and Ethiopian highlands). Note that NCEP exhibits northward and southward gradient in the northern and southern flank of the ITCZ respectively for both seasons. Both models capture the prominent features in the rainfall distribution, including the zone of maximum and minimum rainfall as well as the northward and southward gradients found in NCEP. However, there are some disagreements (see figure 4.4) between the simulated and observed rainfall patterns. For example, in January, CAM3 displaces the zone of maximum rainfall along the dry western half of southern Africa. In addition, CAM3 significantly overestimates the magnitude of rainfall along the ITCZ in July, whereas HadAM3 captures it pretty well but misses the centers of maxima over the complex terrains probably as an artifact of resolution.

Overall the models are able to simulate well the main features in the spatial distribution of temperature and rainfall although some biases exist in the magnitude and location of maxima (mostly in CAM3). Comparing the two models, it is thus evident that they have different dynamics in defining rainfall over the region, which should reflect in the circulation patterns.

4.2 Synoptic Circulations

Having examined the temperature and rainfall climatologies and in an effort to understand the differences between observation and simulations, we here analyse and intercompare some of the relevant circulation features, including mean sea level pressure and wind fields over Africa, and circumpolar waves, subtropical jet and TTTs over southern Africa.

4.2.1 Climatology of pressure and wind fields

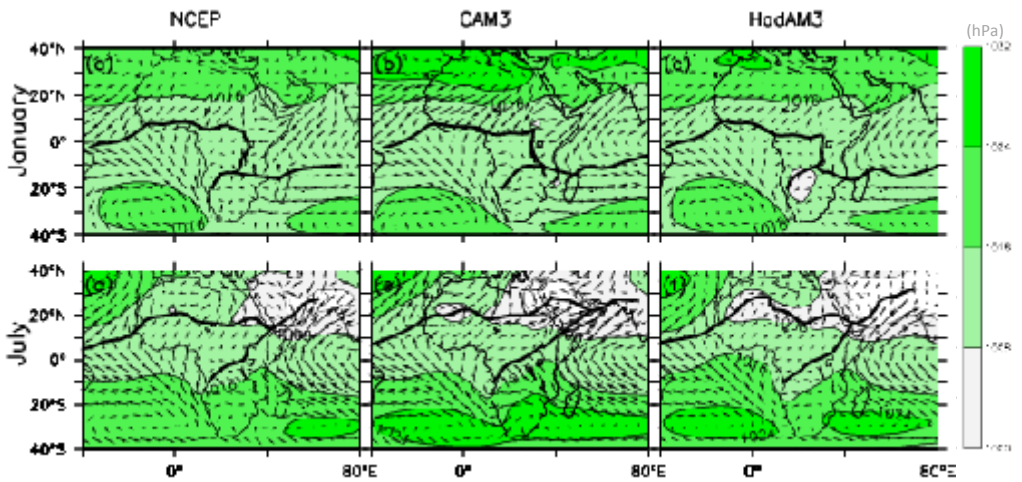

Figure 4.5*: Comparison of observed and simulated mean sea level pressure distribution (shaded) with wind flow (vectors) over Africa in January (upper panels) and in July (lower panels), from NCEP reanalysis (left panels), CAM3 (middle panels), and HadAM3 (right panels). In each panel, the arrows show the winds; the lengths of the arrows indicate the wind strengths.*

In the pressure fields (Figure 4.5), the models capture the locations of the anticyclones very well, although the simulated maximum pressure (especially in CAM3) is about 4mb higher than observed in January and July. The locations of

ITCZ in both seasons are also fairly well simulated over southern Africa. They show that the two trade wind systems converge at the low pressure zones. However, CAM3 pushes the ITCZ a bit far to northeast over Saudi Arabia because the south-westerly is too strong over the area, while HadAM3 pushes it to far north over Mali, because northeasterlies are weaker over the area.

In addition, the effect of temperature on mean sea level pressure distribution is distinct in the models. Both models show that high pressure weakens over the continent in winter but are thermally intensified in summer over the continent. This winter-summer processes is more pronounced at the north and south ends of the continent. However, these circulation are not able to fully explain the biases in rainfall distribution over southern Africa in the models, therefore other synoptic features over the region should be important.

4.2.2 Waves over southern Africa

Since semi-stationary waves are dominant features of the mean southern-hemisphere circulations, it is necessary to know how the GCMs simulate the location and amplitude of wave 1 and wave 3, which strongly influence the southern Africa weather and climate (e.g. Mason and Jury , 1997; Tyson *et al*., 1997). The waves are obtained from the 500mb geopotential height using spectral analysis as explained in section 3.3.2.

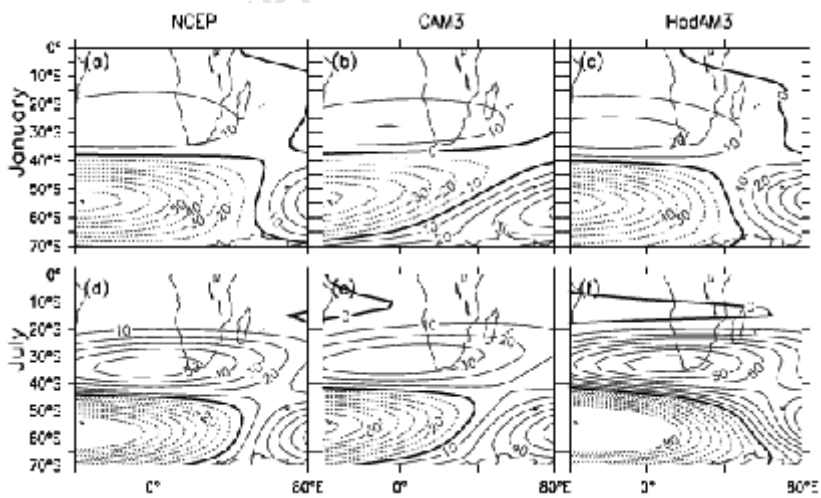

Figure 4.6*: Comparison of observed and simulated Wave 1 over southern Africa: for January (upper panels) and July (lower panels), from NCEP reanalysis (left panels), CAM3 (middle panels), and HadAM3 (right panels).*

NCEP reanalysis exhibits a sub-tropical ridge north of 40°S and trough south of it extended towards the high latitudes in both seasons. The magnitude of these features are more developed in July than in January (Figure 4.6). The models correctly capture the location of ridges and troughs as well as the differences in the magnitudes of the seasons. However, the amplitudes of the wave are generally lower in CAM3 simulation and larger in HadAM3 indicating more subsidence in the latter over the sub-continent, consistent with the rainfall pattern.

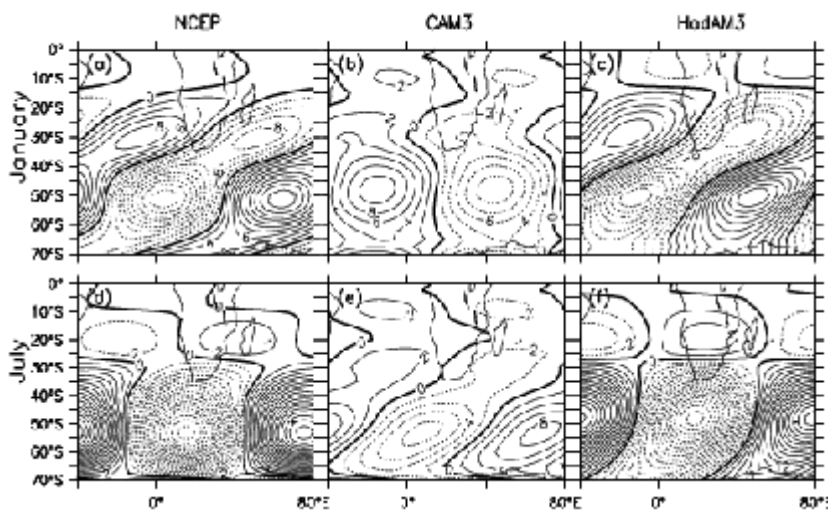

Figure 4.7*: Same as Figure 4.6 but for Wave 3.*

Another circumpolar semi-stationary disturbance is Wave 3, which responds to semi-annual oscillation in the southern hemispheric pressure, therefore, the longitudinal position of its peak varies seasonally (Tyson and Preston-Whyte, 2000). In January, CAM3 fails to capture the location and orientation of the most prominent troughs and ridges, which have south-west to north-east orientation in the NCEP reanalysis, whereas HadAM3 reproduce these features very well in location, orientation and magnitude. Similarly in July, HadAM3 simulates more realistic wave pattern as shown in the NCEP (Figure 4.7). Correct simulation of the wave is critical because it influences substantially the location of blocking anticyclones (Tyson, 1981), consistent with the simulated pressure field. Therefore, comparing this wave pattern to that of rainfall distribution, it is logical that the trough simulated by CAM3 over

the southern most part of the sub-continent along with the weak accompanying ridge might have contributed to the large overestimate of rainfall at the western half of the region.

4.2.3 The subtropical jet

Figure (4.8) shows the cross section of observed and simulated zonal wind fields over southern Africa. The most prominent feature in the fields is the subtropical easterly jets, which both GCMs simulated well (Figure 4.8), although the models overestimate the strength of the jet by 5 m/s.

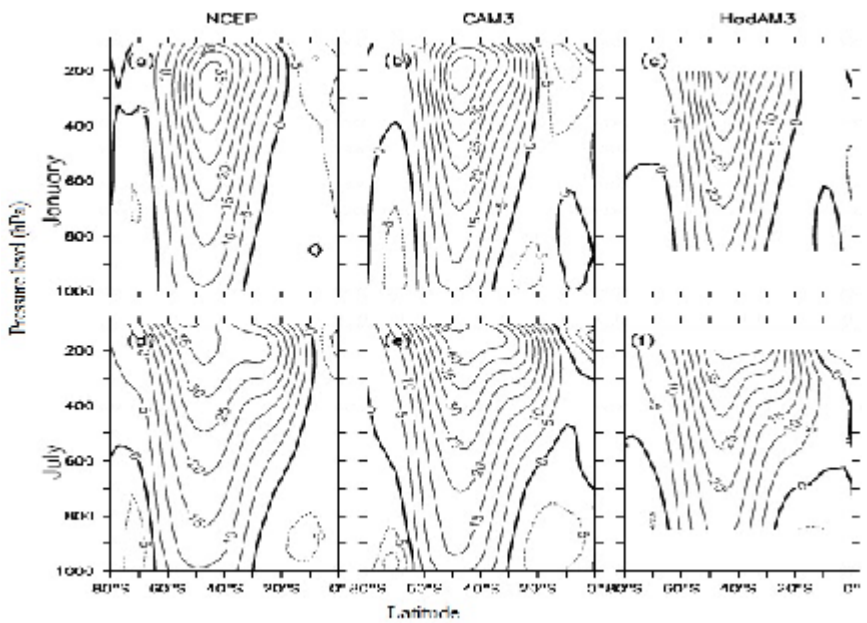

Figure 4.8*: The vertical structure of zonal wind measures in m/s, average between 20W and 60E. For January (upper panels) and in July (lower panels), from NCEP reanalysis (left panels), CAM3 (middle panels), and HadAM3 (right panels).*

The observed and simulated jets shift from 200mb in January to 100mb in July. This shift is accompanied by the strengthening and southwards displacement of its core away from the sub-continent, implying less (more) sinks of water vapor in January (July) over the region. Comparing the two models, although they simulate the position of the core around the same latitude, the magnitude is much larger in CAM3 indicating more moisture transport (Thorncroft and Flocas, 1997; Uccellini and Johnson, 1979; Nakamura and Shimpo, 2004; Roca *et al*., 2005). Other important

features which the models also capture well are the low-level and upper-level easterlies, although this is not well depicted in HadAM3. However, in January, CAM3 simulates stronger easterlies than observed.

4.2.4 Tropical Temperate Troughs

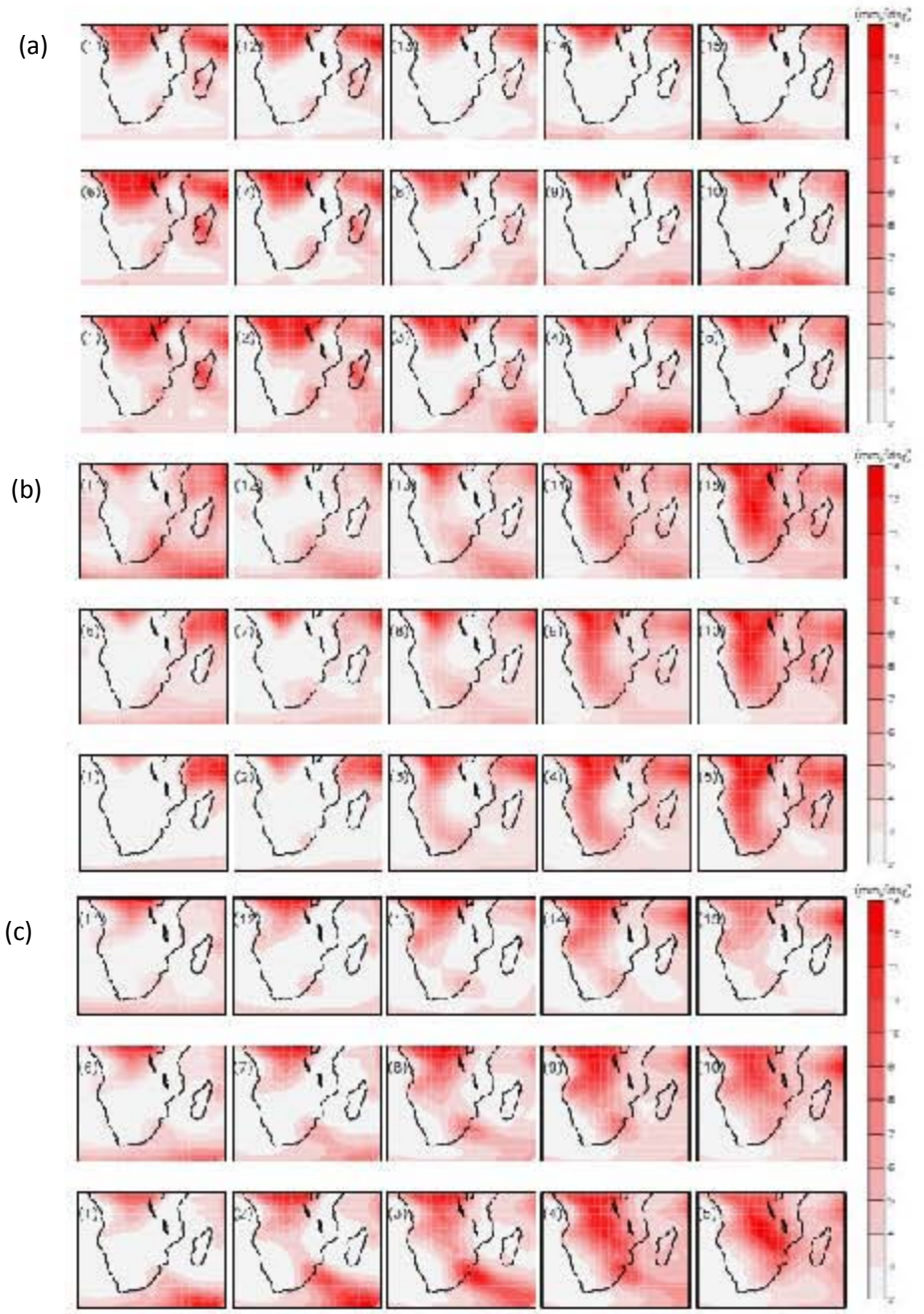

***Figure 4.9**: SOMs composite (1971-2000) of SON rainfall showing TTT formation at each of the 15 nodes for (a) NCEP reanalysis (b) CAM3 and (c) HadAM3.*

In this sub-section, we investigate how well CAM3 and HadAM3 simulate TTTs over southern Africa using a group of 5x3 node SOMs. SOMs technique (explained in section 3.3.2) is used to characterised TTTs over southern Africa. The presentation of the SOMs from daily rainfall for the summer seasons shows how alike the pattern is to the node and the percentage of contribution to the TTTs pattern.

In figure 4.9, September-October-November (SON) rainfall pattern exhibits potential TTT patterns in all nodes at south east across the eastern half of southern Africa except nodes 13 to 15 in NCEP (Figure 4.9a). This pattern is expected since SON is a transition season from the winter to the summer season. A study by Washington and Todd (1999) confirmed the orientation of TTT from north-west to south-east across the eastern half of tropical southern Africa in November. The SOMs process show a pattern of a continuous high rainfall accumulation along the equator. Such pattern can be seen in all the 15 nodes. It is clear that there are two particular type of circulation, located in the left-hand side of the SOMs; one with the rainfall pattern over Madagascar and the other along the Eastern Cape. All the nodes show some dryness over most part of the region. In the case of the models, the dominant circulation pattern is represented in all 15 nodes except in nodes 1 and 2 for CAM3. CAM3 (Figure 4.9b) exhibits the TTTs only at nodes 11-15 of the SOMs. The patterns in nodes 3-5 and 8-10 indicate west coast troughs because of the dryness it simulates at the eastern part of the region. Further explanation can be found in Tyson (1986). HadAM3 (Figure 4.9c) shows the continuous diagonal rainfall accumulation (TTTs) within all the 15 nodes more prominently except in nodes 11 and 12.

(a)

NCEP					CAM3					HadAM3				
8.8	6.5	8.2	8	8.1	12.2	3.6	7.7	14.3	9.3	4.7	1.6	2.2	6.6	10.4
5.2	8.3	4.9	5.9	4.6	4.6	2.6	1.8	11.9	3.3	2.2	4.4	6.7	19.7	5.7
9.5	4.6	6.1	4.7	6	13.6	1.4	3.2	4.5	5.4	9.8	6.3	7.7	6.3	5

(b)

NCEP					CAM3					HadAM3				
50.2	40.4	35.7	33.6	38.4	87.5	65.7	58.4	43.2	43.3	79.9	55.7	45.7	33.6	35.1
51.7	44.5	41	35.4	46.1	79.6	65.8	54	44.6	52.5	76.3	54.9	44.7	36.2	42.7
58.9	52.2	60.2	53.9	64	84.3	79.4	76.5	67.3	75.3	92.2	67.1	67	57.9	63.6

Figure 4.10: *(a) Standard frequency (%) and (b) associated errors (%) of SOM for each node from NCEP reanalysis, CAM3, and HadAM3 SON TTT formation. In (a) The dark shaded squares (high) are nodes above 10%, grey shaded squares (moderate) are nodes between 6 and 10% and non-shaded squares (less) are nodes less than 6%. In (b) the shaded squares have errors below 60%.*

Figure 4.10 shows the standard frequency (a) and associated errors (b) of TTT formation mapped to each node over the 30 year SON rainfall. Each shaded square in figure 4.10 represents 1 node in the SOM array, while the numbers are the percentage frequency (Figure 4.10a) or frequency error (Figure 4.10b) of occurrence. The figure indicates that frequencies are distributed fairly evenly over the nodes but with some errors. From NCEP, the standard frequency shows moderate modes of TTT pattern in most nodes with errors below 60% in all nodes except two nodes of errors of 60.2 and 64%. TTT is dominated by six nodes in CAM3. Out of these nodes, four are highly dominating (dark shaded) with TTT pattern and two are moderately dominating with TTT pattern. Two of the high modes are associated with frequency errors above 60% and the other two with below 60% frequency errors. The moderate modes have frequency errors below 60%. Frequency errors above 60% are concentrated over the bottom and left side on nine nodes of the map. Similarly in HadAM3, the frequency errors above 60% are concentrated over the bottom and left side but on seven nodes of the map. The highest mode of TTT formation from HadAM3 with 19.7% standard frequency has a frequency error of 36.2% associated with it. A moderate mode of 9.8% has the highest frequency error of 92.2%. However, the least dominating mode of TTT at a frequency of 1.6% has an error of 55.7% associated with it. Both models follow fairly well the variation across the nodes in the NCEP but have higher frequency errors for either the high or moderate modes of TTTs. In general, for all the frequency modes, error in the models may trace their sources to their limitations in simulating rainfall as explained in the earlier sections.

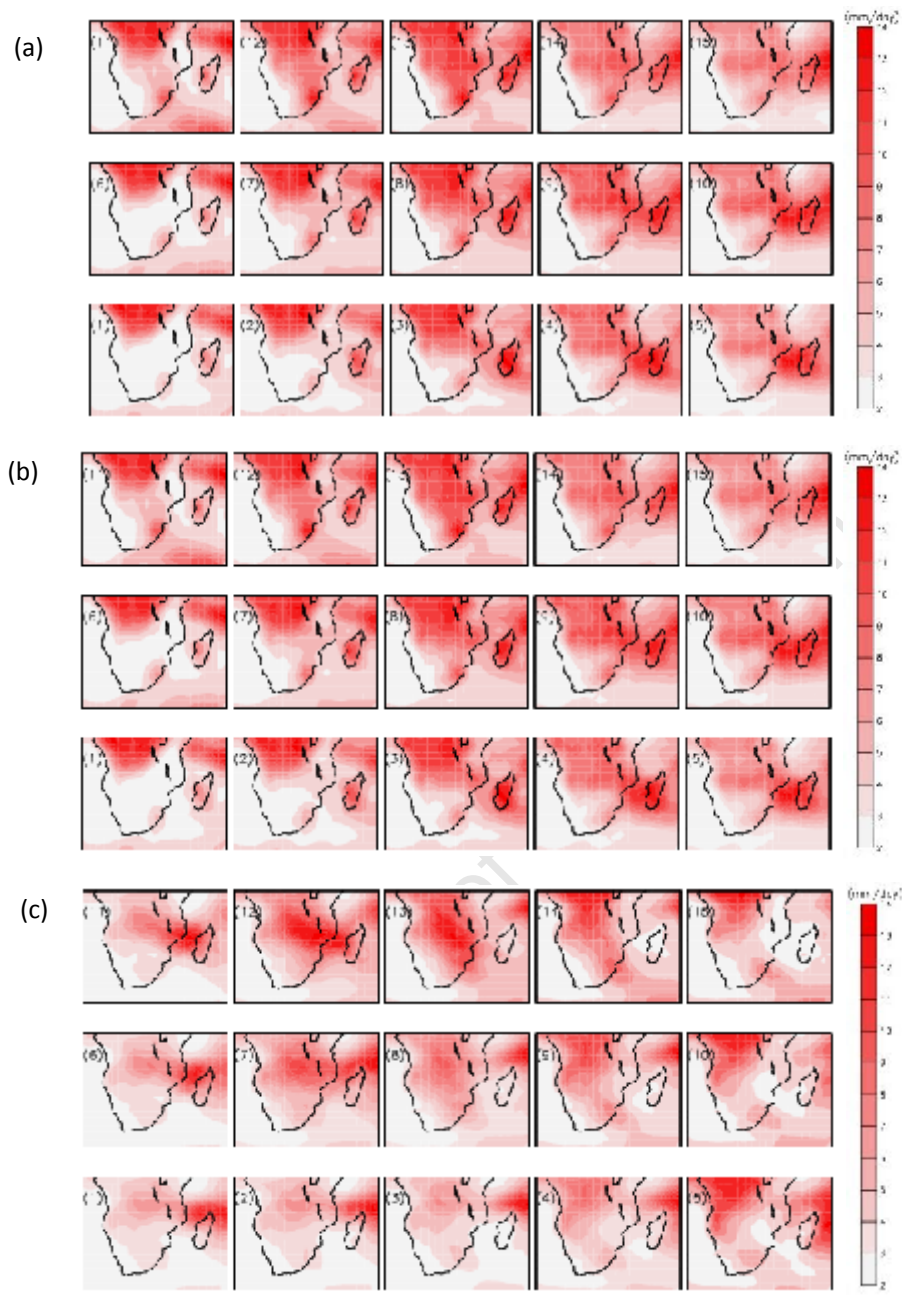

Figure 4.11*: Same as Figure 4.9 but for DJF.*

TTT patterns shown for December-January-February (DJF; Figure 4.11) are clearly defined as the feature matures in summer season (van den Heever *et al.,* 1997; Washington and Todd, 1999). In figure 4.11, NCEP show strong and more clearer TTTs in nodes 11, 12 and 13. Other nodes except node 1 and 2 only show moderate

to weak formation of TTTs. The models equally show clearer formation of TTT in this season.

It can been seen from the percentage frequency (Figure 4.12a) that the TTT pattern is formed in most of the nodes with node 1 most dominating with 12.4% in the NCEP data space. The least represented pattern in NCEP is node 10 with 4.6%. CAM3 present small number of nodes of TTT pattern but also shows it most dominating TTT pattern in node 1 with 24.5% depicting overestimation of rainfall. In HadAM3, TTT pattern is formed in most of the nodes.

(a)

NCEP					CAM3					HadAM3				
5.5	5.3	8	6.3	6.6	5.9	5.3	6.5	4.7	8.8	9.7	8.5	7.1	5.6	12.4
6	6	6.5	5.3	4.6	6.4	4.3	2.9	4.7	7.2	6	7.4	4.1	3.3	3.1
12.4	6.1	7.3	6	7.2	24.5	3.8	3.6	4.2	6.6	12.9	8.1	4	2.3	4.8

(b)

NCEP					CAM3					HadAM3				
69.2	67.1	63.1	65.9	70.9	83.2	82.2	84.3	89.1	99.9	74.8	78.3	87.7	95.9	114
50.5	54.3	57.6	62.6	69.7	72.9	81.6	79.8	85.3	97.8	60.7	70.6	76.6	93.7	122.7
42.4	49.9	57.9	63.9	75.5	54	67.6	78.7	84.6	102.2	46.1	57.6	79.3	97.8	123.6

Figure 4.12: *Same as Figure 4.10 but for DJF.*

In their respective frequency errors (Figure 4.12b), both models and NCEP show low frequency errors at the left side with NCEP recording more nodes of errors below 60%. Both models have errors above 60% in all nodes except 1 node for CAM3 and 2 nodes for HadAM3. Although, the models have higher errors than observed, the pattern of the mean errors is similar to that of NCEP. However, these errors are less important since most of those nodes have relatively low frequencies.

4.3 Summary

In this chapter we evaluated the performance of two global models (CAM3 and HadAM3) used for seasonal forecasts, in simulating the southern African general circulation features that control rainfall over the region. To do this, we compared the model simulations for 30 years (1971 to 2000) over southern Africa with NCEP.

The results show that both models reproduce the climate features over southern Africa but with some biases. In particular, they capture rainfall and temperature spatial distributions, the wind systems, the ITCZ location, Zaire Air Boundary (ZAB), sub-tropical jet, sub-tropical anticyclones, wave systems and TTTs. The main error in CAM3 simulated rainfall distribution is that, in summer, the maximum rainfall zone is located at the west instead of east as in the observed and HadAM3 rainfall. HadAM3 shows underestimation of rainfall over the entire domain. For both models, the errors in simulating the temperature field are within 3^{o}C. For the synoptic features, CAM3 performs well in representing the winds (speed and direction) and the location of ITCZ, while HadAM3 performs better in simulating the circumpolar waves over the region. TTTs analysis shows consistent results with regards to the simulated rainfall among the models but the high frequency errors simulated by the models in the SOMs confirms the models' limitations to reproduce rainfall at the right position and in right amount over southern Africa.

In conclusion, we explain the overestimation of rainfall over the western part of the sub-continent in CAM3 with it limitation in reproducing the proper location and magnitude of the observed trough of wave 3. The underestimation of rainfall shown in HadAM3 simulation over the region may be attributed to the simulation of weak wind flow of the model.

Chapter 5

Simulation of inter-annual variability and impacts of SST in El Niño and La Niña years

ENSO event causes extreme weather conditions such as floods, droughts and other weather disturbances in many regions of the world. In effect, a quantitative assessment of possible effects of changes in the climate with relation to the ENSO events will provide important information for managing the effects of such changes. As an initial step in estimating possible future changes caused by ENSO phenomenon from global models, it is necessary to carefully show how the models reproduce the current rainfall variability based on investigation of the atmospheric circulations, which form the main forcing factors for controlling variability during the El Niño and La Niña years.

The previous chapter considered how CAM3 and HadAM3 models reproduce the main climate circulation features. The present chapter aims to shed more light on the models capability and suitability for seasonal forecasting over southern Africa. In this part, the inter-annual variability of rainfall and the impact of SST during the summer of El Niño and La Niña years over different parts of southern Africa are investigated.

5.1 Seasonal Variability of Rainfall and Temperature

In this section, we discuss the capability of the models in reproducing the seasonal variability of annual rainfall and temperature over the four climatic regions (defined in figure 3.2) in southern Africa.

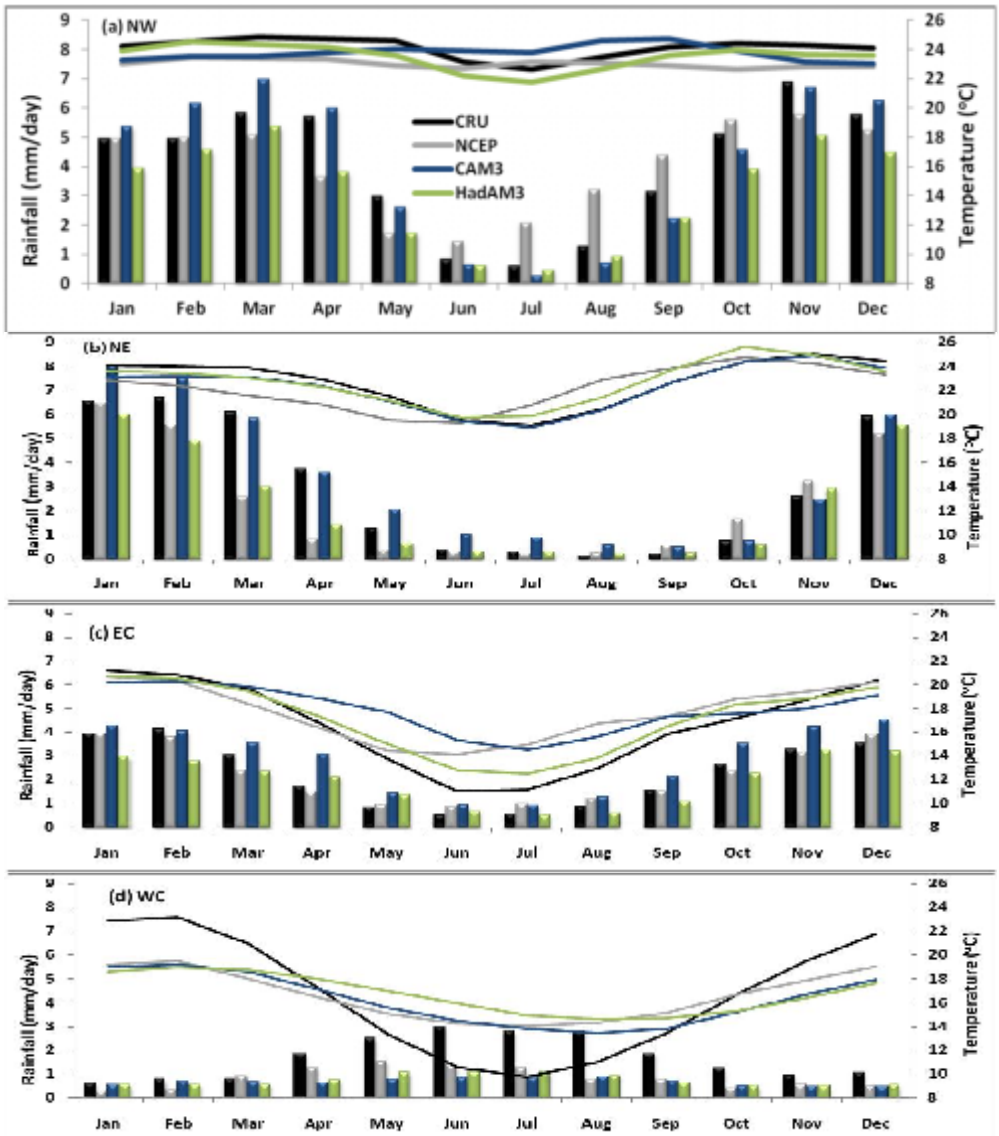

***Figure 5.1**: Monthly variation of simulated and observed mean annual rainfall (bars) and temperature (lines) over different sub-regions in southern Africa.*

Figure 5.1 compares NCEP, the simulated, and CRU monthly rainfall and temperature patterns over the sub-regions in southern Africa. The distribution of the monthly temperature differs across the four sub-regions. For instance, CRU shows

that, over NW, the maximum temperature (about 25^{o}C) occurs in February/March and peak rainfall (about 7 mm/day) in November; but over NE the maximum temperature (about 25^{o}C) is in November and the peak rainfall (about 7 mm/day) is in February. Over EC and WC, the maximum temperature (about 8^{o}C and 7^{o}C, respectively) in January/February, but the peak rainfalls (4.0 mm/day and 3.0 mm/day, respectively) are in February and June, respectively. Over NW, NE, and WC the minimum temperature occurs in July, but over EC it is in June. Both models closely reproduced the seasonal patterns of temperature and rainfall over the sub-regions, with few biases. The main bias is that the simulated minimum temperature is a month late over all the sub-regions. The maximum error in the simulated temperature is about 2.5^{o}C (Figure 5.1d) for both models. In most cases, CAM3 overestimates the monthly rainfall, while HadAM3 underestimates it, but both models correctly reproduce well the seasonal cycle.

5.2 Inter-annual variability of summer rainfall over southern Africa

Figure 5.2 compares the observed, simulated, and NCEP anomalies in the inter-annual DJF rainfall over the four sub-regions. Only the summer rainfall variability is considered here because of its large contribution on the regions' annual rainfall and its connection with synoptic circulation patterns over southern Africa. The anomalies are calculated for 30-year and are expressed in percentage of the mean.

Over the NW, the models agree with both CRU and NCEP in 1972, 1982, 1985, 1994, and 1996. In other years, the models do not agree with either CRU or NCEP. The observed rainfall over NE shows a varying trend from both NCEP and models. Models are able to capture the rainfall patterns in some years well, compared with CRU and NCEP but disagree in other years with both CRU and NCEP. Mean percentage of rainfall over EC is generally low during the summer season. Apart from 1971, where CRU rainfall over EC disagrees with the pattern from the models and reanalysis, the models agree more with CRU than with NCEP reanalysis.

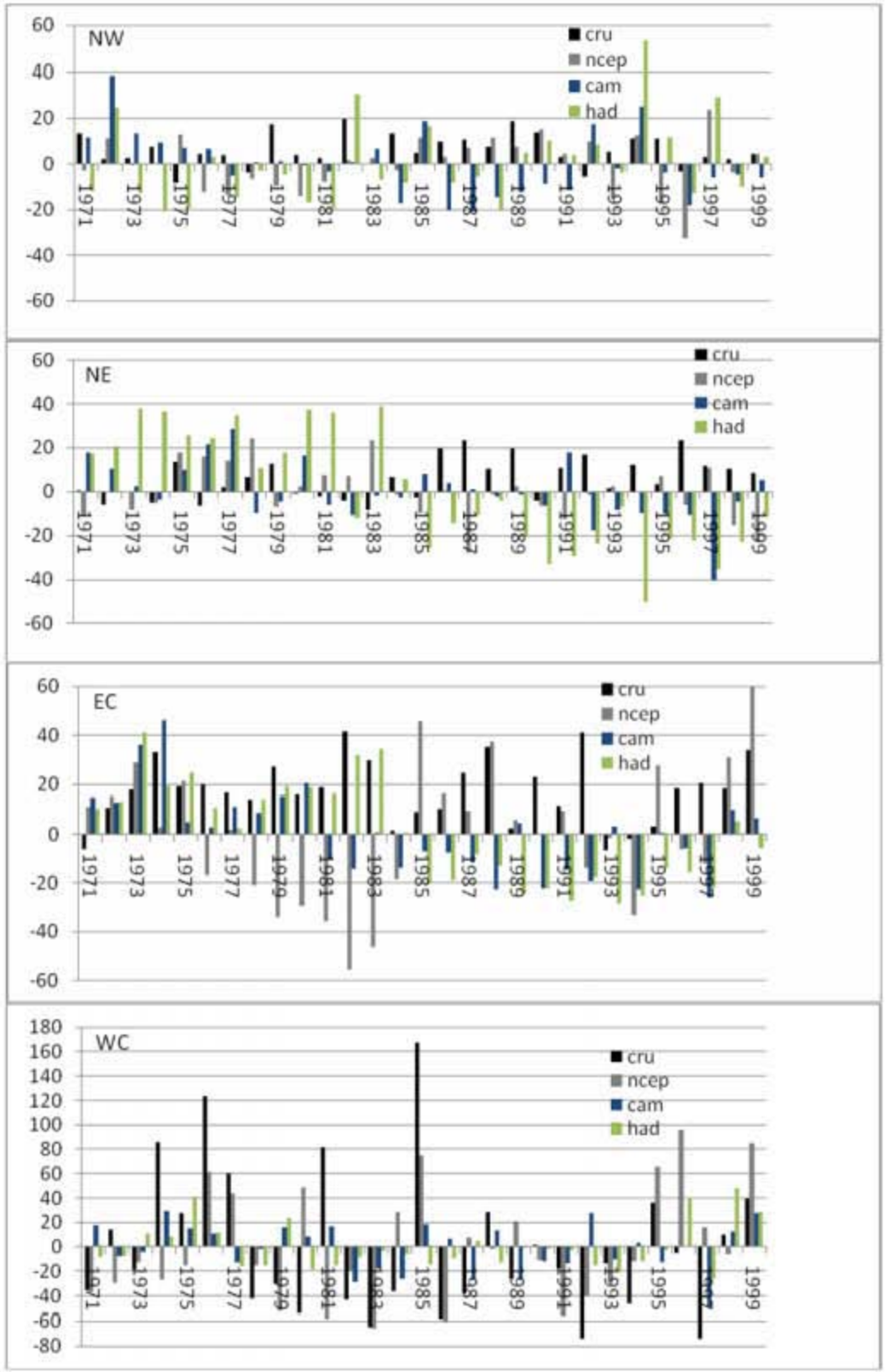

***Figure 5.2**: Anomalies in DJF rainfall (%) over the sub-regions in southern Africa.*

However, the models fail to capture the rainfall pattern between 1984 and 1992. The models and CRU show that WC has the highest percentage variation in the inter-annual variability. This may be because the mean average over WC (being a relatively smaller area) was ENSO years between 1971 and 2000 as against the mean of the entire period (1971-2000). Rainfall over the WC follows the El Niño-La Niña phenomenon. The observation and models largely capture the positive anomaly patterns during these cases. For example, the 1982/83, 1991/1992, 1994/95, 1997/98 El Niño periods which brought dry conditions over the region. The observation and models equally captured the negative anomaly patterns in La Niña years, example 1985/86, 1998/99 and 1999/2000. However, reanalysis did not agree with the pattern from CRU in 1997/98 El Niño year and 1998/99 La Niña year.

The magnitudes of anomalies from the models (and reanalysis) are compared with that from CRU using normalized standard deviation (σ), defined as

$$\sigma = \frac{\sigma_m}{\sigma_c}$$

where σ_m is the standard deviation of the anomalies from the a model (or NCEP reanalysis) and σ_c is standard deviation of anomalies from CRU. The values of σ for models and reanalysis over the four domains are present in figure 5.3. For the models, the standard deviation of the anomalies is close to that of CRU over NE and EC, but higher in NW and lower in WC. NCEP gives a σ of 1.3 and. 1.7 over NE and WC respectively but about 2 over NW and EC.

The values of correlation coefficients (R), also used to further quantify the agreement of the rainfall anomalies from the GCMs (and reanalysis) and those from CRU, are in figure 5.3. In general, the correlation between the model and CRU anomalies is weak. For CAM3, the highest correlation coefficient (R=0.40) occurs over WC and the lowest (R=0.04) over EC. For HadAM3, the highest correlation coefficient (R=0.50) occurs over NE and the lowest over WC (R=0.17). For the reanalysis, the correlation coefficients are also weak (R<0.5), even lower than those for the models in all the domains except over WC. For instance, over NW, the correlation for reanalysis is lower than those for both models.

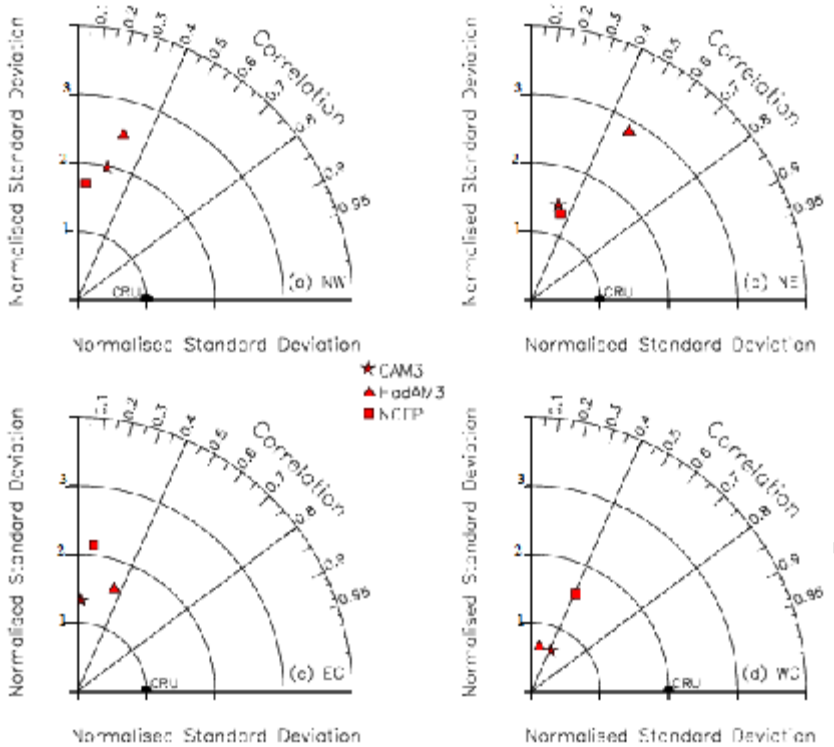

***Figure 5.3**: Comparison of NCEP (square), CAM3 (star), and HadAM3 (triangle) with CRU in simulating the DJF rainfall over (a) NW, (b) NE, (c) EC, and (d) WC.*

This raises the question on the confidence of using reanalysis data for model validation (or evaluation) over southern Africa. Several studies have shown similar concern and evaluation of the reanalysis rainfall over different part of the world using station or CRU datasets. But results they obtained vary. For example, Rao *et al*. (2002) demonstrated that the NCEP rainfall data agree well with observational data in some regions of Brazil, while in others the agreement is poor. Similar conclusions were derived from the studies of Yang *et al*. (1999), Hines *et al*. (2000), Smith *et al*. (2001), Rusticucci and Kousky (2002), and Flocas *et al*. (2004). These studies suggested that parameterization of physical processes is what limits the skill of both GCMs and reanalysis data in reproducing rainfall as observed.

The agreement between the rainfall anomalies from the models (and reanalysis) and CRU is also quantified in terms of phase synchronization (η;Misra, 1991), defined as

$$\eta = \frac{n - n'}{n} \times 100$$

where n is the total number of event (30 here) and η′ is the number of cases for which the anomalies have opposite signs (out of phase) with that of CRU. Therefore η is equal zero if all the anomalies are out of phase with their CRU counterparts, while η =100 when all of them are in phase with their CRU counterparts. The values of η for the four domains, models and reanalysis are given in Table 5.1.

Table 5.1: Phase synchronization

η (%)	NCEP	CAM3	HadAM3
NW	56.7	40.0	50.0
NE	46.7	43.3	33.3
EC	56.7	53.3	56.7
WC	56.7	63.3	63.3

For the models, the phase synchronization is high over EC and WC (η>50) indicating that the models are able to capture the occurences of individual anomalies most of time with respect to CRU observations. Over the tropical sub-regions (NE, NW) where η is lower or equal to 50%, the models fail to represent the proper sign of most of the specific events. The phase synchronization of NCEP is 56.6% for all sub-regions (except over NE, which has 46.7%), which is within the range of the simulated ones over EC, lower in WC and greater in NE and NW.

5.3 Synoptic modulation of El Niño and La Niña years in DJF rainfall

The following results give the composite of the differences between the DJF El Niño/La Niña fields and climatology fields. All anomalies fields are deviations from 30-year (1971-2000) DJF average. The observed fields are computed from CRU (only for rainfall) and NCEP/NCAR reanalysis dataset, and the corresponding simulated fields are from the ensemble mean of the models simulations (equation 5.1). The table shows the ENSO years used in the study, which the models capture their signs in the interannual variability.

Table 5.2: Years representing specific El Niño and La Niña period from 1971-2000 considered in the study.

El Niño	1972/73 1976/77 1977/78 1982/83 1986/87 1987/88 1991/92 1994/95 1997/98
La Niña	1971/72 1973/74 1974/75 1975/76 1985/86 1988/89 1998/99 1999/2000

$$Var_{anomaly} = Var - Var_{meanenso} \quad (5.1)$$

Where Var is CRU, NCEP, CAM3 or HadAM, $Var_{anomaly}$ is the anomaly computed for each case, and $Var_{meanenso}$ is the mean of either ElNino or LaNina years as indicated in table 5.2.

5.3.1 Anomalies in ENSO Rainfall (DJF composite)

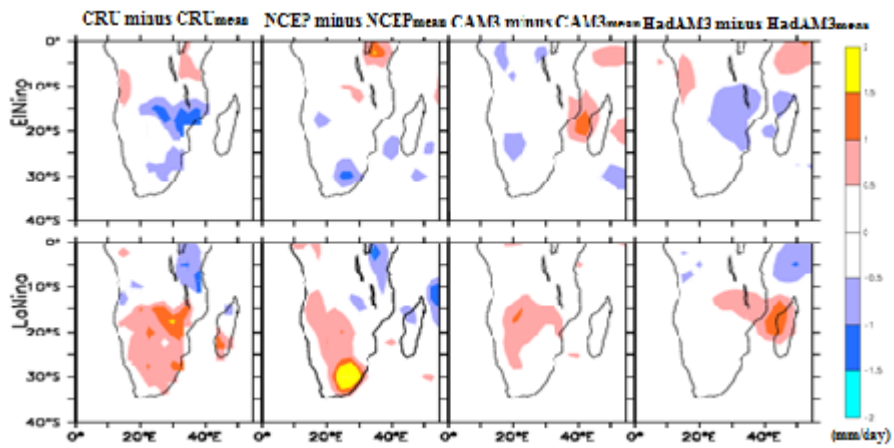

***Figure 5.4**: Comparison of simulated (CAM3 and HadAM3) ENSO years minus mean climatology composite DJF rainfall with CRU and NCEP reanalysis.*

Figure 5.4 depicts the dry anomalies during El Niño and wet anomalies during La Niña years. NCEP anomaly significantly captures drought in El Niño and large intense rainfall in La Niña years over the eastern part of southern Africa, which agrees with previous studies (Ropelewski and Halpert, 1987; Philander, 1990; Ogallo, 1994) of the regional impacts of El Niño on weather and climate in boreal winter (astral summer). The models are able to get the basic structure of the ENSO phenomenon in most part of southern Africa, especially in the La Niña composite.

5.3.2 Anomalies in Mean Sea Level Pressure

The examination of the composite mean sea level pressure (slp) field exhibits high positive anomalies in the El Niño than the La Niña. In the El Niño composite, positive pressure anomalies are more pronounced especially over the Atlantic Ocean, in contrast to the La Niña composite in which the negative anomalies are much lower. This demonstrates that the intensified activity over the oceans has a considerable effect on the rainfall during these years. A closer study exposes an additional difference between the composites, this time over southern Africa (Figure 5.5).

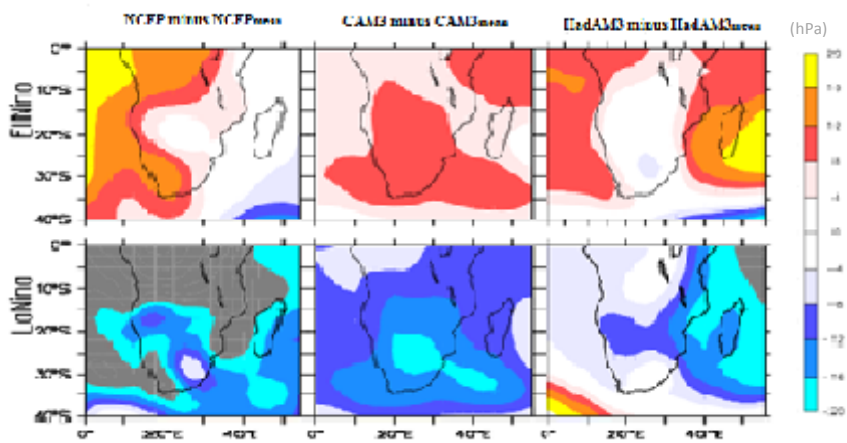

***Figure 5.5**: Comparison of simulated (CAM3 and HadAM3) ENSO years minus mean climatology composite DJF mean sea level pressure with NCEP reanalysis. Values lower than -20 are shaded grey.*

The western half of the region experiences higher positive pressure anomalies than the eastern half with lower positive pressure anomalies in El Niño years. Negative anomalies are only in the Indian Ocean in El Niño. In La Niña composite, high negative values are everywhere over the region with more negative anomalies lower than -20 (shown with grey shades in the figure 5.5) over the northern, western part of the region and over the Atlantic Ocean. Both models reproduce this pattern to some extent. For instance, CAM3 shows high positive anomalies everywhere over the region in El Niño and high negative anomalies everywhere over the region in La Niña. Similarly, HadAM3 shows the negative anomalies emerging from the Indian Ocean and the positive anomalies from the Atlantic Ocean but it fails to simulate the negative anomalies over Madagascar as in NCEP in El Niño but captures the pattern well in La Niña.

5.3.3 Anomalies in Geopotential Height

While in the previous section the El Niño and La Niña impact on rainfall was diagnosed in terms of surface perturbation and since our main interest is on rainfall, which originates essentially in the mid-troposphere, we here examine the composite map of the 500hPa geopotential height. The 500hPa anomalies composites in El Niño years point to positive geopotential height anomalies over most part of the region, which indicate more subsidence and therefore less rainfall as shown above. In the El Niño anomalies, higher than normal geopotential heights is produced over southern Africa. This is associated with anomalous easterly flow over the northeastern part of the region and a suppression of tropical air-masses and subsequent rainfall.

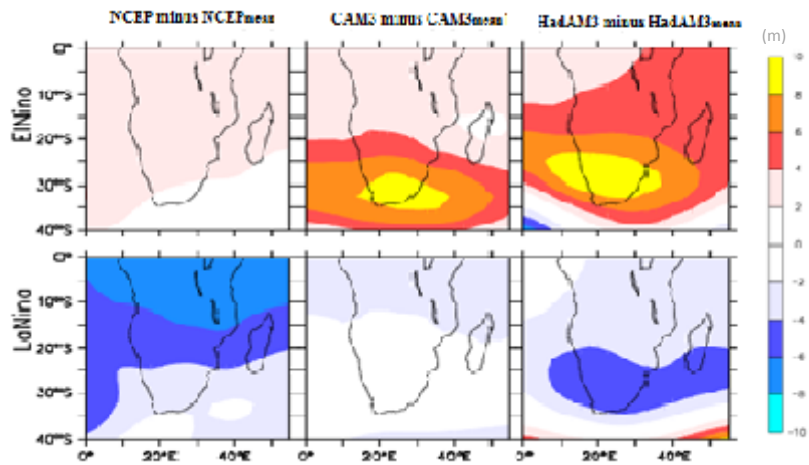

***Figure 5.6**: Comparison of simulated (CAM3 and HadAM3) ENSO years minus mean climatology composite DJF geopotential height at 500 hPa with NCEP reanalysis.*

In both models, positive anomalies of geopotential height are more marked over the southern part of the region, which extends to the north in HadAM3. Furthermore, the lower than normal 500 hPa heights over the northern part of the region did not extend to the south of the region, resulting in typical rather than especially wet events that seem to play an important role in the pattern of rainfall during La Niña years. Both models display the negative pattern over the region. For example, CAM3 has zero to low negative anomalies in La Niña years while HadAM3 has a high

negative over the south central part of the region, consistent to the rainfall anomalies.

5.4 The role of Global SST on the Inter-annual Variability of DJF Rainfall

To assess how the models simulate the relationship between southern Africa rainfall and SST, the distribution of inter-annual temporal correlation coefficients between DJF mean rainfall, and DJF mean SST during the El Niño and La Niña years are shown with figures 5.7 – 5.10 for different sub-regions of southern Africa.

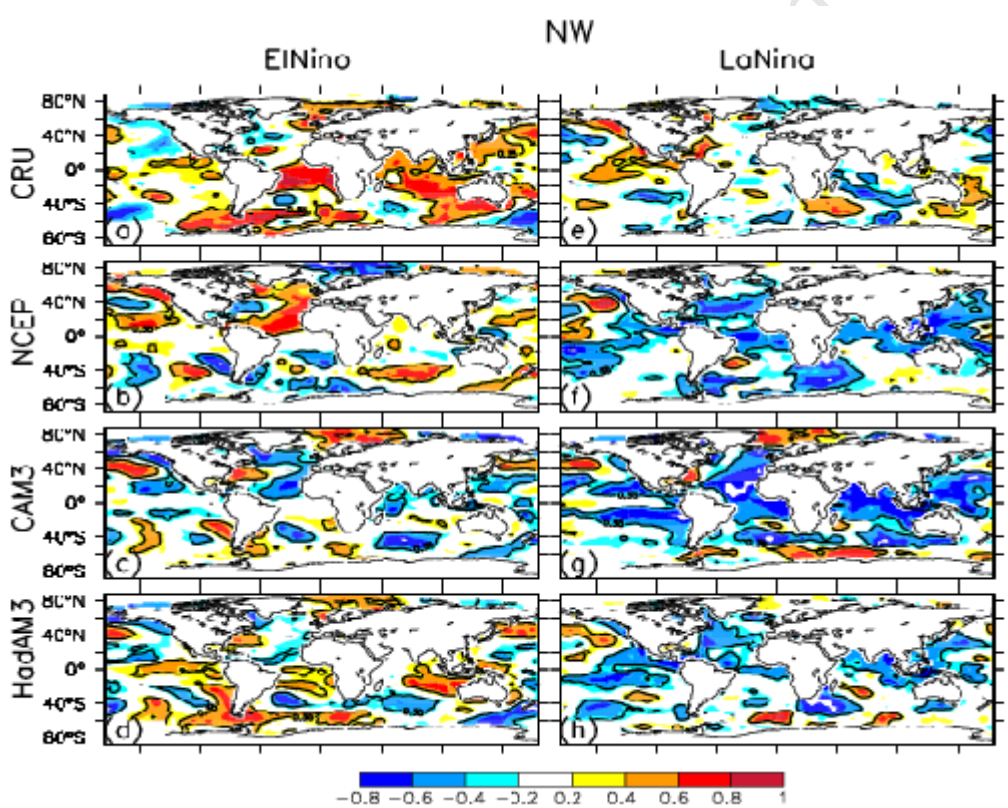

***Figure 5.7**: Distribution of inter-annual temporal correlation coefficients between DJF mean rainfall over NW sub-region and DJF mean global SST for ENSO years from observed, simulated and reanalysis. Significant values (r > 0.37) are in enclosed contours.*

In the NW correlation field (Figure 5.7), CRU disagrees with NCEP on how well the seasonal rainfall over the region correlates with the SST, but shows some agreements with respect to the models. Particularly for the El Niño composite, the positive

correlation in the oceans around Africa shown in CRU is not present in NCEP reanalysis and CAM3. HadAM3 shows this correlation, but with lower values. While CRU suggests significant positive correlations over the South Atlantic Ocean and over south Indian Ocean, NCEP reanalysis show contrasting negative correlation patterns. Both models show comparable correlation patterns. For instance, both show that the seasonal rainfall over the region has a significant negative correlation ($r > 0.4$) pattern over the Indian Ocean, North Pacific and South Pacific Oceans. On the other hand in the La Niña composite, CRU show low correlation coefficients over all the oceans. Again, no significant correlations are found in the Atlantic Ocean as in the case of El Niño but positive correlations are significant in the south Indian Ocean. The models agree more with NCEP than with CRU although they simulate the dipole at the North Pacific Ocean as shown in CRU. In both NCEP and the models, negative correlation values are found everywhere except in a small area in the South Atlantic Ocean near South America and in the North Pacific Ocean.

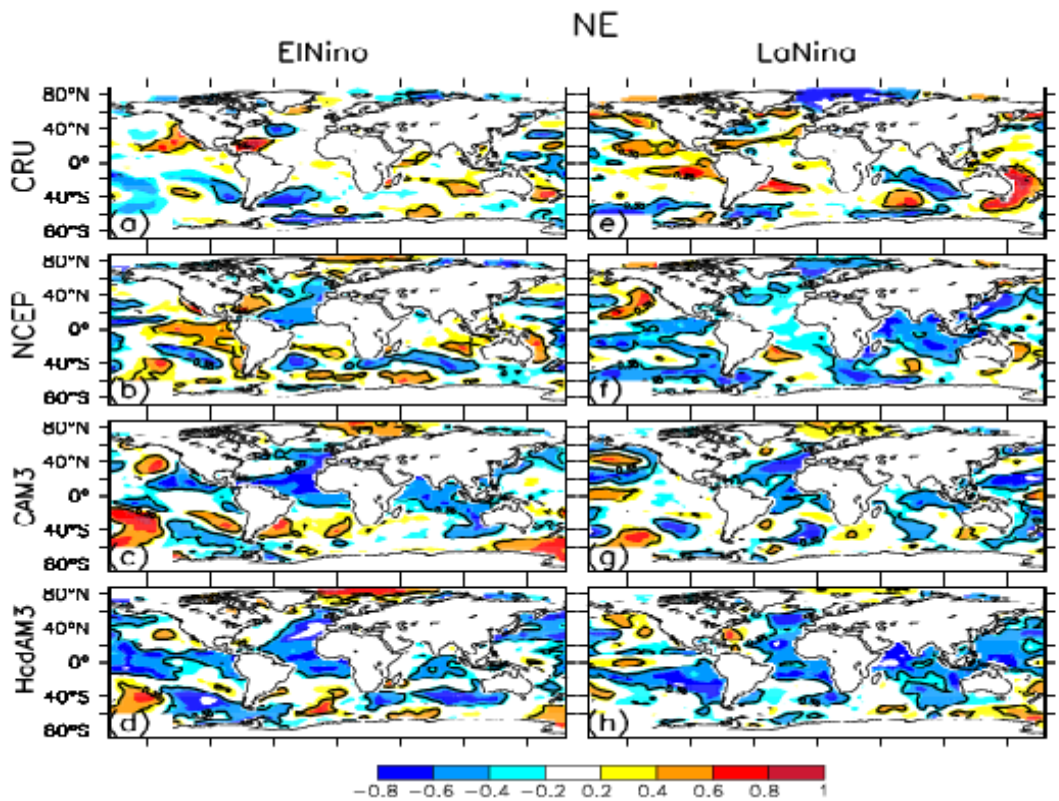

Figure 5.8: *Same as Figure 5.7 but for NE.*

The rainfall-SST correlation field for NE shows disagreements among the models, CRU and NCEP in both El Niño and La Niña composites. Although CRU shows less significant correlation coefficients over the oceans, NCEP and the models show various degrees of significant correlations. CAM3 agrees with CRU for the correlation over the south Indian Ocean in El Niño and both models in La Niña. In addition, the models show that the seasonal rainfall is negatively correlated (r = -0.4, significant at 90%) with SST over the Pacific Ocean and the Indian Ocean in both composites.

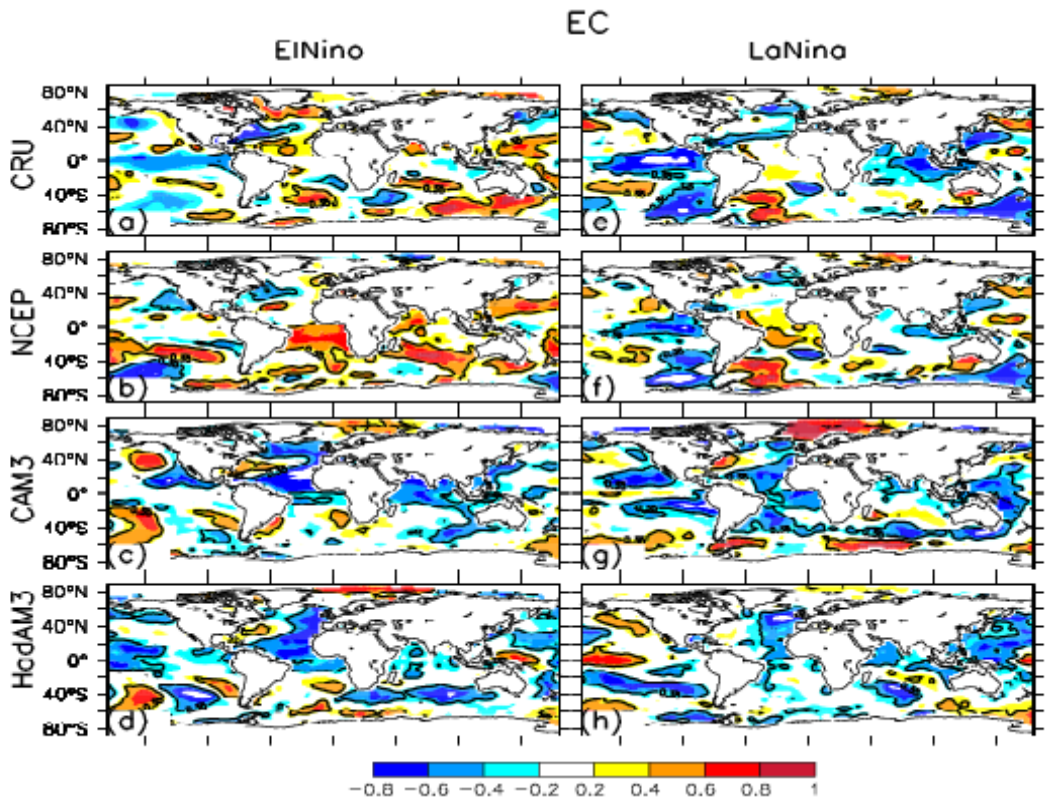

Figure 5.9: *Same as Figure 5.7 but for EC.*

In the rainfall-SST correlation fields for EC, there is a good agreement between the models and CRU, to some extent but not with NCEP (Figure 5.9). In general, the models suggest a negative correlation between the rainfall over this region and SST over the Pacific Ocean in both composites. The models also suggest a negative correlation between the regional rainfall and SST over the North Atlantic Ocean, in both composites which disagree with CRU. However the correlation pattern of

NCEP only agrees with CRU over the Indian Ocean. It shows a positive correlation with SST over the South Atlantic Ocean and Indian Ocean in El Niño and a negative correlation with North Pacific Ocean in La Niña.

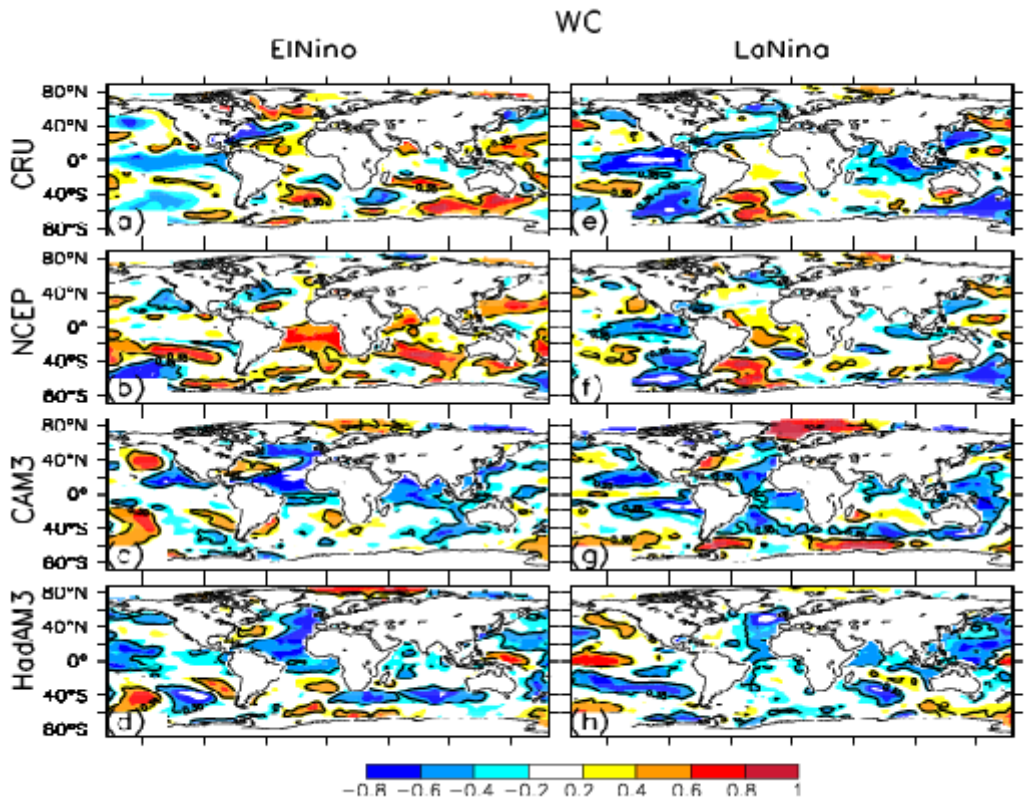

***Figure 5.10**: Same as Figure 5.7 but for WC.*

Similarly, for WC, the simulated correlation fields and NCEP show disagreement with the observed. NCEP has close correlation patterns with CRU than with the models but the models have similar patterns. For instance in El Niño, NCEP and CRU show that the rainfall is positively correlated with SST over the South Indian and Atlantic Oceans, contrary to the models, which show significant negative correlations (for HadAM3) or no significant correlations (for CAM3) over the south Indian Ocean.

The disagreement between observation and the reanalysis here shows how difficult it is to link the summer rainfall over the sub-regions with global SST. This could be

because, in observation, there are other smaller scale circulations that control connection between the SST and the seasonal rainfall over the region, but in the reanalysis and models those smaller scale features may not be fully resolved. The degree to which those smaller scales are resolved depends on the physics parameterizations in the GCMs and the reanalysis. However, the models are able to capture the impact of Nino signal on regional rainfall over WC although HadAM3 performs better than CAM3.

5.5 Summary

This study has explored the capability of CAM3 and HadAM3 in representing the inter-annual rainfall and circulations during ENSO years. It also investigated the relationship between the regional rainfall from the models and global SST during the El Niño and La Niña years. Typical synoptic conditions during the ENSO years appear to be coupled with rainfall variations. For instance, more intense circulation activities advocate strengthening of advection and dry southerly air mass into the most part of the region, which cause the consequential dry rainfall pattern in El Niño years. In La Niña years, more intense conditions prevail which favor stronger circulation and tropical convection resulting in above normal rainfall over the southern Africa.

The models did a good job in simulating the correlation pattern between the SST and seasonal rainfall over NW and EC (compared to CRU), but not over NE and WC, where the simulations disagree with CRU. However, in most of the cases, there are good agreements between the simulated rainfall-SST correlation patterns produced by CAM3 and HAdAM3, and sometime the correlation pattern agree with CRU better than the reanalysis. Simulating the influence of SST on the seasonal rainfall over these four regions as observed is challenging for the models, even for the reanalysis. This could be because, the models do not fully resolve smaller scale circulations (Gates, 1985; Bryan, 1984) that control connection between the SST and the seasonal rainfall over southern Africa. Nonetheless, it is interesting to note that both models give a consistent pattern, which agrees with the observation in some sub-regions and does not in other sub-regions. However, this study stresses that the

results of the models show a better agreement with observation than the reanalysis do.

In conclusion, although they show some biases, both CAM3 and HadAM3 give credible simulations of essential climatic features and significant relationship between the regional rainfall and SST over the Nino region, which strongly drives the climate of southern Africa. Their simulations could contribute to understanding the climate of the region and improve seasonal forecasts over southern Africa if models can fully resolve small scale circulations.

Chapter 6

Evaluation of seasonal forecasts from the CAM3 and HadAM3

Evaluation is necessary for understanding the strength and weaknesses in forecast models. As part of the long term aim of employing CAM3 and HadAM3 in seasonal forecasting over southern Africa, this study will allow the Climate Systems Analysis Group and the South African Weather Service to identify strengths and weaknesses of the models as well as identify areas where efforts and resources can be applied to improve the forecasts.

The previous chapters demostrated how CAM3 and HadAM3 represent climatology and variability of southern Africa and why they show such results. This chapter is a case study focusing on the rainfall forecast of 2002/2003 El Niño and 2007/2008 La Niña years. The study investigates and discusses the skills of the seasonal forecasts produced from CAM3 and HadAM3 over southern Africa during those years. The forecasts from the models are produced with persisted SSTs as explained in Chapter 3. In the investigation, the two global models are assessed on their ability to predict probabilities of summer rainfall during the two ENSO cases in comparison with CMAP observation data. The sections below describe the skills of the models in forecasting the southern Africa rainfall using different verification measures.

6.1 Seasonal Rainfall Forecast

The relationship between the models ensemble mean DJF rainfall and the observed DJF rainfall is presented in the table below with the correlation coefficients for 2002/2003 El Niño and 2007/2008 La Niña years. These correlations provide good

agreements between the forecasts and the observation over southern Africa (SA) and for each case, considering the period of the forecast. The correlations are repeated but for rainfall from four different sub-regions of southern Africa having varying rainfall patterns. These sub-regions have been discussed in section 3.4 of the thesis.

Table 6.1: Spatial correlation between the models DJF rainfall forecasts and CMAP DJF rainfall of (a) 2002/2003 El Niño and (b) 2007/2008 La Niña.

(a)

	SA	**NW**	**NE**	**EC**	**WC**
CAM3	0.568	0.570	0.356	0.620	0.498
HadAM3	0.679	0.585	0.226	0.791	0.911

(b)

	SA	**NW**	**NE**	**EC**	**WC**
CAM3	0.561	0.557	-0.02	0.582	0.510
HadAM3	0.669	0.720	0.40	0.762	0.806

Rainfall from SA and the all the sub-regions show a good relationship with the observed rainfall but not NE from both models. The poor relationship between the observed and models rainfall over NE confirms the phase synchronization of the models with CRU rainfall in Chapter 5, where the number of rainfall anomalies in phase with the observed rainfall anomalies is lower (below 50%) than other sub-regions.

The following results show the main skill of the models in reproducing the spatial rainfall forecasts of the 2002/2003 El Niño and 2007/2008 La Niña years.

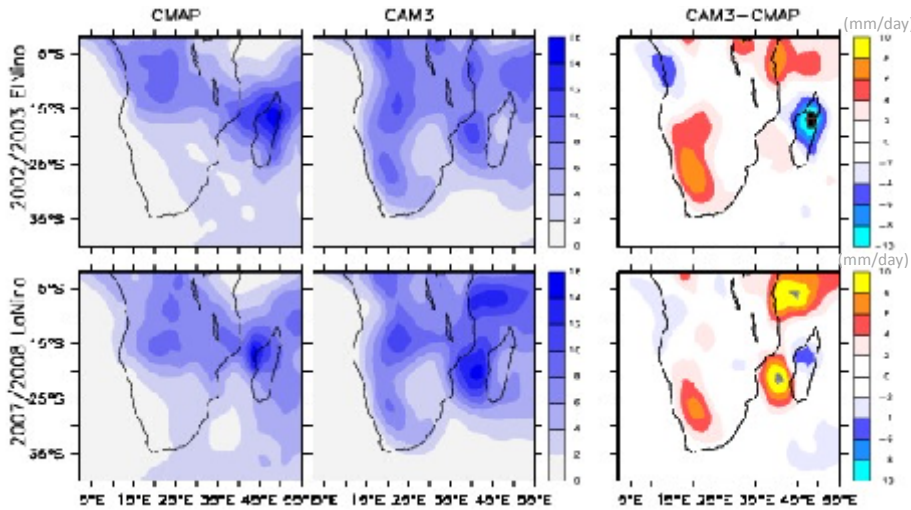

***Figure 6.1**: DJF rainfall (mm/day) over southern Africa from CMAP (left panel), CAM3 (middle panel), and the bias (right panel). The upper row represents the 2002/2003 DJF rainfall and the lower row represents the 2007/2008 DJF rainfall. Field shaded grey are bias more than 10mm/day and black are values less than -10mm/day.*

From figure 6.1, the observed mean rainfall is greatest in the northern portion of the region, along the equator in both cases. The maximum at this portion gradually decreases southward until 15^{o}S. Another peak of rainfall is located over Madagascar and it decreases from that region. The dryness over the western part of the sub-continent covers a wider area towards the north covering Namibia and southern part of Angola during the 2002/2003 El Niño year. The La Niña year covered relatively smaller area of the western part. Low rainfall is experienced over the Eastern part of the sub-continent with some dry patches during the 2002/2003 El Niño. CAM3 forecast a different pattern of rainfall in these cases. In both cases, CAM3 misses the drying pattern over the western part of the region. The zone of maximum rainfall lies along the western half of southern Africa. However, it captures the low rainfall over the eastern part of the region. The bias shown in the left panel of figure 6.1 shows that CAM3 has a strong bias (overestimation) along the western part of the sub-continent during both events. This behaviour of CAM3 is similar to its representation of the climatology, which has been explained in Chapter 4.

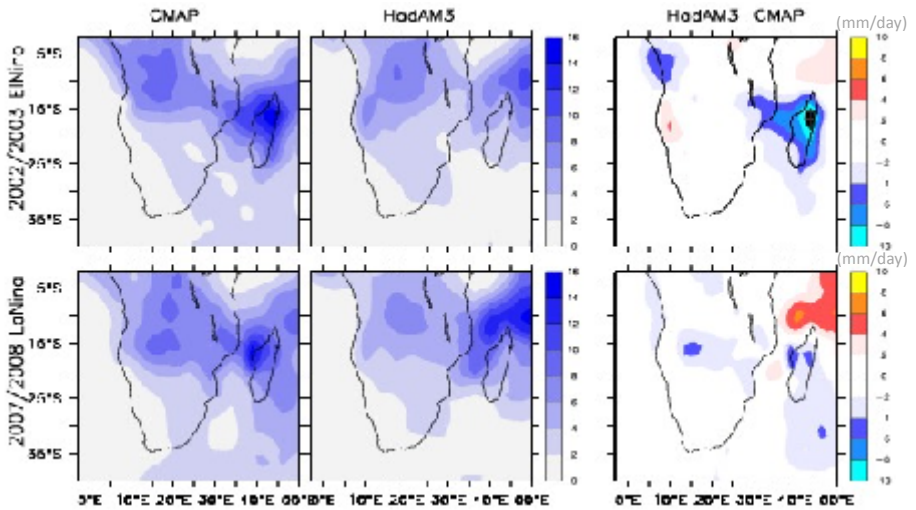

Figure 6.2 *Same as figure 6.1 but for HadAM3*

In the HadAM3 forecast, the rainfall distribution is closer to that from the CMAP observation (Figure 6.2). The model captures all the essential features in the observed, except that it generally under-forecast the rainfall amount over the western part of the region in El Niño and the central in La Niña cases. Elsewhere, the differences are between 0 and +/-2. HadAM3 showed similar rainfall climatology when compared with NCEP in the previous chapters. The model showed good circulation patterns compared with NCEP reanalysis.

6.2 Forecast Verification

6.2.1 Relative Operative Characteristics Score

The ROC score, defined as the area under the ROC curve is tested for forecast in the El Niño and La Niña year from CAM3 and HadAM3 (Figure 6.3). Areas shaded red have ROC score between 0.8 and 1 showing a good performance of the models' forecasts while the areas shaded blue have scores between 0.6 and 0.8 and the green shaded areas have scores between 0.5 and 0.6. A score of 1 means perfect forecast from the model. Both models showed close to perfect forecast. Score between 0.7 and 0.8 are good forecast but not excellent, and score between 0.6 and 0.7 are fair,

but scores close to 0.5 or below are poor. The scores below 0.5 are not shaded and are the white spaces in the figure.

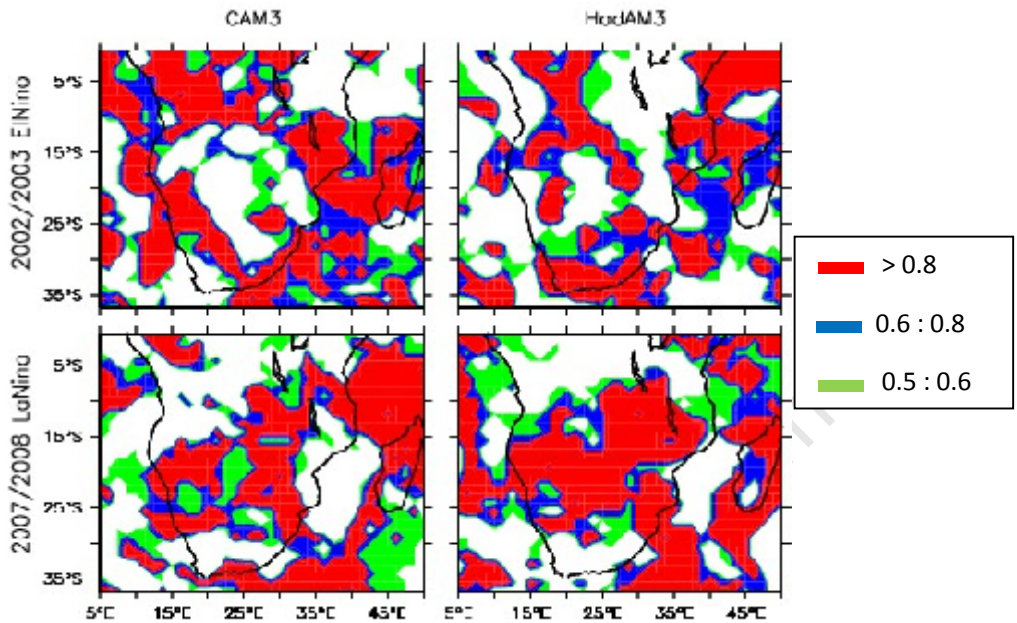

***Figure 6.3**: Relative Operative Characteristics Score from CAM3 and HadAM3 DJF rainfall (mm/day) over southern Africa. Only significant values are plotted with shaded areas signifying skill (values between 0.5 and 1 inclusive) and white areas show no skill or scores below 0.5.*

From figure 6.3, El Niño rainfall forecast from CAM3 shows good scores over most part of the region except over the central part, the Western Cape and the north eastern part of the sub-continent, where the score is below 0.5. Unlike the El Niño year, the La Niña rainfall forecast shows high scores over most central and the north eastern part of the sub-continent. However, patches of low ROC scores are visible over the high score regions. In the case of HadAM3 forecast, high scores are shown over the western part of the sub-continent in El Niño rainfall but not in the La Niña year. The model show good scores over most central and eastern part of the sub-continent in La Niña year.

6.2.2 Brier Score

The score (Figure 6.4) is the mean squared error of the probability forecasts for rainfall over southern Africa. The forecast shows some skills at the shaded areas. Red shaded areas have mean squared errors between 0 and 0.3 showing a good

performance of the models' forecasts. Blue shaded areas have errors between 0.3 and 0.6 and the green shaded areas have errors more than 0.6. An error that is 1 means a high error from the model. Both models showed some errors but none has errors of 1. The worse error from the models is 0.9. Low errors are shown over most part of the region.

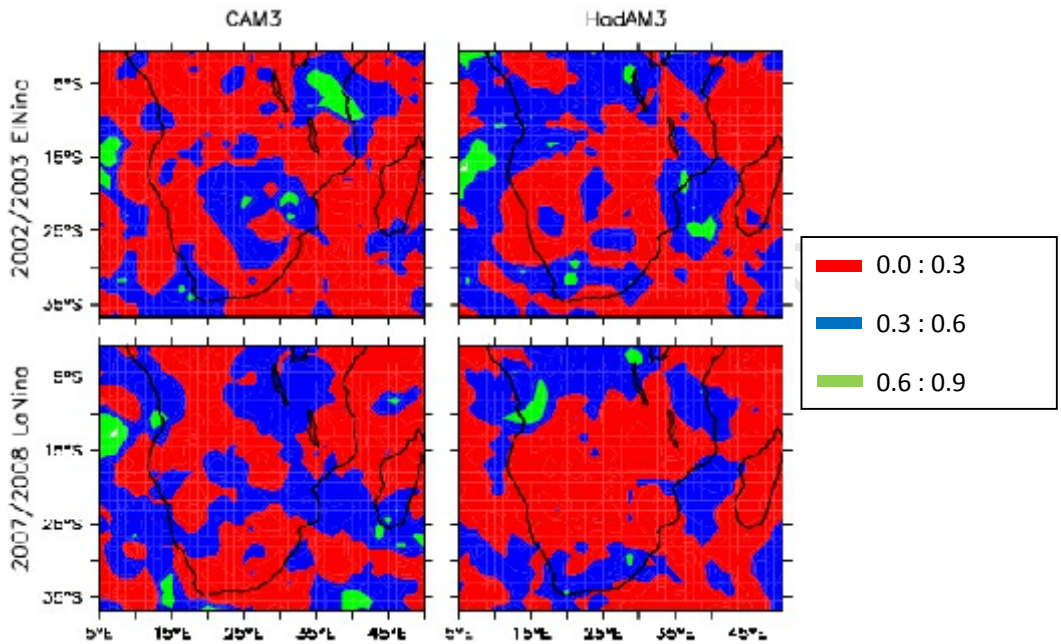

***Figure 6.4**: Brier Score from CAM3 and HadAM3 DJF rainfall forecast over southern Africa. The shaded areas signify skill (values below 0.9) with low scores close to zero representing good skills.*

Both models show good scores over most part of the sub-continent. However, CAM3 forecast in the El Niño year shows low skill over Western Cape, between the northern part of South Africa and southern part of Botswana, and an area at the north eastern part of the sub-continent. The model has a representation of good skills during the 2007/2008 La Niña. HadAM3 on the other hand show good scores in most areas in all cases but shows some patches of low skill over some selected places in both cases. The low skill may be due the inability of both models to resolve processes over the topography over those areas.

6.2.3 Ranked Probability Score

Figure 6.5 shows the RPS from the models forecasts for various cases with climatology as the reference. Like the Brier scores, the forecast shows some skills at

the shaded areas. Both models show good scores over most part of the sub-continent. However, CAM3 forecast for El Niño shows low skill over Western Cape, northern part of South Africa to southern part of Botswana, and an area at the north eastern part of the sub-continent. The RPS from HadAM3 shows good score.

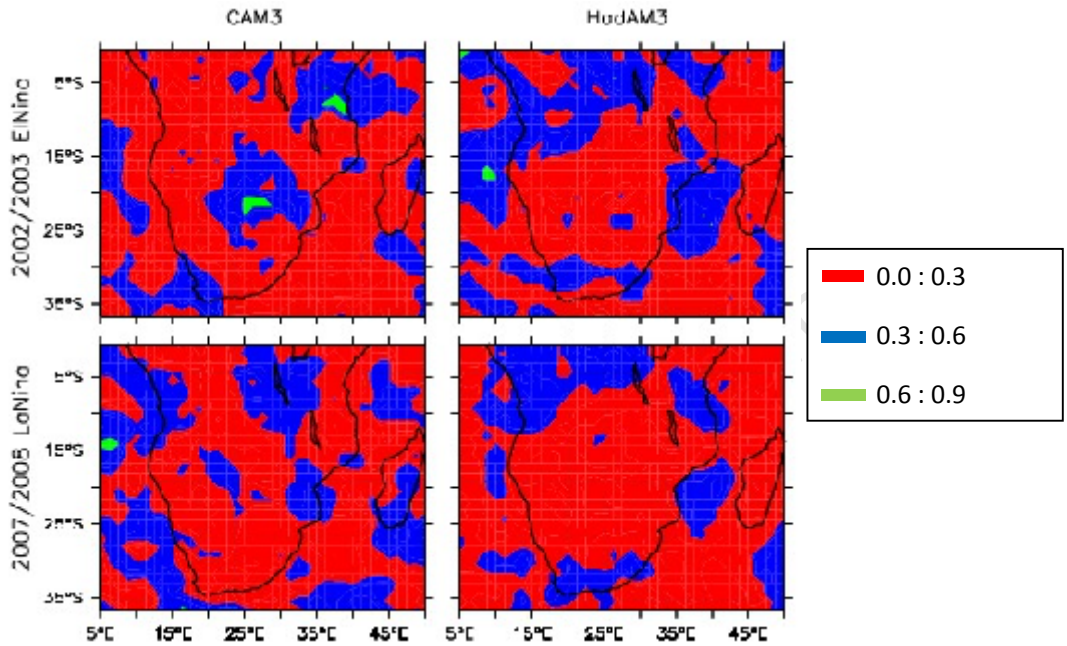

***Figure 6.5**: Ranked Probability Score from CAM3 and HadAM3 DJF rainfall forecast over southern Africa. The shaded areas signify skill (values below 0.9) with low scores close to zero representing good skills.*

6.2.4 Area under the ROC curve

From CAM3 (HadAM3) forecast, the hit rate versus the false alarm rate of the area averaged rainfall for the southern is 0.611 (0.535) for 2002/2003 El Niño, and 0.548 (0.571) for 2007/2008 La Niña year as the area under the ROC curve. The ROC diagrams below show the plot of the area under the ROC curve over southern Africa (Figure 6.6) and over the various sub-regions (Figure 6.7). In figure 6.6, CAM3 shows a good skill for the DJF rainfall for 2002/2003 El Niño, while less but not worse skill for La Niña years. HadAM3 on the other hand, has less skill for 2002/2003 El Niño and good skill for La Niña years.

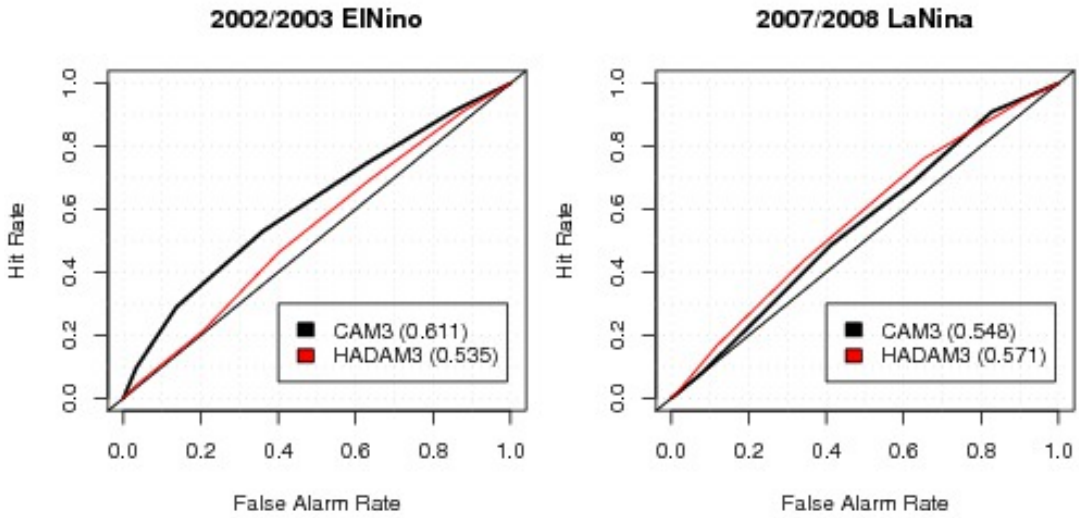

***Figure 6.6**: ROC diagram showing the area under the curve of DJF rainfall for El Niño and La Niña phenomenon from CAM3 and HadAM3 forecasts. The area under the ROC curve is shown in parenthesis by the models. The plot is averaged over 36S:0 and 5E:50E*

In the El Niño year, CAM3 forecast shows a good AUC (values above 0.6) in all the sub-regions whereas HadAM3 gave a poor skill (values around 0.5) in all the sub-regions except over the WC where the AUC is 0.695. In particular, CAM3 shows it best skill (with AUC above 0.7) over NW and it worst skill over the WC with AUC of 0.607. Ironically, HadAM3 shows its best skill over WC and the worse skill over NW where CAM3 shows its best skill over NW and the worse over WC. Reasons why the models have contrasting skill is not clear but for CAM3, it may be attributed to its inability to simulate the rainfall over that sub-region well compared to observation as shown in the previous chapters. That of HadAM3 may be attributed to underestimation of rainfall over the region.

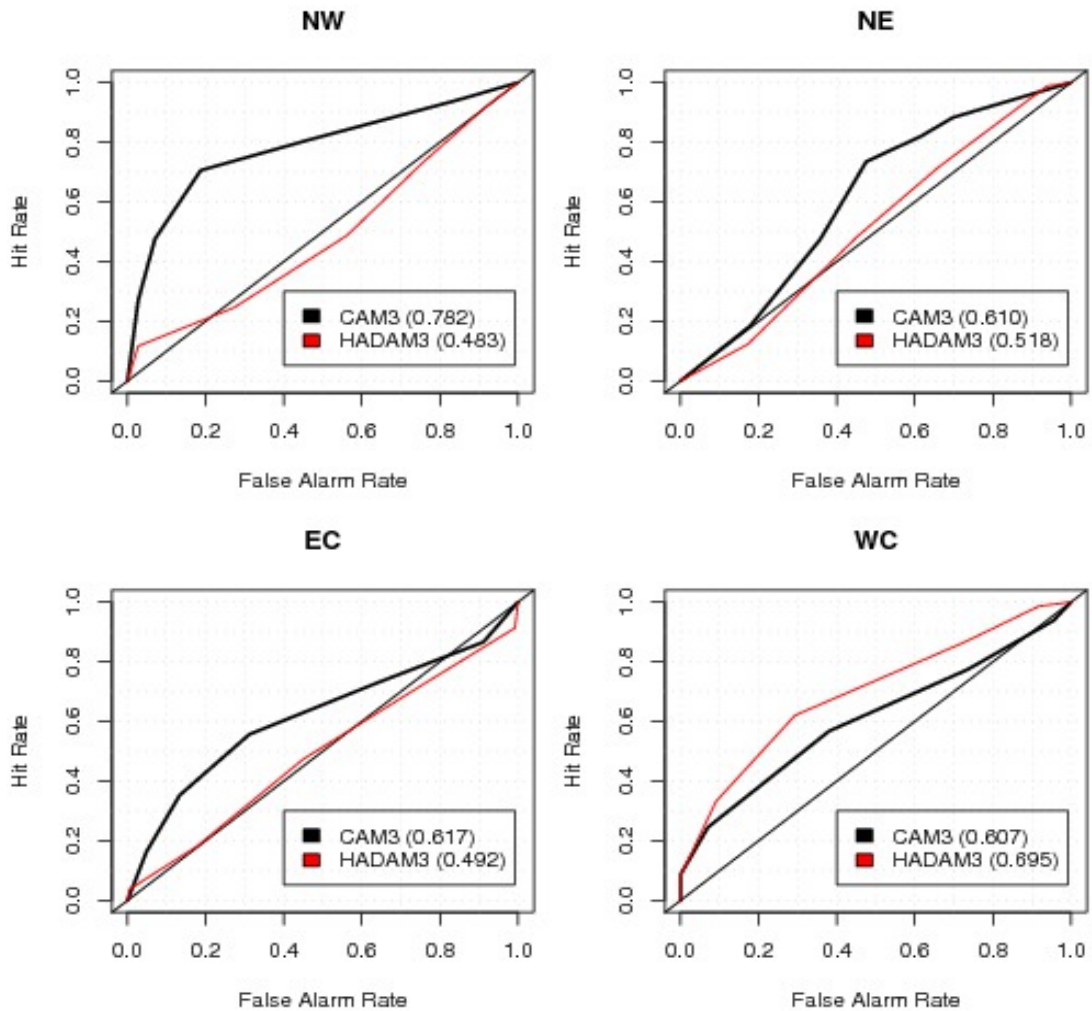

Figure 6.7*: ROC diagram showing the area under the curve for various sub-regions of southern Africa for El Niño phenomenon from CAM3 and HadAM3 DJF rainfall forecasts. The area under the ROC curve is shown in parenthesis by the models.*

In the La Niña year (Figure 6.8), both models produce poor skill over the sub-regions, especially over the NW where CAM gives an AUC of 0.456 and HadAM3 gives 0.384. They equally give poor skill over the WC. However, both models agree and give fairly good skill over the NE and EC.

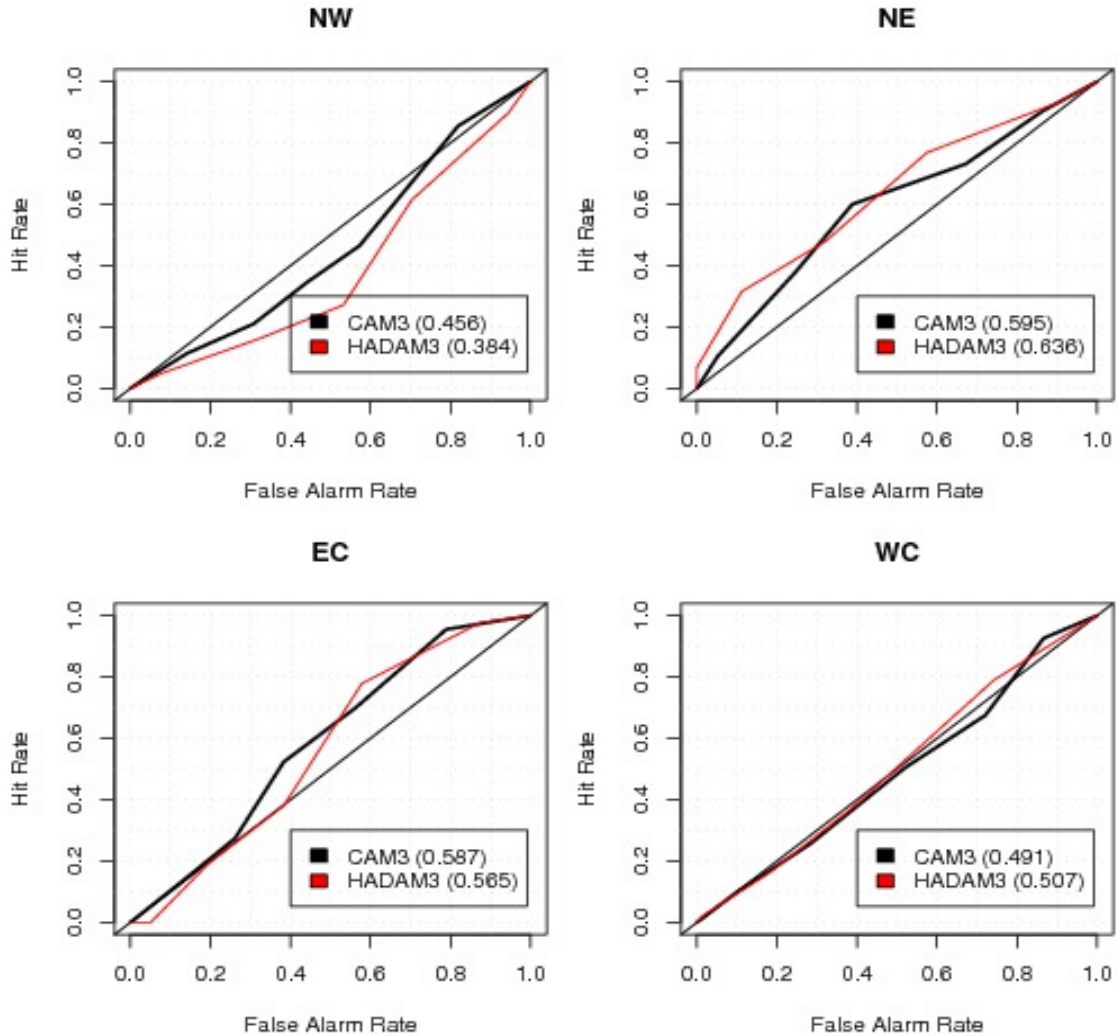

Figure 6.8: *Same as Figure 6.7 but for La Niña phenomenon.*

6.3 Summary

The seasonal forecast over southern Africa from CAM3 and HadAM3 has been evaluated for their available rainfall forecasts during the summer seasons of an El Niño and a La Niña year with ten member ensembles produced from each model. This has been done to investigate the skill of the models. In the investigation, both models were compared with the observed frequencies associated with the different forecast probability values. The summer season is December-January-February, where January and February are for the succeeding year. Both models show a good correlation between their DJF rainfall and observed DJF rainfall. The study uses

rainfall from the four different sub-regions of southern Africa defined in the Chapter 3 for further analyses of the models' potentials in capturing the varying rainfall pattern. In the correlation coefficient tables showing the various models' relationship with observed rainfall from the sub-regions, rainfall from all the regions show good relationship with observation except NE showing very weak relationship from both models in both El Niño and La Niña cases.

A number of skill and accuracy measures, including the Brier score, Ranked probability Score, and Relative Operative Characteristics curve were employed to give a robust account of the models skills. It was found that CAM3 forecast shows strong biases over southern Africa while HadAM3 show only weak biases in both El Niño and La Niña cases. Rainfall from both models shows some skills over the entire study domain, however, the story is not the same for the sub-regions. Rainfall over each sub-region has a unique skill from the models and in El Niño and La Niña cases. The CAM3 forecast show good score over all the sub-regions in the El Niño year but HadAM3 has poor skill over all the sub-regions except for the western cape where the model give an AUC of 0.695. Both models show poor AUC in the La Niña year with NW having a negative skill.

Various skill measures used have helped identify the strengths and weaknesses of the forecasts produced from CAM3 and HadAM3. The models are able to produce skills in some cases over some sub-regions but not over others. There is no clear cut on where the models are showing their strengths and weakness over the different sub-regions of southern Africa.

Chapter 7

Synthesis

This study is a contribution to model development process, which model evaluation is an essential part and determines models to be accepted and used to support decision making. In this contest, the thesis evaluated two global models to be used for seasonal forecasting over southern Africa. The thesis contributes to our understanding of model skill in simulating seasonal variability and how model performance may constrain seasonal forecast skills. The study investigated models' ability to simulate the synoptic features that modulate rainfall and temperature, and the relationship of regional rainfall with global SST. The aim of the thesis therefore is to add to our understanding of why global models show marked limitations in representing southern African climate and how these affect their seasonal forecast skills. The following specific questions assisted in addressing the aim of the thesis:

- How well do global models reproduce the synoptic circulations that control the climate of southern Africa?
- How well do global models reproduce teleconnections between regional rainfall and global SST?
- How predictable is the seasonal climate over southern Africa using these global models?

Answers to the following questions have advanced our understanding in why models represent the climate of southern Africa the way they do. Each question is answered with a result chapter addressing the pertinent information on the models skills.

To address the question of how well models reproduce the synoptic circulations, 30-year climate simulation datasets from CAM3 (2.0^o x 2.5^o resolution, 26 levels) and HadAM3 (2.5^o by 3.75^o resolution, 19 levels) models were used. By perturbing the Reynold's historical SST data for the ocean boundary state, five member ensembles

were produced from each model, and relevant averages computed for further analysis. Monthly parameters from models and observations were used to assess the models' ability to correctly simulate the mean state of synoptic features. The investigation included the climate dynamics, with emphasis on the influences of the anticyclones (over the southern oceans), wind flow, position of ITCZ, and mean sea level pressure variation on rainfall during the summer and winter seasons. For transient features like TTTs, daily summer rainfall data was used.

In the investigation of the second question, rainfall data for El Niño and La Niña years between 1971 and 2000 were used to assess the models to know how well the models represent the mean state of synoptic scale modulation caused by El Niño and La Niña phenomena. All results were presented as composites – average of the anomalies fields, which are calculated as the differences between the DJF El Niño/La Niña fields and DJF climatology fields of the 30-year (1971-2000) period. The observed fields were computed from CRU (only for rainfall) and NCEP/NCAR reanalysis dataset, and the corresponding simulated fields are from the ensemble mean of the models simulations. Results from this analysis improved our understanding of the relationship between regional rainfall and global SSTs.

The last objective was addressed with a case study of available historical rainfall forecasts during recent ENSO events. We considered the 2002/2003 El Niño and 2007/2008 La Niña events using ten-member ensembles produced from each model. Monthly rainfall rates were averaged over southern Africa for December, January and February (DJF). The probabilistic forecasts were created by counting the ensemble members that exceeded any given one month accumulated rainfall amount, and then dividing that number by the total number (10) of ensemble forecasts. Forecasts were presented as the probability of the rainfall above the mean of historical rainfall; the threshold used was the climatological mean. Model forecasts were compared with CMAP observation data. Here, models demonstrated their forecast skill and when linked with the other results we understood why models show such skill.

With the understanding that the mean state of synoptic features play an important role in the climate of southern Africa, the models' evaluation included the simulation of these features. We found that although the models fairly simulated features like

the ITCZ, and anticyclones, which directly and indirectly affect rainfall variability of southern Africa, these models failed to establish a good relationship between the regional rainfall and global SST. The following section specifically discusses various aspects of the models' performances.

7.1 Discussion

Chapters 4-6 presented findings regarding the performance of CAM3 and HadAM3 in reproducing key atmospheric processes over southern Africa. It is evident from the results that the models are capable of adequately reproducing the mean climatology and seasonal variations of some features but they struggle to reproduce same for other features. Some features are represented well in one model but not in another model, admitting the fact that each model has different parameterization schemes and physics, thus having different internal variability and biases associated with it.

HadAM3 underestimates rainfall over southern Africa because it simulates weak wind flow over the region. The wind systems influence rainfall over southern Africa suggesting that strong wind cause more evaporation and together with other favourable factors, increase the chance for rainfall (Tyson and Preston-Whyte, 2000). Weak wind flow on the other hand causes less or no evaporation and low rainfall. The weak winds simulated by HadAM3 leads to weak convection and then decrease the chance of rainfall over the region. A study by Reason and Jagadheesha (2005) with HadAM3 forced with observed SST anomalies found evidence of the mean flow of the low-level cyclonic response.

CAM3 produces the largest bias during summer, overestimating rainfall amount and wrongly representing the spatial position of the rainfall peak to the western part of the region instead of east (in observations). The discrepancy is due to CAM3 simulating a trough of circumpolar wave 3 along the western part of the region between 10^{o}S and 35^{o}S with an associated weak ridge over the Indian Ocean. The trough-ridge system of wave 3 influences the location of blocking anticyclones (Tyson, 1981), which inturn controls rainfall over the region. Further investigation of

the summer rainfall simulated by CAM3 shows that the convective rainfall dominates the total rainfall. Figure A.1 shows that the percentage convective rainfall for January (the peak of the summer season) is almost 100% along the western part of southern Africa, which explains the overestimation of rainfall by CAM3.

Synoptic circulation features are of major importance to southern African climate, since they control rainfall in all seasons over the region. It is critical that models adequately represent these rainfall controlling features over southern Africa for a meaningful study of the climate of the region. Both model results provided a satisfactory description of the mean state of the synoptic features of southern Africa although there are pertinent issues about their performances which cannot be overlooked. For example, wind system can be viewed as a response of the boundary layer to pressure perturbations produced by convection and sea surface temperature gradients. A model's simulation of the wind system suggests how the model interacts with ocean boundary layers. An underestimation or overestimation of the wind pattern as seen in the results implies that the simulated boundary layer stability is not strong. As seen in the results, both models have only a fair representation of the wind system over Africa. HadAM3 underestimates the wind pattern because the region is covered by a large high pressure system especially during the summer season. However, both models show that high pressure weakens over the continent in winter but are thermally intensified in summer over the continent as seen in the observation.

Simulation of the wind system also affect the location and convergence of tropical winds at the low pressure zones (ITCZ). Variation in the location of the ITCZ drastically affects rainfall in many equatorial regions, resulting in the wet and dry seasons of the tropics. Simulation of the position of the ITCZ is interesting in the climate of Africa because the position affects the seasonal rainfall patterns. The models inadequately simulated the position of this important feature in summer; CAM3 pushed the ITCZ a bit far to northeast over Saudi Arabia because the south-westerly is too strong over the area, while HadAM3 pushes it to far north over Mali, because northeasterlies are weaker over the area.

The models adequately simulated the locations of the anticyclones, but overestimated the magnitudes of pressure over the south and north Atlantic Oceans. Since pressure differences evolve due to interactions of temperature differentials in

the atmosphere, temperature differences between the atmosphere and oceans, the influence of upper-level troughs and shortwaves, as well as other factors, we admit that the models fail to establish such interactions properly.

The importance of TTTs cannot be overemphasized, since they are the dominant rain-producing synoptic type over southern Africa (Todd *et al*., 2004). TTT event is considered as the zone of absolute vapour flux convergence and are associated with deep convection. If the relationship between atmospheric processes and rainfall can be well established by the models, the TTT events can be well understood. In the SOMs, the nodes identified TTT patterns from 30 years of daily rainfall data and clearly showed the percentage frequency at which each model simulated the TTTs. CAM3 showed greater errors than HadAM3 in the standard frequencies confirming its limitation to correctly reproduce rainfall over southern Africa.

Additionally, the models showed a good representation of the inter-annual rainfall and circulations during ENSO years. They showed that typical synoptic conditions during the ENSO years appeared to be coupled with rainfall variations in those years. Simulating a realistic influence of SST on seasonal rainfall over the sub-regions was challenging for the models. But it was interesting that both models gave a consistent pattern, which agrees with the observation in some sub-regions and does not in other sub-regions. It is not clear why the models have different patterns from the observed in some sub-regions but the disagreements showed how difficult it is to link the summer rainfall over the sub-regions with global SST. There is the question on the confidence of using reanalysis rainfall data for model validation (or evaluation) over southern Africa. Several studies have shown similar concern in studies over different parts of the world using reanalysis. For example, Rao *et al*. (2002) demonstrated that the NCEP rainfall data agree well with observational data in some regions of Brazil, while in others the agreement is poor. Similar conclusions were derived from the studies of Yang *et al*. (1999), Hines *et al*. (2000), Smith *et al*. (2001), Rusticucci and Kousky (2002), and Flocas *et al*. (2004). These studies suggested that parameterization of physical processes is what limits the skill of both GCMs and reanalysis data in reproducing rainfall as observed. Rainfall data from both NCEP reanalysis and CRU observation were used for comparisons. The rainfall from NCEP was particularly used to enhance consistency in the study because its

large-scale circulation which is more realistic was used in the models validation of the mean state of the synoptic circulation.

Various metrics used to evaluate the seasonal forecasts from CAM3 and HadAM3 models during the recent El Niño and La Niña years showed that models' skill in predicting seasonal rainfall varies from one sub-region to the other. Although, the model forecasts showed bias when compared with observed frequencies, they demonstrated some skill over southern Africa. On the other hand, the low skill over the sub-regions (especially over the Western Cape) during the La Niña year could generally be partly attributed to the increased chaotic instability associated with rainfall. More specifically, at the peak of the summer season, when the ITCZ is at the southern part of Africa, tropical circulation dominates implying a more direct influence from local forcing mechanisms on the regional rainfall. GCMs are limited in resolving important sub-grid scale features such as clouds and topography and in capturing the effect of local forcings in areas of complex surface physiography. This limitation can greatly influence the performance of models in regional climate simulation.

This study suggests that there are significant limitations in the performances of the models in simulating atmospheric processes over southern Africa. Each model has different parameterization schemes and physics, thus having different internal variability and biases associated with it. Typical examples include the overestimation of rainfall over the western part of southern Africa simulated by CAM3 during summer and the underestimation of rainfall by HadAM3 in many parts of the region in all seasons. GCM horizontal resolution is known to play a role in model accuracy by reducing climate drift (Palmer *et al*., 1990; Tibaldi *et al*., 1990) and capturing observed atmospheric processes better (Stratton, 1999; Chandrasekar *et al*., 1999). The biases and errors noted serve a useful purpose, being in essence pointers to those aspect of the models which need improvement. Models' physical parameterization and convective scheme may be improved to address their limitations.

A necessary condition for confidence in a seasonal forecast of a region's climate is that the model should be able to adequately simulate past and present climate. In addition, the judgment of whether a climate model is skillful or not does not come from its prediction of the future, but from its ability to replicate the mean climatic

conditions, climate variability and transient changes for which we have observations; and from its ability to simulate well-understood climate processes. In the thesis, it has been demonstrated that CAM3 and HadAM3 are able to represent the climate conditions of southern Africa and the variability therein but with some bias. There is evidence that both models can be used for reliable seasonal forecasts of rainfall and temperature over southern Africa if the models are improved. The thesis focused on model performance and how the performance may affect its seasonal forecast skills. The work did not consider the errors that may be associated with the models' internal physics. However, CAM3 has a peculiar error, which is attributed to the convective scheme used in the simulation, and which could limit its forecast skill.

Given that the seasonality of rainfall varies greatly from one region to another over southern Africa, it is difficult to explain the mean seasonal rainfall of the entire region. The study again used rainfall from four different sub-regions of southern Africa for further analyses of the models' potentials. In most cases, the variation in regional rainfall was well simulated by the models but their inability to simulate the correlation between regional rainfall and SST indicates that the models do not simulate realistic teleconnections for the regions. A good example is the rainfall-SST correlation over the North Eastern part of the region, which gives a good variability in the regional rainfall pattern but has poor correlation coefficient with global SST. As the boundary conditions used to generate the seasonal forecasts are from the global SST, this poor representation of the teleconnections could be a key determinant of the models' limitation to produce skillful seasonal forecasts. This recommend the need to assess GCMs' relationship with SSTs before used to produce seasonal forecasts.

7.2 Caveats

As with all exploratory studies, this body of work is not without caveats and assumptions that should be taken into consideration when interpreting the results. Limiting issues regarding but not limited to general model simulations and seasonal forecasting are mentioned in the paragraphs below.

The ensemble approach used to run each simulation is limited in its ability to capture the full range of uncertainties in the models' representation of the true climate system (Houtekamer and Lefaivre, 1997). In general, because the true climate system is highly complex, it remains fundamentally impossible to describe all its processes in a climate model, no matter how complex the model itself is.

In addition, seasonal forecast systems suffer from biases in location and intensity of rainfall over southern Africa which require correction especially if used for impacts modeling. Bias corrections have the advantage of maintaining the spatial coherence of precipitation anomalies. They are particularly useful on regional scales with a dominant mode of variability that could be well represented by models. This thesis investigated how the models represent synoptic features and rainfall forecast over southern Africa and no attempt was made for bias correction of the models since that is more applicable to impacts studies.

7.3 Recommendations

It is expected that most of the remaining uncertaintities in model simulations of the features will be difficult to reduce even when models are improved, because uncertainities are due to random and stochastic fluctuations. The gap between model simulations and the real climate may never be completely closed, but models will continue to be important tools for improving our understanding of the climate. However, if the forecasting community aims to provide more skillful forecasts at the seasonal time scale, then further studies with a focus on the evaluation of different global models should provide a more robust understanding of the connection between regional rainfall and global SST.

Although there is low predictability of rainfall over southern Africa due to its high variability over the region, GCMs are able to reproduce the controlling circulation features. If the link between the circulation features and the local features is well understood, downscaling methods could be developed and applied more effectively to predict regional rainfall. Seasonal forecasts are still far from perfect, thus more research is needed towards improving their skills over southern Africa. The results

obtained in the thesis highlight the critical shortcomings of GCMs to be used for seasonal forecasting over southern Africa. At present the only apparent approach to such end user needs appears to be some form of downscaling, either empirical or through nested models.

REFERENCES

Anderson, D.L.T. (2008). Overview of Seasonal Forecasting. *Seasonal Climate: Forecasting and Managing Risk.* NATO Science Series: IV: Earth and Environmental Sciences. Springer Netherlands. 82, 45-65.

Anderson, J. and Stern, W. (1996). Evaluating the Potential Predictive Utility of Ensemble Forecasts. *Journal of Climate*, 9(2):260–269.

Anyah, R., Semazzi, F. and Xie, L. (2006). Simulated Physical Mechanisms Associated with Climate Variability over Lake Victoria Basin in East Africa. *Monthly Weather Review*, 134(12):3588–3609.

Asnani, G.C. (1993). Tropical meteorology. Noble Printers, Pune Chang CP (1977) Some theoretical problems of planetary scale monsoons. *Pure Appl Geophys* 115:1089–1109.

Bard, E. (2002). Climate shock: Abrupt changes, over millennial time scales. *Physics Today*, 55(12), 32-38.

Barnston, A. (1994). Linear Statistical Short-Term Climate Predictive Skill in the Northern Hemisphere. *Journal of Climate*, 7(10):1513–1564.

Barnston, A., Kumar, A., Goddard, L., and Hoerling, M. (2005). Improving seasonal prediction practices through attribution of climate variability. *Bulletin of the American Meteorological Society*, 86(1):59–72.

Barnston, A., Mason, S., Goddard, L., Dewitt, D., and Zebiak, S. (2003). Multimodel Ensembling in Seasonal Climate Forecasting at IRI. *Bulletin of the American Meteorological Society*, 84(12):1783–1796.

Barnston, A., Thiao, W. and Kumar, V. (1996). Long-Lead Forecasts of Seasonal Precipitation in Africa Using CCA. *Weather and Forecasting*, 11(4):506–520.

Bengtsson, L., Schlese, U., Roeckner, E., Latif, M., Barnett, T., and Graham, N. (1993). A Two-Tiered Approach to Long-Range Climate Forecasting. *Science*, 261(5124):1026–1029.

Bonnardot, V., Planchon, O. and Cautenet, S. (2005). The sea breeze development under an offshore synoptic wind in the South Western Cape and implications over the Stellenbosch wine-producing area. *Theor. Appl. Climatol*., 81, 203–218.

Brier, G. (1950). Verification of forecasts expressed in terms of probability. *Monthly Weather Review*, 78:1–3.

Browning, K. and Mason, J. (1980). Air motion and precipitation growth in frontal systems. *Pure and Applied Geophysics*, 119(3):577–593.

Bryan, K. (1984). Accelerating the convergence to equilibrium of ocean-climate models. J. Phys Oceanogr., 14 666-673.

Buizza, R., Miller, M. and Palmer, T.N. (1999). Stochastic representation of model uncertainties in the ECMWF EPS. *Quarterly Journal of the Royal Meteorological Society*, 125, No. 560, 2887-2908.

Cane, M.A., Zebiak, S.E. and Dolan, S.C. (1986). Experimental forecasts of El Nino. *Nature*, 321, 827-832.

Cantelaube, P. and Terres, J.M. (2005). Seasonal weather forecasts for crop yield modelling in Europe. *Tellus*, 57 (3):476–487.

Cavalcanti, I.F.A. Pezzi, L.P. Nobre P. Sampaio G., Camargo Jr H. (1998). Climate prediction of precipitation in Brazil for the Northeast raining season (MAM) 1998. *Experimental Long -Lead Forecast Bulletin*, **7**, No. 1; 24-27.

Cavazos, T. (1999). Large-scale circulation anomalies conducive to extreme precipitation events and derivation of daily rainfall in northeastern Mexico and southeastern Texas. *Journal of Climate*, 12:1506–1523.

Cavazos, T. (2000). Using self-organizing maps to investigate extreme climate events: An application to wintertime precipitation in the Balkans. *Journal of Climate*, 13:1718–1732.

Chandrasekar, A., Rao, D.V.B. and Kitoh, A. (1999). Effect of horizontal resolution of Asian summer monsoons using the MRI GCM-II. *Pap. Meteor. Geophys.*, 50, 65–80.

Charney, J. and Shukla, J. (1981). Predictability of monsoons. *Monsoon Dynamics*, pages 99–109.

Chase, B.M., and Meadows, M.E. (2007). Late Quaternary dynamics of southern Africa's winter rainfall zone: *Earth-Science Reviews*, 84, 103–138, doi: 10.1016/j. earscirev.2007.06.002.

Collins, W.D., Ramaswamy, V., Schwarzkopf, M.D., Sun, Y., Portmann, R.W., Fu, Q., Casanova, S.E.B., Dufresne, J.-L., Fillmore, D.W., Forster, P.M.D., Galin, V.Y., Gohar, L.K., Ingram, W.J., Kratz, D.P., Lefebvre, M.-P., Li, J., Marquet, P., Oinas, V., Tsushima, Y., Uchiyama, T., and Zhong, W.Y. (2006). Radiative forcing by well-mixed greenhouse gases: Estimates from climate models in the Intergovernmental Panel on Climate Change (IPCC) Fourth Assessment Report (AR4). *J. Geophys. Res.*, **111**, D14317, doi:10.1029/2005JD006713.

Collins, M. and Senior, C.A. (2002). Projections of future climate change. *Weather*, 57, pp. 283–287.

Collins, W., Rasch, P., Boville, B., Hack, J., McCaa, J., Williamson, D., Kiehl, J., Briegleb, B., Bitz, C., Lin, S., *et al*. (2004). Description of the NCAR Community Atmosphere Model (CAM 3.0). *NCAR Technical Note*. National Center for Atmospheric Research, Boulder, Colorado, http://www. ccsm.ucar.edu/models/atm-cam.

Cook, K. (2000). The South Indian convergence zone and interannual rainfall variability over southern Africa. *Journal of Climate*, 13:3789–3804.

Crimp, S. (1997). A Sea-Surface Temperature Sensitivity test using the Colorado State University Regional Atmospheric Modelling System. *South African Journal of Science*, 93(3):133–141.

d'Abreton, P. and Tyson, P. (1996). Three-dimensional kinematic trajectory modelling of water vapour transport over southern Africa. *WATER SA-PRETORIA*-, 22:297–306.

Doblas-Reyes, F.J., Hagedorn, R. and Palmer, T.N. (2005). The rationale behind the success of multi-model ensembles in seasonal forecasting-II. Calibration and combination, *Tellus* A, 57(3): 234—252. Blackwell Synergy.

Engelbrecht, F., McGregor, J., and Engelbrecht, C. (2009). Dynamics of the Conformal-Cubic Atmospheric Model projected climate-change signal over southern Africa. *International Journal of Climatology*, 29(7):1013–1033.

Epstein, E. (1969). The Role of Initial Uncertainties in Predicion. *Journal of Applied Meteorology*, 8(2):190–198.

FAO corporate Document Repository. (1994). Small water bodies and their fisheries in southern Africa. *CIFA Technical Paper*, T29(76). http://www.fao.org/docrep/008/v5345e/v5345e00.htm

Feddersen, H., Navarra, A., and Ward, M. (1999). Reduction of Model Systematic Error by Statistical Correction for Dynamical Seasonal Predictions. *Journal of Climate*, 12(7):1974–1989.

Ferro, C. (2007). Comparing probabilistic forecasting systems with the Brier score. *Weather and forecasting*, 22:1076–1088.

Flocas, H., Tolika, K., Anagnostopoulou, C., Patrikas, I., Maheras, P., Vafiadis, M. (2004). Evaluation of maximum and minimum temperature NCEP-NCAR reanalysis data over the Greek area. *Theoretical and Applied Climatology* 80: 49–65.

Freiman, M.T. and Tyson, P.D. (2000). The thermodynamic structure of the atmosphere over South Africa: Implications for water vapour transport. *Water SA,* 26, 153–158.

Fuenzalida, H., Sanchez, R. and Garreaud, R. (2005). A climatology of cuto lows in the a Southern Hemisphere *Journal of Geophysical Research*, 110, D1801, doi: 10.1029/2005JD005934

Garreaud, R. (2000). Cold Air Incursions over Subtropical South America: Mean Structure and Dynamics. *Monthly Weather Review*, 128(7):2544–2559.

Garstang, M., Tyson, P., Swap, R., Edwards, M., Kallberg, P., and Lindesay, J. (1996). Horizontal and vertical transport of air over southern Africa, *Journal of Geophysical Research* 10 (D19), 23,721-23,736.

Gates, W.L. (1985). The use of general circulation models in the analysis of the ecosystem impacts of climatic change. *Clim Change* 7:267-284.

Giorgi, F. and Mearns, L. (1999). Regional climate modeling revisited: an introduction to the special issue. *Journal of Geophysical Research*, 104(D6):6335–6352.

Goddard, L. and Graham, N.E. (1999). The importance of the Indian Ocean for simulating rainfall anomalies over eastern and southern Africa. *J. Geophys. Res*., 104, 19099-19116.

Goddard, L. and Mason, S. (2002). Sensitivity of seasonal climate forecasts to persisted SST anomalies. *Climate Dynamics*, 19(7):619–632.

Goddard L, Mason S.J., Zebiak S.E., Ropelewski C.F., Basher R, Cane M.A. (2001) Current approaches to seasonal to interannual climate predictions. *Int J Climatol* 21: 1111-1152.

Goddard, L., Mason, S., Zebiak, S., Ropelewski, C., Basher, R., and Cane, M. (2001). Current approaches to seasonal to interannual climate predictions. *International Journal of Climatology*, 21(9):1111–1152.

Gordon, C., Cooper, C., Senior, C., Banks, H., Gregory, J., Johns, T., Mitchell, J., and Wood, R. (2000). The simulation of SST, sea ice extents and ocean heat

transports in a version of the Hadley Centre coupled model without flux adjustments. *Climate Dynamics*, 16(2):147–168.

Grabowski,W. and Moncrieff, M. (2004). Moisture-convection feedback in the tropics. *Quart. J. Roy. Meteor. Soc*., 130 (604), 3081–3104.

Gregory, D. and Allen, S. (1991). The effect of convective scale downdroughts upon NWP and climate simulations. Preprints. *Ninth conf. on Numerical Weather Prediction*.

Gregory, D. and Rowntree, P. (1990). A mass flux convection scheme with representation of cloud ensemble characteristics and stability dependent closure. *Monthly Weather Review,* 118(17):1483–1506.

Hack, J. (1994). Parameterization of moist convection in the National Center for Atmospheric Research community climate model (CCM2). *Journal of Geophysical Research*, 99(D3):5551–5568.

Halpert, M.S. and Ropelewski, C.F. (1992). Surface temperature patterns associated with the Southern Oscillation. *J. Climate*, 5, 577-593.

Harangozo, S. and Harrison, M. (1983). On the use of synoptic data indicating the presence of cloud bands over southern Africa. *South Africa Journal of Science*, 79:413–414.

Harrison, M. (1984a). A generalized classification of South African summer rain-earing synoptic systems. *International Journal of Climatology*, 4, 547–560.

Harrison, M. (1984b). The annual rainfall cycle over the central interior of South Africa. *South Africa Geogr. Journal,* 66:47–64.

Hastenrath, S., Greischar, L., and van Heepden, J. (1995). Prediction of the Summer Rainfall over South Africa. *Journal of Climate*, 8(6):1511–1518.

Hastenrath, S. (1995). *Climate Dynamics of the Tropics.* Kluwer Academic, 488 pp.

Hewitson, B. and Crane, R. (2002). Self-organizing maps: applications to synoptic climatology. *Climate Research*, 22(1):13–26.

Hines, K.M., Bromwich, D.H. and Marshall, G.J. (2000). Artificial Surface Pressure Trends in the NCEP–NCAR Reanalysis over the Southern Ocean and Antarctica. *J. Climate*, 13, 3940–3952.

Hirst, A. and Hastenrath, S. (1983). Atmosphere-ocean mechanisms of climate anomalies in the Angola-tropical Atlantic sector. *Journal of Physical Oceanography*, 13(7):1146–1157.

Hobbs, J. (1998). Present Climates of Australia and New Zealand. In: Climates of the. Southern Continents: Present, Past and Future, (eds J.E Hobbs, J.A. Lindesay, & H.A., Bridgman), pp. 63-105. John Wiley & Sons Ltd, Chichester.

Hoerling, M.P. and Kumar, A. (2002). Atmospheric response patterns associated with tropical forcing. *J. Climate,* 15, 2184–2203.

Hoerling, M.P., Hurrell, J.W. and Xu, T. (2001). Tropical origins for recent North Atlantic climate change. *Science*, 292, 90–92.

Horel, J.D., and J.M. Wallace (1981), Planetary-scale atmospheric phenomena associated with the Southern Oscillation, *Mon. Weather Rev*., 109, 813–829.

Houtekamer, P.L., Lefaivre, L., Derome, J., Ritchie, H., Mitchell, H.L. (1996). A System Simulation Approach to Ensemble Prediction. *Monthly Weather Review*, 124, 1225–1242. doi: 10.1175/1520-0493(1996)124.

Houtekamer, P.L. and Lefaivre, L. (1997). Using ensemble forecasts for model validation. *Monthly Weather Review*, 125, 2416-2426.

Hudson, D. and Jones, R. (2002). Simulations of present-day and future climate over southern Africa using HadAM3H. *Hadley Centre Technical Note*, 38.

Hulme, M., Osborn,T.J. and Johns T.C. (1998). Precipitation sensitivity to global warming: Comparison of observations with HadCM2 simulations. *Geophysical Research Letters*, 25, 3379-3382.

Hunt, B. (1997). Prospects and Problems for Multi-Seasonal Predictions: Some Issues Arissng From a Study of 1992. *International Journal of Climatology*, 17(2):137–154.

Hurrell, J., Meehl, G.A., Bader, D., Delworth, T.L., Kirtman, B.and Wielicki, B. (2009). A unified modelling approach to climate system prediction. *Bulletin of the American Meteorological Society*, 90, 1819-1832.

IPCC (2007). Climate change 2007: Impacts, adaptation and vulnerability. IN Parry, M. L., Canzioni, O. F., Palutikof, J. P., van der Linden, P. J. & Hanson, C. E. (Eds.). Cambridge, UK, Contribution of Working Group II to the Fourth Assessment Report of the Intergovernmental Panel on Climate Change. *Cambridge University Press*.

Indeje, M., Semazzi, F.H.M. and Ogallo, L.J. (2000). ENSO signals in East African rainfall seasons. *Int. J. Climatol*., 20, 19-46.

Janowiak, J. (1988). An investigation of interannual variability in Africa, *J. Climate*, **1**, 240–255.

Jolliffe, I. and Stephenson, D.B. (2003). Forecast Verification, *A practitioner's Guide in Atmospheric Science*. Wiley & Sons Inc.

Jones, C., Gregory, J., Thorpe, R., Cox, P., Murphy, J., Sexton, D., and Valdes, P. (2005). Systematic optimisation and climate simulation of FAMOUS, a fast version of HadCM3. *Climate Dynamics*, 25(2):189–204.

Jones, D. and Simmonds, I. (1993). A climatology of Southern Hemisphere extratropical cyclones. *Climate Dynamics*, 9(3):131–145.

Jury, M. and Pathack, B. (1993). Composite climatic patterns associated with extreme modes of summer rainfall over southern Africa: 1975–1984. *Theoretical and Applied Climatology*, 47(3):137–145.

Kalnay, E., Kanamitsuand, M., Kistler, R., Collins, W., Deaven, D., Gandin, L., Iredell, M., Saha, S., WHite, G., Woollen, J., Zhu, Y., Chelliah, M., Ebisuzaki, W., Higgins, W., Janoeiah, J., Mo, K. C., Ropelewski, C., Wang, J., Leetmaa, A., Jenne,

R., and Jeseph, D. (1996). The NCEP/NCAR 40-year reanalysis project. *Bulletin of the American Meteorological Society*, 77(2):437–471.

Kang, I.S. and Yoo, J.H. (2006). Examination of multi-model ensemble seasonal prediction methods using a simple climate system. *Climate Dynamics*, 26(2):285-294, Springer.

Kiehl, J., and Ramanathan, V. (2006). Frontiers of climate modeling. *Cambridge University Press*.

Klaus, D. (1978). Spatial distribution and periodicity of mean annual precipitation south of the Sahara. *Theoretical and Applied Climatology*, 26(1):17–27.

Kraus, E. (1977). Subtropical droughts and cross-equatorial energy transports. *Monthly Weather Review*, 105(8):1009–1018.

Krishnamurti, T., Kishtawal, C., LaRow, T., Bachiochi, D., Zhang, Z., Williford, C., Gadgil, S., and Surendran, S. (1999). Improved Weather and Seasonal Climate Forecasts from Multimodel Superensemble. *Science*, 285(5433):1548.

Kumar, A. and Hoerling, M. (1998). Annual cycle of Pacific–North American seasonal predictability associated with different phases of ENSO. *Journal of Climate*, 11(12):3295–3308.

Landman, W. and Beraki, A. (2010). Multi-model forecast skill for mid-summer rainfall over southern Africa. *International Journal of Climatology*, n/a. DOI: 10.1002/joc.2273

Landman, W. and Goddard, L. (2002). Statistical Recalibration of GCM Forecasts over Southern Africa Using Model Output Statistics. *Journal of Climate*, 15(15):2038–2055.

Landman, W.A., Kgatuke, M.-J., Mbedzi, M., Beraki, A., Bartman, A., and Piesanie, A. (2009). Performance comparison of some dynamical and empirical downscaling methods for South Africa from a seasonal climate modelling perspective. *International Journal of Climatology*, 29:1535–1549.

Landman, W. and Mason, S. (1999). Operational long-lead prediction of South African rainfall using canonical correlation analysis. *International Journal of Climatology*, 19(10):1073–1090.

Landman, W. and Mason, S. (2001). Forecasts of Near-Global Sea Surface Temperatures Using Canonical Correlation Analysis. *Journal of Climate*, 14(18):3819–3833.

Landman, W. and Tennant, W. (2000). Statistical downscaling of monthly forecasts. *International Journal of Climatology*, 20(13):1521–1532.

Latif, M, Barnett T.P, Cane M.A, Flügel M, Graham N.E, von Storch H, Xu J.S, Zebiak SE (1994) A review of ENSO prediction studies. *Clim Dyn* 9: 167 179.

Latif M, Anderson DLT, Barnett TP, Cane MA, Kleeman R, Leetmaa A, O'Brien J, Rosati A, Schneider E (1998) A review of the predictability and prediction of ENSO. *J Geophys Res* 103: 14375 14393.

Leith, C. (1974). Theoretical Skill of Monte Carlo Forecasts. *Monthly Weather Review*, 102(6):409–418.

Lin, S. and Rood, R. (1996). Multidimensional flux-form semi-Lagrangian transport schemes. *Monthly Weather Review*, 124(9):2046–2070.

Lindesay, J.A. (1988). South African rainfall, the Southern Oscillation and a Southern Hemisphere semi-annual cycle. *J. Climatol.,* 8, 17–30.

Lindesay, J.A., Harrison, M.S.J., Haffner M.P. (1986). The Southern Oscillation and South African rainfall. *South African Journal of Science* 82: 196–198.

Lorenz, E. (1982). Atmospheric predictability experiments with a large numerical model. *Tellus*, 24.

Madden, R.A., and Julian, P.R. (1972). Description of global scale circulation cells in the Tropics with 40–50 day period. *J. Atmos. Sci.,* 29**,** 1109–1123.

Madden, R.A., and Julian, P.R. (2005). Historical perspective. *Intraseasonal Variability in the Atmosphere–Ocean Climate System,* W. K.-M. Lau and D. Waliser, (Eds.), Springer-Praxis, 1–16.

Mason, S. (1998). Seasonal forecasting of South African rainfall using a non-linear discriminant analysis model. *International Journal of Climatology*, 18(2):147–164.

Mason, S. (2004). On using climatology as a reference strategy in the Brier and ranked probability skill scores. *Monthly Weather Review*, 132:1891–1895.

Mason, S., Goddard, L., Graham, N., Yulaeva, E., Sun, L. and Arkin, P. (1999). The IRI seasonal climate prediction system and the 1997/98 El Nino event. *Bulletin of the American Meteorological Society*, 80(9):1853–1873.

Mason, S., Joubert, A., Cosijn, C. and Crimp, S. (1996). Review of seasonal forecasting techniques and their applicability to Southern Africa. *WATER SA-PRETORIA*-, 22:203–210.

Mason, S. and Jury, M. (1997). Climatic variability and change over southern Africa: a reflection on underlying processes. *Progress in Physical Geography*, 21(1):23.

Mason, S. and Mimmack, G. (2002). Comparison of some statistical methods of probabilistic forecasting of ENSO. *Journal of Climate*, 15:8–29.

Matheson, J. and Winkler, R. (1976). Scoring rules for continuous probability distributions. *Management Science*, 22(10):1087–1096.

McGregor, G. and Nieuwolt, S. (1998). Tropical climatology: an introduction to the climates of the low latitudes. ed. 2. John Wiley and Sons, England.

McGregor, J. (1997). Regional climate modelling. *Meteorology and Atmospheric Physics*, 63(1), 105-117.

Misra, J. (1991). Phase synchronization, *Information Processing Letters* 38 (2), pp. 101–105.

Mitchell, T., Carter, T., Jones, P., Hulme, M. and New, M. (2003). A comprehensive set of high-resolution grids of monthly climate for Europe and globe; The observed records (1901-2000) and 16 scenarios (2001-2100). *Journal of Climate*.

Mo, R., and Straus, D.M. (2002). Statistical–dynamical seasonal prediction based on principal component regression of GCM ensemble integrations. *Mon. Wea. Rev.*, 130, 2167–2187.

Mo, R., Fyfe, J. and Derome, J. (1998). Phase-locked and asymmetric correlations of the wintertime atmospheric patters with ENSO, Atmosphere-Ocean, 36, 213-239.

Murphy, A. (1973). A new vector partition of the probability score. *Journal of Applied Meteorology*, 12:595600.

Murphy, A. (1993). What Is a Good Forecast? An Essay on the Nature of Goodness in Weather Forecasting. *Weather and Forecasting*, 8(2):281–293.

Murphy, A. (1996). The Finley affair: A signal event in the history of forecast verification. *Weather and Forecasting*, 11(1):3–20.

Murphy, B., Marsiat, I., and Valdes, P. (2002). Atmospheric contributions to the surface mass balance of Greenland in the HadAM3 atmospheric model. *Journal of Geophysical Research* (Atmospheres, 107(D21).

Mutai, C.C. and Ward, M.N. (2000). East African rainfall and the tropical circulation/convection on intraseasonal to interannual timescales. *J. Climate*, **13**, 3915-3939.

Mutai, C.C., Ward, M.N. and Colman, A.W. (1998). Towards the prediction of the East African short rains based on sea-surface temperature and atmosphere coupling. *Int. J. Climatol.*, 18, 975-997.

Nakamura, H. and Shimpo, A. (2004). Seasonal variations in the Southern Hemisphere storm tracks and jet streams as revealed in a reanalysis dataset. *Journal of Climate*, 17, 1828–1844.

New, M., Hulme, M. and Jones, P.D., 2000: Representing twentieth century space-time climate variability. Part 2: development of 1901-96 monthly grids of terrestrial surface climate. *Journal of Climate* **13**, 2217-2238.

Newell, R. and Kidson, I. (1984). African mean wind changes between Sahelian wet and dry periods. *International Journal of Climatology*, 4:27–33.

Nicholson, S.E. (2000). The nature of rainfall variability over Africa on time scales of decades to millenia. *Global and planetary change*, 26(1-3):137–158.

Nicholson, S.E. (1986). The spatial coherence of African rainfall anomalies-interhemispheric teleconnections, *J. Clim. Appl. Meteorol.*, **25**, 1365–1381.

Nicholson, S., Ba, M. and Kim, J. (1996). Rainfall in the Sahel during 1994. *Journal of Climate*, 9(7):1673–1676.

Nicholson, S.E. and Entekhabi, D. (1986). The quasi-periodic behavior of rainfall variability in Africa and its relationship to the Southern Oscillation. *Journal of Climate and Applied Meteorology* 34: 331–348.

Nicholson, S.E and Selato, J.C. (2000). The influence of La Niña on African rainfall. *International Journal of Climatology* 20: 1761–1776.

Nieto, R., Gimeno, L., d la Torre, L., Ribera, P., Gallego, D., Garcı´Herrera, R., and Garcı´, J. (2005). Climatological features of cut-off low systems in the northern hemisphere. *Journal of Climate*, 108:3085–3103.

North, G.R. (1975). Theory of energy-balance climate models. *J. Atmos. Sci.,* 32, 2033–2043.

North, G.R. (1984). The small ice cap instability in diffusive climate models. *J. Atmos. Sci.*, 41, 3390–3395.

Ogallo, L.A. (1994). Validity of the ENSO-related impacts in Eastern and Southern Africa, in *Proceedings of the Workshop on ENSO/FEWS*, Budapest, Hungary, pp. 179–184

Ogallo, L.A., Janowiak, J.E. and Halpert, M.S. (1988). Teleconnections between east African seasonal rainfall and global sea surface temperature anomalies. *Journal of the Meteorological Society of Japan*, 66(6), 807-822.

Palmer, T. N., C. Brankovic, F. Molteni, S. Tibaldi, L. Ferranti, A. Hollingsworth, U. Cubasch, and E. Klinker, (1990). The European Centre for Medium-Range Weather Forecasts (ECMWF) program on extended-range prediction. *Bull. Amer. Meteor. Soc.*, 71, 1317–1330.

Palmer, T., Alessandri, A., Andersen, U., Cantelaube, P., Davey, M., D´l´cluse, P., D´qu´, M., D´ E., Doblas-Reyes, F., Feddersen, H., *et al*. (2004). Development of European Multimodel Ensemble system for seasonal to interannual prediction (DEMETER). *Bulletin of the American Meteorological Society*, 85(6):853–872.

Palmer, T. and Anderson, D. (1994). The prospects for seasonal forecasting-A review paper. *Quarterly Journal of the Royal Meteorological Society*, 120(518):755–793.

Palmer, T., Doblas-Reyes, F., Hagedorn, R., and Weisheimer, A. (2005). Probabilistic prediction of climate using multi-model ensembles: from basics to applications. *Philosophical Transactions- Royal Society of London Series B Biological Sciences*, 360(1463):1991–1998.

Philander, S. (1990). El Niño, La Niña, and the Southern Oscillation: Academic Press.

Philander, G. (1989). *El Niño. La Niña, and the Southern Oscillation.* Academic Press, San Diego, California.

Pocernich, M. (2009). Verification Package: examples using weather forecasts. R package, 408.

Pohl, B., Richard, Y. and Fauchereau, N. (2007). Influence of the Madden-Julian Oscillation on Southern African Summer Rainfall. *American Meteorological Society.* DOI: 10.1175/JCLI4231.1

Pohl, B, Fauchereau, N., Richard, Y., Rouault, M., Reason, C.J.C. (2009). Interactions between synoptic, intraseasonal and interannual convective variability over southern Africa. *Climate Dynamics* 33: 1033–1050.

Pope, V., Gallani, M., Rowntree, P., and Stratton, R. (2000). The impact of new physical parametrizations in the Hadley Centre climate model: HadAM3. *Climate Dynamics*, 16(2):–146.

Preston-Whyte, R.A., Tyson, P.D. (1988). *The Atmosphere and Weather of Southern Africa*, Oxford University Press: Cape Town.

R Development Core Team (2008). R: A Language and Environment for Statistical Computing. R Foundation for Statistical Computing, Vienna, Austria. ISBN 3-900051-07-0.

Rao, V.B., Chapa, S.R. Fernandez, J.P.R. and Franchito, S.H. (2002). A diagnosis of rainfall over South America during the 1997/98 El Niño event. Part II: Roles of water vapor transport and stationarywaves. *J. Climate,* 15**,** 512–521.

Rasch, P. and Kristjansson, J. (1998). A comparison of the CCM3 model climate using a diagnosed and predicted condensate parameterizations. *Journal of Climate*, 11(7):1587–1614.

Rasmusson, E.M. and Carpenter, T.H. (1982). Variations in tropical sea surface temperature and surface wind fields associated with the Southern Oscillation/El Niño. *Mon Wea. Rev*., 110, 354-384.

Rasmusson, E.M. and Wallace, J.M. (1983). Meteorological aspects of the El Niño/Southern Oscillation. *Science*, 222, 1195-1202.

Reason, C. (2002). Sensitivity of the southern African circulation to dipole sea-surface temperature patterns in the south Indian Ocean. *International Journal of Climatology*, 22(4):377–393.

Reason, C. and Jagadheesha, D. (2005). A model investigation of recent ENSO impacts over southern Africa. *Meteorology and Atmospheric Physics*, 89(1):181–205.

Reynolds, R. (1988). A real-time global sea surface temperature analysis. *Journal of Climate*, 1(1):75–87.

Reynolds, R.W. and T. M. Smith, (1994). Improved global sea surface temperatureanalyses using optimum interpolation. *J. Climate*, 7, 929–948.

Reynolds, R. W., N. A. Rayner, T. M. Smith, D. C. Stokes and W. Wang, (2002). An improved in situ and satellite SST analysis for climate. *J. Climate*, 15, 1609-1625.

Richardson, D. (2000). Skill and relative economic value of the ECMWF ensemble prediction system. *Quarterly Journal of the Royal Meteorological Society*, 126(563):649–667.

Robock, A. (2002). Pinatubo eruption: The climatic aftermath, *Science*, 295, 1242-1244.

Roca, R., Lafore, J., Piriou, C., and Redelsperger, J. (2005). Extratropical dry-air intrusions into the West African monsoon midtroposphere: An important factor for the convective activity over the Sahel. *Journal of the Atmospheric Sciences*, 62:390–407.

Rocha, A. and Simmonds, I. (1997). Interannual variability of south-eastern African summer rainfall. Part 1: relationships with air-sea interaction processes. *International Journal of Climatology*, 17, 235–265. doi: 10.1002/(SICI)1097-0088(19970315).

Roncoli, C., Ingram, K. Kirshen P. (2001). The cost and risks of coping with drought: livelihood impacts and farmers' responses in Burkina Faso. *Climate Research*, 19, 119-132.

Ropelewski, C.F., Halpert, M.S. (1987). Global and regional scale precipitation associated with El Nino:Southern Oscillation. *Monthly Weather Review*, 115: 985–996.

Rusticucci, M.M., Kousky, V.E. (2002). A Comparative study of maximum and minimum temperatures over Argentina: NCEP-NCAR reanalysis *versus* station data. *Journal of Climate* 15: 2089–2101.

Shongwe, M.E., Landman, W.A. and Mason, S.J. (2006). Performance of recalibration systems for GCM forecasts for southern Africa. *Int. J. Climatol*., 17, 1567–1585.

Shukla, J. (1998). Predictability in the Midst of Chaos: A Scientific Basis for Climate Forecasting. *Science*, 282(5389):728.

Singleton, A. and Reason, C.J.C. (2007). Variability in the characteristics of cut-off low pressure systems over subtropical southern Africa. *International Journal of Climatology*, 27(3):295–310.

Singleton, A. and Reason, C.J.C. (2006). Numerical simulations of a severe rainfall event over the Eastern Cape coast of South Africa: sensitivity to sea surface temperature and topography. *Tellus A* 58(3), 355–367.

Sloan, L.C. (2006). A framework for regional modeling of past climates. *Theoretical and Applied Climatology*, 86(1-4), 271-279. doi: DOI 10.1007/s00704-005-0207-3.

Soden, B.J., Held, I.M. (2005). An assessment of Climate Feedbacks in Coupled Ocean-Atmosphere Models. *J. Climate,* 19**,** 3354-3360.

Smith, T.M., and Livezey, R.E. (1999). GCM systematic error correction and specification of the seasonal mean Pacific–North America region atmosphere from global SSTs. *J. Climate*, 12, 273–288.

Smith, R. and Reeder, M. (1988). On the Movement and Low-Level Structure of Cold Fronts. *Monthly Weather Review*, 116(10):1927–1944.

Smith, S.R., Legler D.M., Verzone K.V. (2001). Quantifying uncertainties in NCEP reanalyses using High-Quality research vessel observations. *Journal of Climate* 14: 4062–4072.

Stanski, H.R., Wilson, L.J. and Burrows, W.R. (1989). *Survey of common verification methods in meteorology*. World Weather Watch Tech. Rept. No.8, WMO/TD No.358, WMO, Geneva, 114 pp.

Steinfeld H., Gerber P., Wassenaar T., Castel V., Rosales M., de Haan C. (2006). *Livestock's Long Shadow: Environmental Issues and Options.* United Nations Food and Agricultural Organization. Rome, Italy.

Stockdale TN, Busalacchi AJ, Harrison DE, Seager R (1998) Ocean modeling for ENSO. *J Geophys Res* 103: 14325 14355

Stratton, R.A. (1999). A high resolution AMIP integration using Hadley Center model HadAm2b, *Climate Dynamics,* 15, 9-28.

Sundqvist, H. (1988). Parameterization of condensation and associated clouds in models for weather prediction and general circulation simulation. *Physically-based modelling and simulation of climate and climatic change*, pages 433–461.

Suzuki, T. (2010). Seasonal variation of the ITCZ and its characteristics over central Africa. *Theoretical and Applied Climatology*, pages 1–22.

Talagrand, O., Vautard, R. and Strauss, B. (1999). Evaluation of probabilistic prediction systems. *Proc. Workshop on Predictability,* Reading, United Kingdom, ECMWF, 1–25.

Taljaard, J. (1986). Change of rainfall distribution and circulation patterns over Southern Africa in summer. *International Journal of Climatology*, 6(6):579–592.

Taljaard, J. and Bureau, W. (1985). Cut-off lows in the South African region. *Weather Bureau, Dept. of Transport*. Paper 14, 153 pp.

Tazalika, L. and Jury, M. R. (2008). Intra-seasonal rainfall oscillations over central Africa space-time character and evolution. *Theoretical and Applied Climatology,* (94):67-80.

Tennant, W. (2003). An assessment of intraseasonal variability from 13-yr GCM simulations. *Monthly Weather Review*, 131:1975–1991.

Tennant, W. and Hewitson, B. (2002). Intra-seasonal rainfall characteristics and their importance to the seasonal prediction problem. *International Journal of Climatology*, 22(9):1033–1048.

Tippett, M.K., Barlow, M. and Lyon, B. (2003). Statistical correction of Central Southwest Asia winter precipitation simulations. *Int. J. Climatol.*, 23**,** 1421–1433.

Thomson, M.C., Doblas-Reyes, F.J., Mason, S.J., Hagedorn, R. Connor, S. J., Phindela, T., Morse, A.P., Palmer, T. N. (2006). Malaria early warnings based on seasonal climate forecasts from multi-model ensembles. *Nature* 439, 576-579.

Thorncroft, C. and Flocas, H. (1997). A case study of Saharan cyclogenesis. *Monthly Weather Review*, 125:1147–1165.

Tibaldi, S., Palmer, T.N. Brankovic, C. and Cubasch, U. (1990). Extended range prediction with ECMWF models: Influence of horizontal resolution on systematic error and forecast skill. *Quart. J. Roy. Meteor. Soc.*, 116, 835–866.

Todd, M., Washington, R. and Palmer, P. I. (2004). Water vapour transport associated with tropical-temperate trough systems over Southern Africa and the southwest Indian Ocean. *Int. J. Climatol.,* 24**,** 555–568.

Tomczak, M, Godfrey J.S. (2003). Regional oceanography: an introduction. 2nd ed, Daya, Delhi.

Tompkins, A. M., and Berner, J. (2008). A stochastic convective approach to account for model uncertainty due to unresolved humidity variability, *Journal of Geophysical Research,* 113, D18101, doi:10.1029/2007JD009284.

Toth, Z. and Kalnay, E. (1993). Ensemble Forecasting at NMC: The Generation of Perturbations. *Bulletin of the American Meteorological Society*, 74(12):2317–2330.

Toth, Z. and Kalnay, E. (1997). Ensemble Forecasting at NCEP and the Breeding Method. *Monthly Weather Review*, 125(12):3297–3319.

Toth, Z., Zhu, Y., Marchok, T., Tracton, S. and Kalnay, E. (1998). Verification of the NCEP global ensemble forecasts. Preprints, 12th Conf. on Numerical Weather Prediction, Phoenix, AZ, *Amer. Meteor. Soc.*, 286-289.

Toth, Z., Talagrand, O., Candille, G., and Zhu, Y. (2003). Probability and ensemble forecasts. Forecast Verification: A Practitioners Guide in Atmospheric Science. Jolliffe I. T. and Stephenson, D. B., Wiley, 137-163.

Tyson, P. (1980). Temporal and spatial variation of rainfall anomalies in Africa south of latitude 22 during the period of meteorological record. *Climatic Change*, 2(4):363 371.

Tyson, P. (1981). Atmospheric circulation variations and the occurrence of extended wet and dry spells over southern Africa. *International Journal of Climatology*, 1(2).

Tyson, P. (1986). Climatic change and variability in southern Africa. Oxford University Press, Cape Town.

Tyson, P. and Preston-Whyte, R. (2000). The Weather and Climate of Southern Africa. Oxford University Press Southern Africa.

Tyson, P., Sturman, A., Fitzharris, B., Mason, S., and Owens, I. (1997). Circulation changes and teleconnections between glacial advances on the west coast of New Zealand and extended spells of drought years in South Africa. *International Journal of Climatology*, 17(14):1499–1512.

Uccellini, L. and Johnson, D. (1979). The coupling of upper and lower tropospheric jet streaks and implications for the development of severe convective storms. *Monthly Weather Review,* 107(6):682–703.

Usman, M. and Reason, C. (2004). Dry spell frequencies and their variability over southern Africa. *Climate Research*, 26(3):199–211.

van den Heever, S., D'Abreton, P., and Tyson, P. (1997). Numerical simulation of tropical-temperate troughs over southern Africa using the CSU RAMS model. *South African Journal of Science*, 93:359–365.

Walker, G.T. (1918). Correlation in seasonal variations of weather. *Quarterly Journal of the Royal Meteorological Society.* 44**,** 223–224.

Wang, B., (2005). Theory. Intraseasonal Variability in the Atmosphere–Ocean Climate System, W. K. M. Lau and D. E. Waliser, Eds., *Springer,* Berlin.

Wang, B., Kang, I., and Lee, J. (2004). Ensemble Simulations of Asian-Australian Monsoon Variability by 11 AGCMs. *Journal of Climate*, 17(4):803–818.

Washington, R., Todd, M.C. (1999). Tropical temperate links in southern African and southwest Indian Ocean daily rainfall. *International Journal of Climatology* 19: 1601–1616.

Widmann, M., Bretherton, C. and Salathé Jr., E.P. (2003) Statistical precipitation downscaling over the northwestern United States using numerically simulated precipitation as a predictor. *J. Climate*, 16**,** 799–816.

Wilks, D. (1995). Probability and Statistics in the Atmospheric Sciences. Academic Press, 467 pp.

Wilks, D. (2006). Comparison of ensemble-MOS methods in the Lorenz'96 setting. *Meteorological Applications*, 13(03):243–256.

WMO/TD-No. 876 Proceedings of the first WCRP international conference on reanalyses (Silver Spring, Maryland, USA, 27-31 October 1997).

Xie, P. and Arkin, P. A. (1996). Analyses of global monthly precipitation using gauge observations, satellite estimates and numerical model predictions. *Journal of Climate*. 9,840-858.

Xie, P. and Arkin, P. (1997). Global Precipitation: A 17-Year Monthly Analysis Based on Guage Observations, Satellite Estimates, and Numerical Model Outputs. *Bulletin of the American Meteorological Society*, 78:2539–2558.

Yang, S.K., Hou Y.T., Miller A.J., Campana K.A. (1999). Evaluation of the Earth radiation budget in NCEP-NCAR reanalysis with ERBE. *Journal of Climate* 12: 477–493.

Yoo J.H. and Kang I.S. (2005). Theoretical examination of a multi-model composite for seasonal prediction. *Geophysical Research Letters*, 32.

Zhang, C. (2005). Madden–Julian Oscillation. *Reviews of Geophysics*, 43, G2003, doi:10.1029/2004RG000158.

Zhang, F., Snyder, C., and Rotunno, R. (2003). Effects of moist convection on mesoscale predictability. *Journal of the Atmospheric Sciences*, 60(9):1173–1185.

Zhang, G. and McFarlane, N. (1995). Sensitivity of climate simulations to the parameterization of cumulus convection in the Canadian Climate Centre general circulation model. *Atmosphere Ocean*, 33:407–407.

APPENDIX

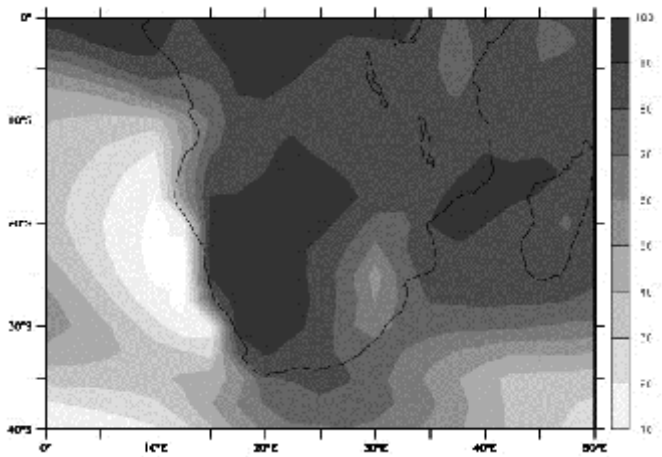

***Figure A.1**: Convective rainfall (%) from CAM3 in January.*